

THERMODYNAMICS OF SOLUTIONS IN LIQUID METHANE.

Thesis submitted for the Degree of

DOCTOR OF PHILOSOPHY

in the

FACULTY OF SCIENCE

in the

UNIVERSITY OF LONDON

by

ARTHUR JOHN DAVENPORT

Department of Chemical Engineering and Chemical Technology,  
Imperial College of Science and Technology,  
London, S.W.7.

July, 1964.

### ACKNOWLEDGEMENTS.

I should like to thank:-

Professor J. S. Rowlinson for his help and guidance at all times during the supervision of this work.

Dr. G. Saville for his help and advice on the vapour pressure studies.

The technicians of the department, and in particular, Mr. C. Onley for his help in the development of the apparatus for the volume measurements.

The Department of Scientific and Industrial Research for a maintenance grant over the past three years.

My parents for financial assistance and every other encouragement.

## CONTENTS.

Page.

### PART I.

CHAPTER I	INTRODUCTION.	1
CHAPTER II	THEORY.	
	Phase Separation in Binary Mixtures.	4
	Thermodynamics of Partially Miscible Liquids.	12
	Structural Considerations for Phase Separation.	30
CHAPTER III	EXPERIMENTAL.	
	Materials.	47
	Preparation of Experimental Sealed Tubes and the High Vacuum Technique.	52
	Measurement of Phase Behaviour of Liquids.	62
CHAPTER IV	RESULTS AND DISCUSSION.	73

### PART II.

CHAPTER I	INTRODUCTION.	102
CHAPTER II	THEORY.	
	Theories of Simple Solutions.	105
	Solution Theory for Molecules of Different Sizes.	112
	Application of the Theory of Molecules of Different sizes to systems showing a L.C.S.T. of the type mentioned in Part I of this thesis.	116

	<u>Page.</u>
CHAPTER III	EXPERIMENTAL.
	Materials. 120
	Volume Measurements. 123
	Details of High Vacuum Apparatus. 124
	The Cryostat. 129
	Vapour Pressure Measurements. 137
	Details of Apparatus. 137
	Experimental Procedure. 139
	Calculation of the excess free energy. 142
CHAPTER IV	RESULTS AND DISCUSSION.
	The Volume Measurements. 145
	The Vapour Pressure Measurements. 147
	Discussion. 148

PART I.

THE SOLUBILITY OF HYDROCARBONS IN LIQUID METHANE.

## CHAPTER I.

### INTRODUCTION.

According to the maxim "like dissolves like", two liquid hydrocarbons would be expected to be completely miscible in all proportions and a solid one should be as soluble in a liquid one as is required by the laws of ideal solutions. However, this principle is found not to hold for pairs of hydrocarbons of very different chain length and intermolecular energies.

The initial disproof of this principle was the observation that the addition of liquid propane to lubricating oil in order to precipitate colloidal asphalt<sup>1, 2</sup>, gives rise to four fluid phases - asphalt, oil with a little propane, propane with a little oil and gaseous propane, if the temperature was above 70° C. The oil is completely miscible with liquid propane below 70° C.

More recent studies<sup>3</sup> on the properties of hydrocarbons in liquid propane and liquid ethane have shown that five hydrocarbons containing between 24 and 32 carbon atoms exhibit a lower critical solution temperature with liquid ethane: that is on heating, the solution separates into two liquid phases. With two hydrocarbons, namely n-octadecyl<sup>cycl</sup>hexane (C<sub>24</sub>H<sub>48</sub>) and 18-ethylpentatriacontane (C<sub>37</sub>H<sub>76</sub>), no single liquid

phase was observed, since solidification of the less volatile liquid phase occurred before the lower critical solution point was reached. In all these systems where there are more than two fluid phases (i.e. liquid I + liquid II + gas), the miscibility gap is found to be within  $30^{\circ}$  of the gas-liquid critical point of pure ethane.

Along similar lines, recent observations<sup>4</sup> on the properties of solutions of non-polar hydrocarbon polymers in non-polar hydrocarbon solvents have shown similar limited miscibility behaviour and it is found that the lower critical solution point for certain of these solutions can lie as much as  $170^{\circ}$  below the gas-liquid critical point of the pure solvent.

In this present work, attention has been turned to the simplest class of hydrocarbon mixtures of this type, namely solutions of hydrocarbons in liquid methane. Twenty-four hydrocarbons containing between four and eight carbon atoms were mixed with liquid methane, and the solutions were investigated from  $113^{\circ}$  K to  $200^{\circ}$  K in a low temperature cryostat. It was found that some hydrocarbons containing five carbon atoms, and almost all those containing six or more carbon atoms were incompletely miscible with liquid methane in the range of temperature investigated. Eight of these systems were found to exhibit lower critical solution points. In

one case, namely methane + hex-1-ene, the solution was completely immiscible at low temperature, but on warming the two liquid phases mixed at an upper critical solution point. On further warming, the single liquid phase re-separated into two liquid phases at a lower critical solution point. In all these systems, the composition and temperature of the lower critical solution point was deduced by investigating the shape of the temperature-composition phase diagram. Ten systems showed no one liquid phase region due to the solidification of the less volatile liquid phase. In these systems, only the temperature at which the four phases [solid + liquid I + liquid II + gas] coexisted in equilibrium was determined, except for the system methane + n-heptane, where the whole temperature-composition phase diagram was studied and the results obtained were found to agree fairly well with those of other workers. 5, 6



CHAPTER II.THEORY.Phase Separation in Binary Mixtures.

Phase separation is quite common in many classes of binary liquid mixtures. Its occurrence depends on the pressure, temperature, composition and molecular properties of the constituents.

The most common class of phase separation in binary liquid mixtures occurs on cooling a homogeneous mixture. The temperature at which phase separation occurs is a function of composition for a given pair of liquids. Perhaps one of the best known examples of this kind of behaviour is the system nitrobenzene + n-hexane and Figure 1 (a) shows the shape of the phase boundary curve. The maximum temperature ( $T_u^c$ ) at which the two phases can coexist is called the Upper Critical Solution Temperature (U.C.S.T.) or Upper Consolute Temperature. At temperatures below this, within the composition range enclosed by the area of the curve, two liquid phases can exist together in thermodynamic equilibrium. If one cuts the phase boundary curve in Fig. 1 (a) with a tie line at temperature  $T'$ , the two liquid phases will have composition  $x_2'$  and  $x_2''$  of component 2 and  $(1 - x_2')$  and  $(1 - x_2'')$

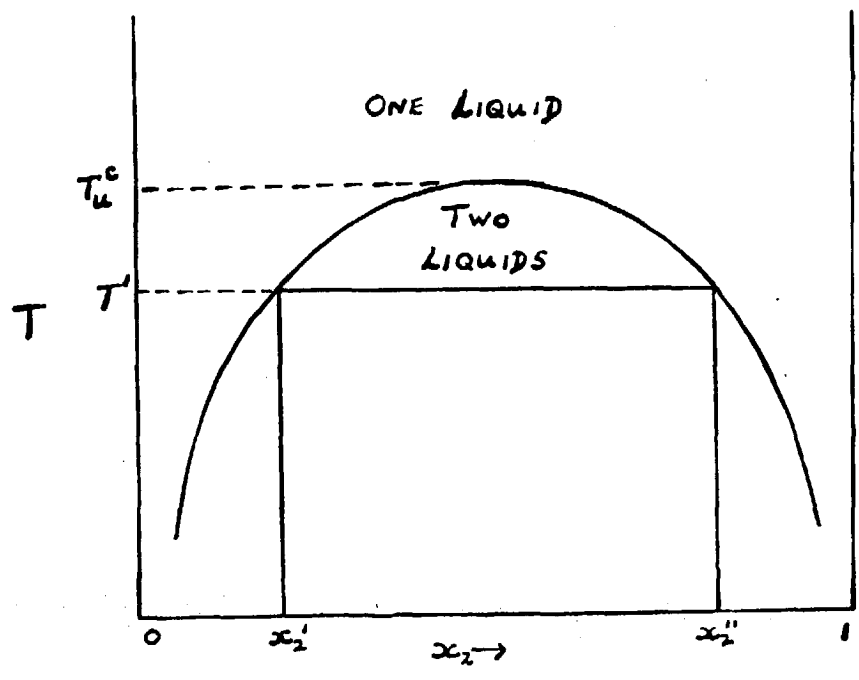


Fig. 1(a)

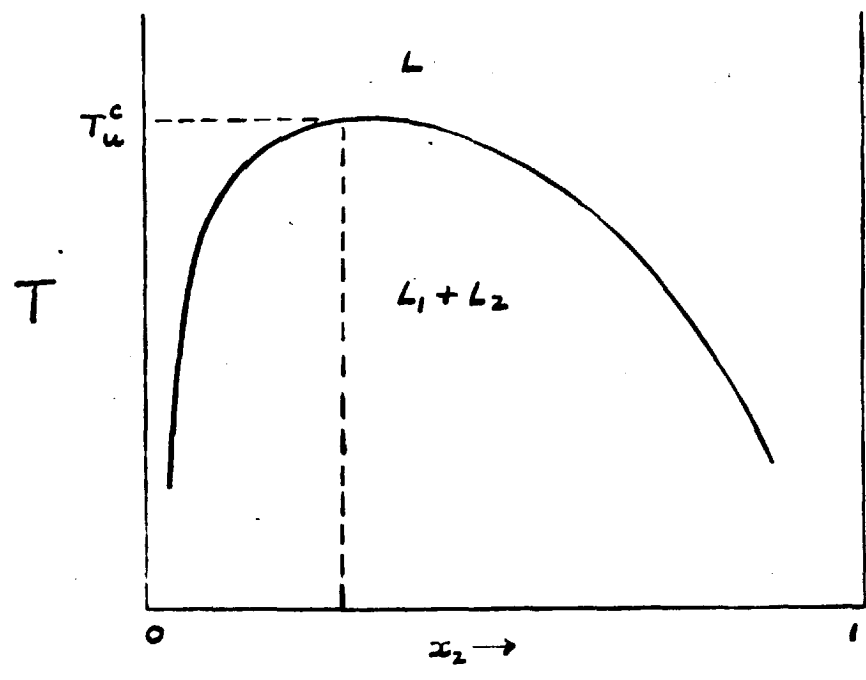


Fig 1 (b)

of component 1. It was found experimentally that the position of the U.C.S.T. lies fairly close to the  $x_2 = 0.5$  composition for two liquids of fairly equal molar volume.

If, however, the components differ vastly in size, e.g. a polymer in a non-polymer solvent, then the phase diagram becomes asymmetric, the ~~symmetry~~<sup>maxima</sup> being displaced towards the component having the ~~larger~~<sup>smaller</sup> molar volume. The degree of displacement increases as the  $\lambda$ <sup>ratio of the</sup> molar volumes increases. Fig. 1 (b) shows a typical phase diagram for a polymer-solvent system of this type, such as polyisobutene + di-isobutyl ketone.

In many cases the cooling of a system exhibiting a U.C.S.T., results in the solidification of the less volatile liquid phase. The phase diagram for this type of system is shown in Fig. 1 (c). The temperature  $T_q$ , where four phases (solid + liquid I + liquid II + gas) coexist is the quadruple point. This is an invariant state of a binary system and corresponds to the triple point in a one component system.

Less common behaviour in binary mixtures is the appearance of phase separation on warming. A similar but inverted curve to that a Fig. 1 (a) shows the variation of temperature with composition for two liquids of nearly equal molar volume - Fig. 2 (a).

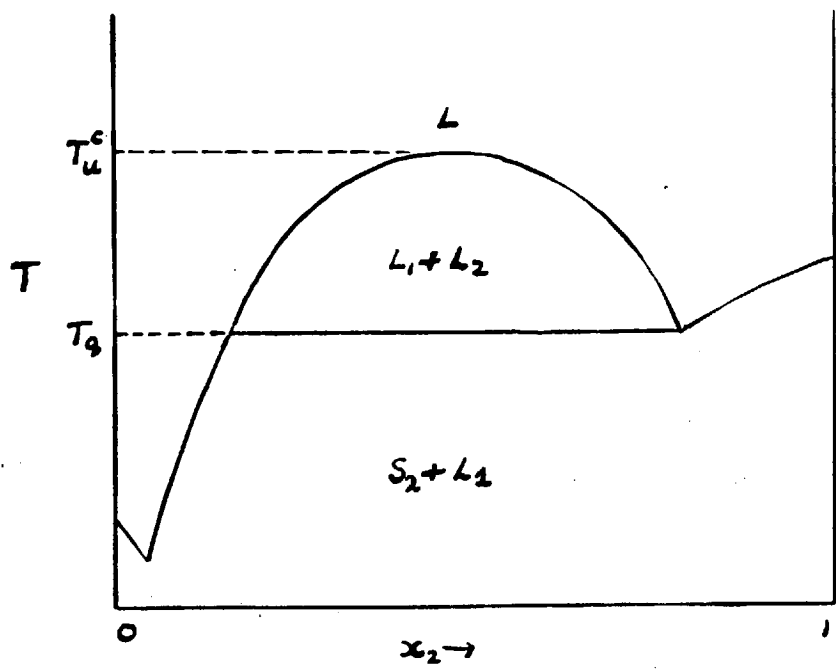


FIG. 1 (c)

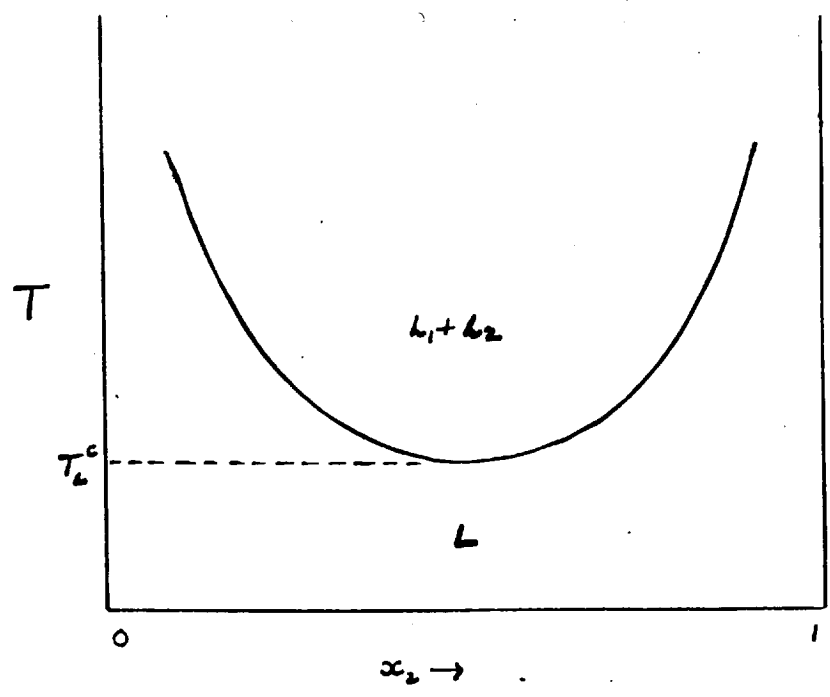


FIG. 2 (a)

The lowest temperature ( $T_L^C$ ) at which the two liquid phases can coexist in equilibrium is called the Lower Critical Solution Temperature (L.C.S.T.) or Lower Consolute Temperature. As with systems exhibiting an U.C.S.T., the phase boundary curve is displaced towards the component of ~~higher~~<sup>smaller</sup> molar volume when the ratio of the molar volumes of the two components is increased. Fig. 2 (b) shows the typical phase boundary curve for the system polyisobutene + n-pentane. In quite a few of the systems which appear to have a similar phase diagram to that of Fig. 2 (a), the exact position of the L.C.S.T. is masked by the solidification of the less volatile liquid phase at the quadruple point ( $T_q$ ). The phase diagram for this type of system is depicted in Fig. 2 (c), the dotted line indicating the position of a metastable L.C.S.T., if the liquid state were extended.

Quite often systems which exhibit lower critical solution phenomena also on warming exhibit upper critical solution points. This results in a phase diagram of the type shown in Fig. 3 where there is a closed solubility loop. The system nicotine + water is an example of this kind of behaviour.

Very recently two new types of phase diagram have come to light. Fig. 4 (a) shows the type of phase diagram exhibited by systems with very different critical

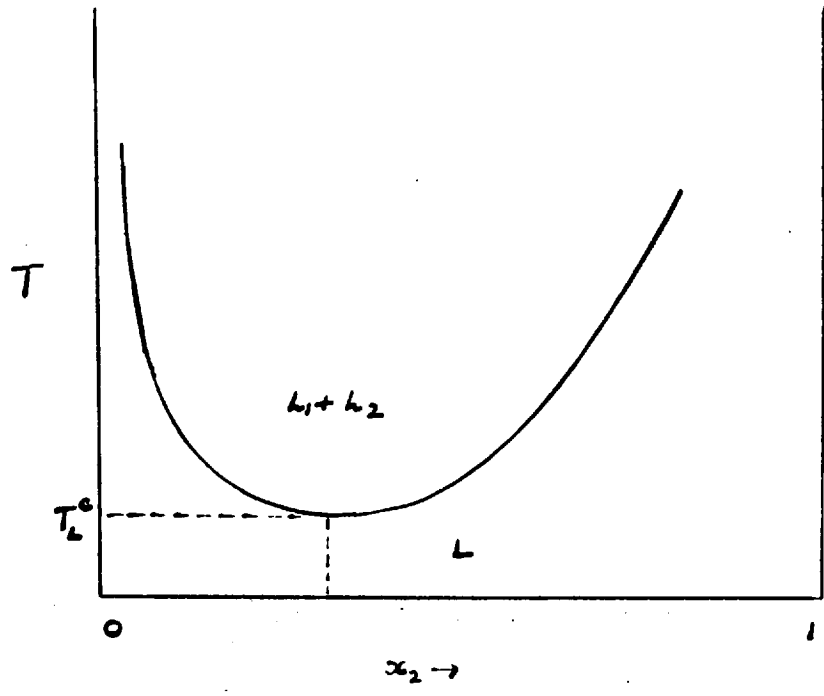


FIG. 2(b)

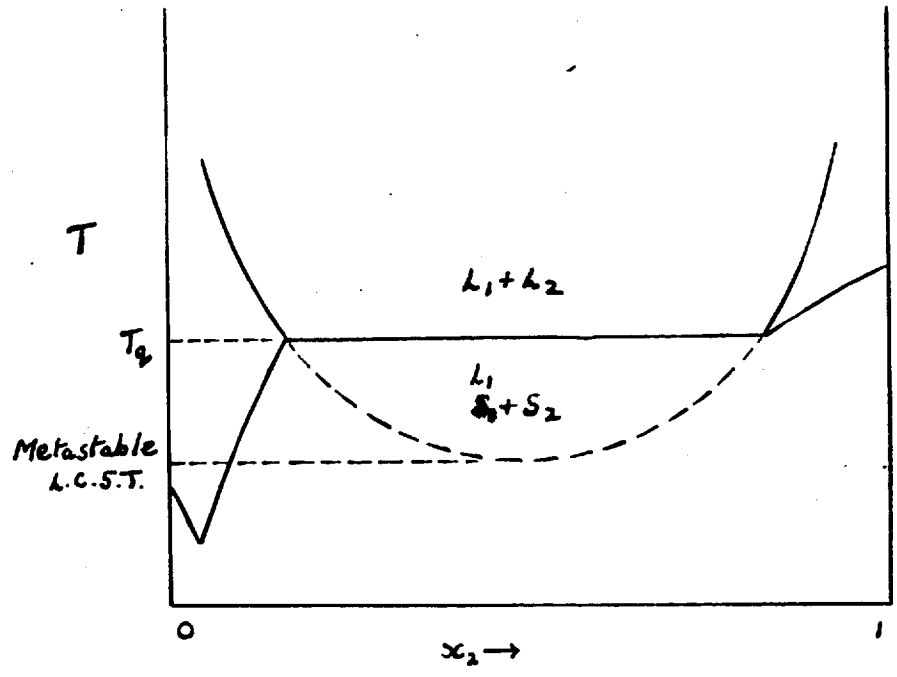


FIG. 2(c)

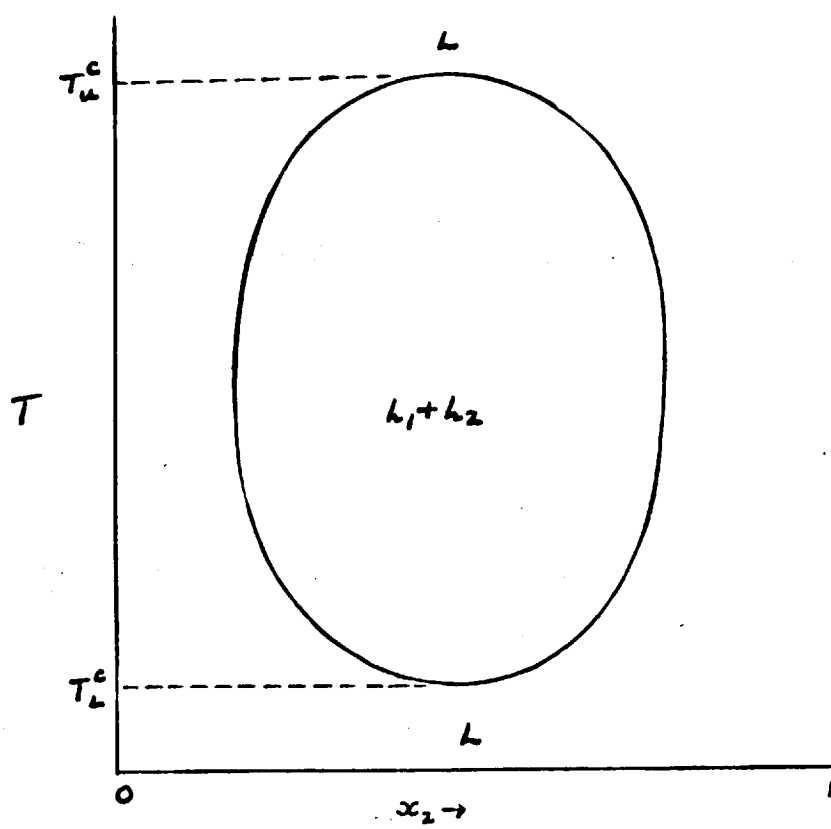


FIG. 3.

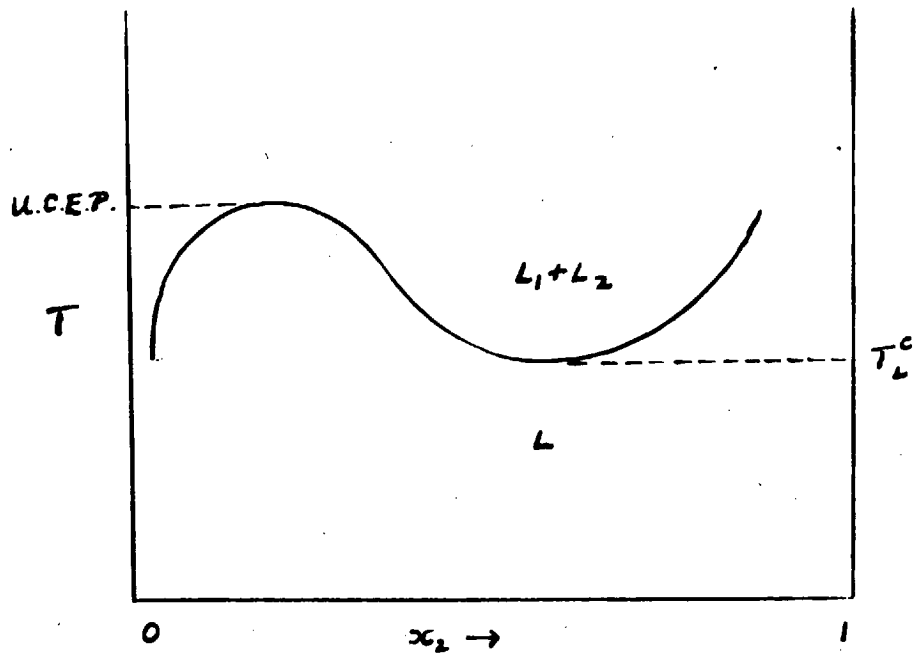


Fig. 4(a)

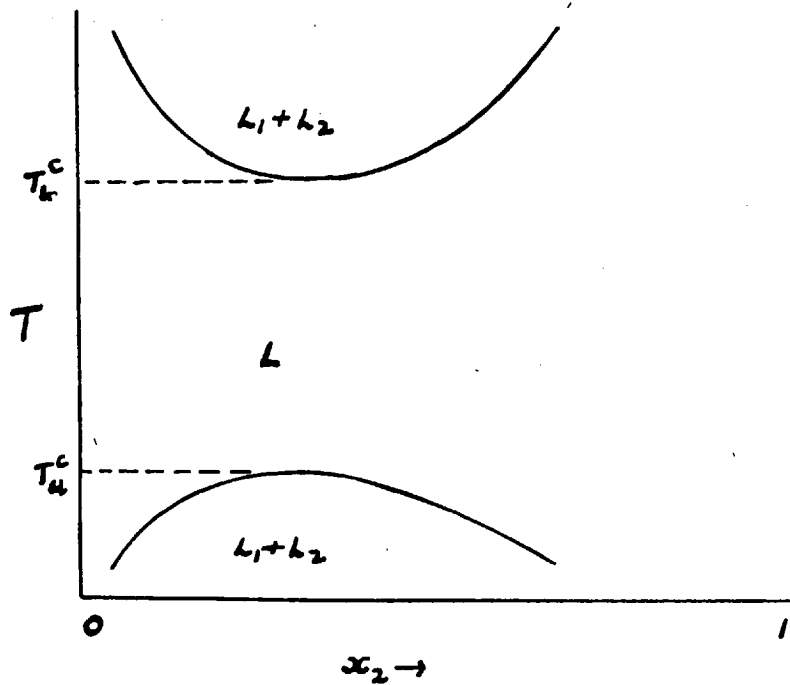


Fig. 4(b)



temperatures. The temperature range of immiscibility is small and lies close to the gas-liquid critical temperature of the more volatile component. It is bounded above by the Upper Critical End Point (U.C.E.P.), where the more volatile liquid phase and the gas phase become identical and below by a L.C.S.T. This type of phase behaviour will be discussed in more detail later in this section. Even more recently, phase behaviour of the type shown in Fig. 4 (b) has been observed. In this case, the system shows a L.C.S.T. fairly close to the gas-liquid critical point but on cooling below the L.C.S.T., the single liquid phase again separates into two liquid phases at a U.C.S.T. This type of behaviour is shown by polyethylene in several hydrocarbon solvents.<sup>7</sup>

#### Thermodynamics of Partially Miscible Liquids.

In a single substance, where the phases solid, liquid and gas are capable of existing in equilibrium, the criteria of mechanical and thermal stability play an essential role in determining which phase is stable with respect to the others. In a homogeneous mixture, however, not only must the conditions of mechanical and thermal stability be satisfied, but a third condition of material or diffusional stability must also be satisfied.

If a binary liquid mixture is to be stable with respect to phase separation, it is essential that the Gibbs Free Energy of the system must be a minimum with respect to composition at constant temperature and pressure.

Now the Gibbs Free Energy per mole ( $g$ ) of a binary liquid mixture is defined at constant temperature and pressure:-

$$\begin{aligned}
 g &= x_1 \mu_1 + x_2 \mu_2 \\
 &= (1-x_2) \mu_1 + x_2 \mu_2 \\
 \left( \frac{\partial g}{\partial x_2} \right)_{T,P} &= \mu_2 - \mu_1 \\
 \left( \frac{\partial^2 g}{\partial x_2^2} \right)_{T,P} &= \left( \frac{\partial \mu_2}{\partial x_2} \right)_{T,P} - \left( \frac{\partial \mu_1}{\partial x_2} \right)_{T,P} \quad \dots \dots (2.1)
 \end{aligned}$$

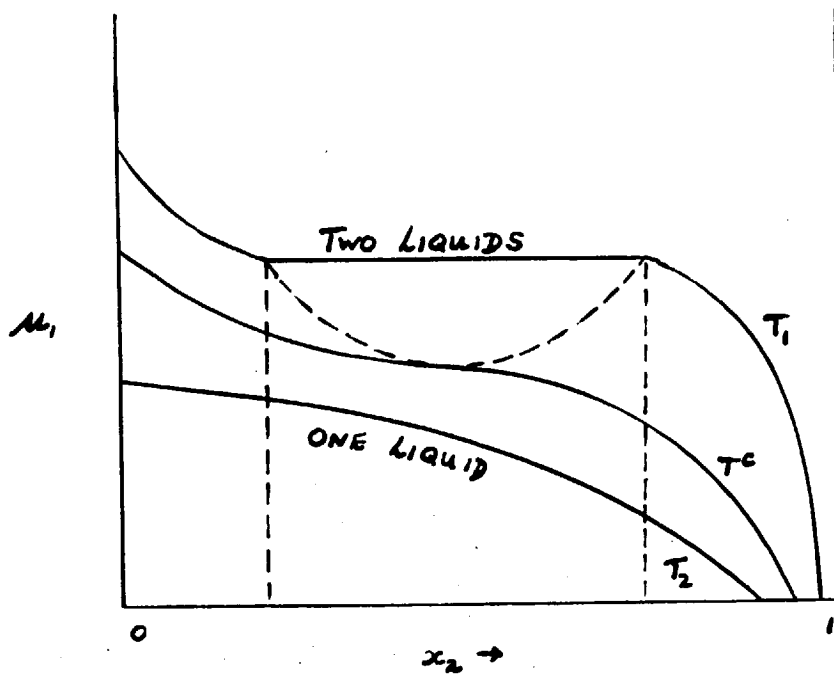
Applying the Gibbs-Duhem equation which for a binary mixture can be written as:-

$$\begin{aligned}
 x_1 \left( \frac{\partial \mu_1}{\partial x_2} \right)_{T,P} + x_2 \left( \frac{\partial \mu_2}{\partial x_2} \right)_{T,P} &= 0 \\
 \therefore \left( \frac{\partial \mu_2}{\partial x_2} \right)_{T,P} &= - \frac{x_1}{x_2} \left( \frac{\partial \mu_1}{\partial x_2} \right)_{T,P} \quad \dots \dots (2.2)
 \end{aligned}$$

Substituting equation (2.2) in (2.1) gives:-

$$\left( \frac{\partial^2 g}{\partial x_2^2} \right)_{T,P} = - \frac{1}{x_2} \left( \frac{\partial \mu_1}{\partial x_2} \right)_{T,P} \quad \dots \dots (2.3)$$

Let us now consider the form of a plot of the chemical potential of component 1 ( $\mu_1$ ) against the mole fraction of component 2 ( $x_2$ ). Fig. 5 shows the



$T_2 > T^c > T_1$  - U.C.S.T.

FIG. 5.

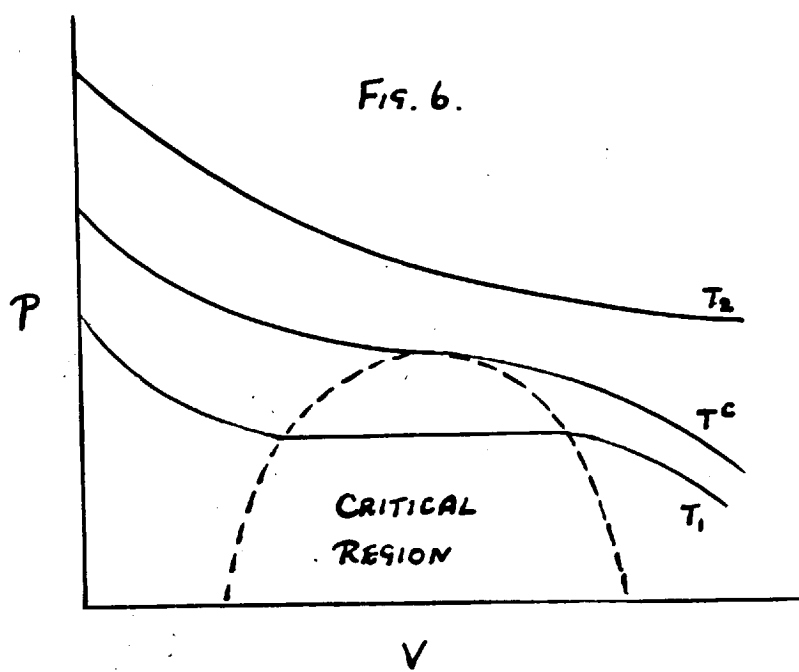


FIG. 6.

$T_2 > T^c > T_1$

type of plot obtained for a system showing a U.C.S.T. This plot corresponds very closely to the plot of pressure against volume for a single substance in the critical region (Fig. 6), where at the gas-liquid critical point, the following conditions hold:-

$$\left(\frac{\partial p}{\partial v}\right)_{T_c} = 0 \quad : \quad \left(\frac{\partial^2 p}{\partial v^2}\right)_{T_c} = 0 \quad : \quad \left(\frac{\partial^3 p}{\partial v^3}\right)_{T_c} < 0$$

In Fig. 5, it can be seen that at temperatures between  $T^c$  and  $T_2$ , there is one liquid phase, whereas at temperatures between  $T_1$  and  $T^c$ , there are two liquid phases, one richer in component 1 ( $x_2'$ ) and the other in component 2 ( $x_2''$ ), the two phases being joined by a horizontal line, indicating that the conditions  $\mu_1' = \mu_1''$  and  $\mu_2' = \mu_2''$  must hold.

Now since:-

$$\mu_1 = g - x_2 \left(\frac{\partial g}{\partial x_2}\right)_{T,P}$$

$$\therefore \mu_1' = g' - x_2' \left(\frac{\partial g}{\partial x_2}\right)'_{T,P} = \mu_1'' = g'' - x_2'' \left(\frac{\partial g}{\partial x_2}\right)''_{T,P}$$

and 
$$\mu_2' = g' + x_1' \left(\frac{\partial g}{\partial x_2}\right)'_{T,P} = \mu_2'' = g'' + x_1'' \left(\frac{\partial g}{\partial x_2}\right)''_{T,P}$$

On subtraction, we obtain the condition that at a liquid-liquid critical point

$$\left(\frac{\partial g}{\partial x_2}\right)'_{T,P} = \left(\frac{\partial g}{\partial x_2}\right)''_{T,P} \quad \dots \dots (2.4)$$

The horizontal line in Fig. 5 reduces to a single point of inflexion at the liquid-liquid critical point, having the conditions:-

$$\left(\frac{\partial \mu_1}{\partial x_2}\right)_{T_c, p_c} = 0 \quad : \quad \left(\frac{\partial^2 \mu_1}{\partial x_2^2}\right)_{T_c, p_c} = 0 \quad : \quad \left(\frac{\partial^3 \mu_1}{\partial x_2^3}\right)_{T_c, p_c} < 0$$

Substituting these conditions in equation (2.3), we obtain the following set of conditions for the derivatives of the Gibbs Free Energy of a mixture with respect to composition at constant temperature and pressure at a liquid-liquid critical point:-

$$\left(\frac{\partial^2 g}{\partial x_2^2}\right)_{T_c, p_c} = 0$$

$$\left(\frac{\partial^3 g}{\partial x_2^3}\right)_{T_c, p_c} = -\frac{1}{x_2} \left(\frac{\partial^2 \mu_1}{\partial x_2^2}\right)_{T_c, p_c} + \frac{1}{x_2^2} \left(\frac{\partial \mu_1}{\partial x_2}\right)_{T_c, p_c} = 0$$

$$\begin{aligned} \left(\frac{\partial^4 g}{\partial x_2^4}\right)_{T_c, p_c} &= -\frac{1}{x_2^2} \left(\frac{\partial^2 \mu_1}{\partial x_2^2}\right)_{T_c, p_c} - \frac{1}{x_2} \left(\frac{\partial^3 \mu_1}{\partial x_2^3}\right)_{T_c, p_c} + \frac{1}{x_2^2} \left(\frac{\partial^2 \mu_1}{\partial x_2^2}\right)_{T_c, p_c} - \frac{2}{x_2^3} \left(\frac{\partial \mu_1}{\partial x_2}\right)_{T_c, p_c} \\ &= -\frac{1}{x_2} \left(\frac{\partial^3 \mu_1}{\partial x_2^3}\right)_{T_c, p_c} \end{aligned}$$

Since  $\left(\frac{\partial^3 \mu_1}{\partial x_2^3}\right)_{T_c, p_c} < 0 \quad \therefore \left(\frac{\partial^4 g}{\partial x_2^4}\right)_{T_c, p_c} > 0$

The existence of a liquid-liquid critical point indicates a certain continuity of state between immiscible liquids becoming identical at a critical point in the same way as a gas-liquid critical point indicates a continuity between two phases in a single component.

If we look at the  $(\mu_1, x_2)$  curve at a temperature where two liquids exist, we can see that it can be regarded as made up of a continuous curve ABCDEF. (Fig. 7). All states between C and D are unstable with  $\left(\frac{\partial \mu_1}{\partial x_2}\right)_{T,P} > 0$ , whilst BC and DE correspond to metastable states with  $\left(\frac{\partial \mu_1}{\partial x_2}\right)_{T,P} < 0$ . The boundary between metastability and instability is determined by  $\left(\frac{\partial \mu_1}{\partial x_2}\right)_{T,P} = 0$ . The stable states have  $\left(\frac{\partial \mu_1}{\partial x_2}\right)_{T,P} < 0$  and are represented by the segments AB and EF in Fig. 7.

As we have previously shown, the thermodynamic conditions for the existence of a liquid-liquid critical point are:-

$$g_{2x_2}^c = 0 : g_{3x_2}^c = 0 : g_{4x_2}^c > 0$$

$$\text{where } g_{2x_2}^c = \left(\frac{\partial^2 g}{\partial x_2^2}\right)_{T_c, P_c} \text{ etc.}$$

The geometrical interpretation for this condition of material stability, namely  $g_{2x_2}^c > 0$ , can only be realised by drawing the plot of  $g$  against  $x_2$  at constant temperature and pressure in the form of a concave upwards curve. (Fig. 8). This curve also satisfies the thermodynamic requirement that all spontaneous fluctuations in a system at equilibrium at constant temperature and pressure must lead to an increase in Gibbs Free Energy.

$$\text{i.e. for stability } \left(\frac{\partial^2 g}{\partial x_2^2}\right)_{T,P} = \left(\frac{\partial^2 g}{\partial x_2^2}\right)_{T,P} > 0 \dots (2.5)$$

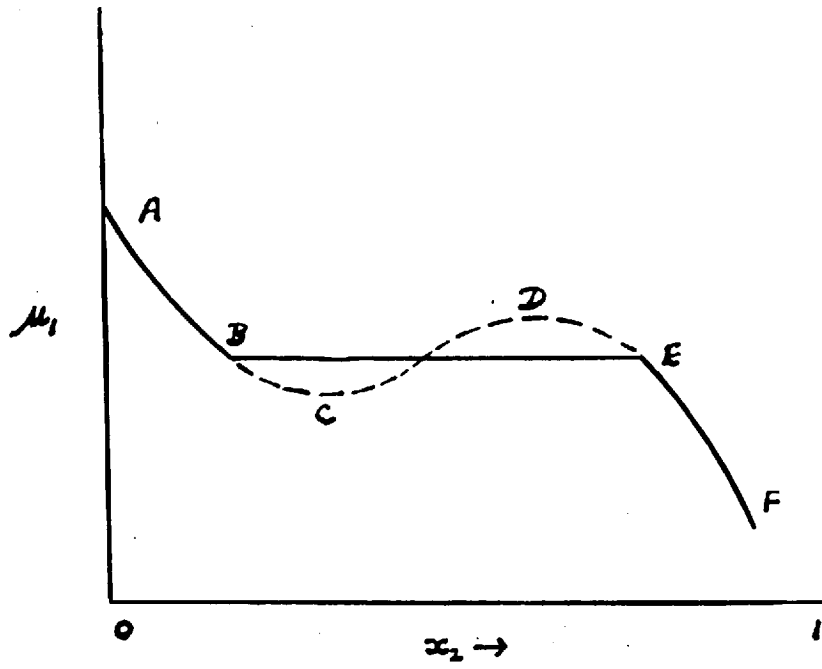


FIG. 7.

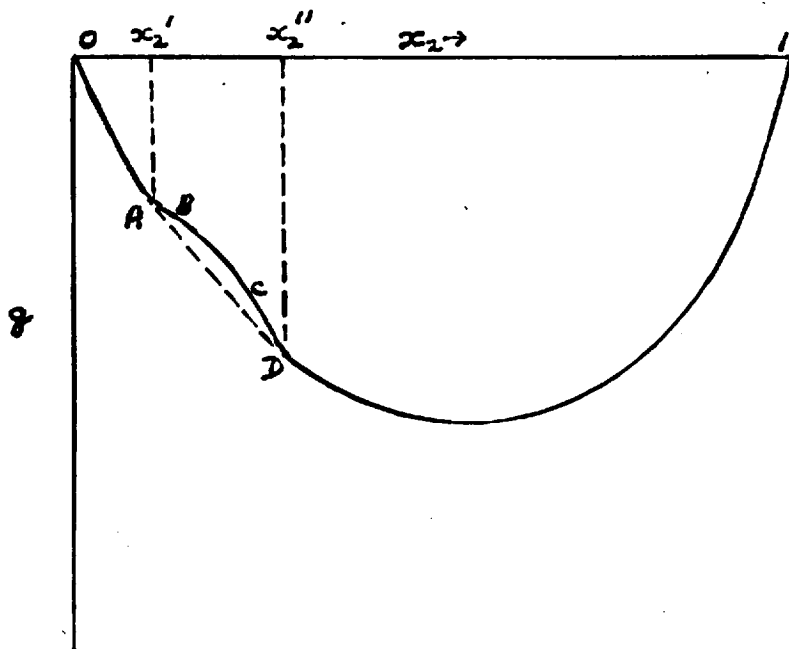


FIG. 8.

The condition of equation (2.5) may also be derived together with the condition of mechanical stability from the  $(F, V, x)$  surface.

In Fig. 8, the curve is concave downwards between B and C and so between this range of composition, the system exhibits immiscibility. At any composition between B and C, the system can only exist as two liquid phases having compositions  $x_2'$  and  $x_2''$  of component 2. The segments AB and CD represent the metastable portion which will tend to revert to the two liquid state. The drawing of the curve in Fig. 8 for  $(g - x_2)$  requires the condition that it is meaningful to express  $g$  as a continuous function of  $x_2$  through stable and unstable phases. This assumption is analogous with the assumption about the continuity of the Helmholtz Free Energy ( $f$ ) with volume for a pure substance at a gas-liquid critical point, but it is very necessary for the useful application of classical thermodynamics to a critical point. The only experimental justification for the prediction of the portion ABCD in Fig. 8 is that under very careful conditions, the metastable portions AB and CD have been shown to exist. The usual experimental curve for  $g(x_2)$  as determined from vapour pressure measurements follows the straight line AD between A and D.

It is now useful to introduce the term excess



function, originally used by Scatchard.<sup>8</sup> An excess function  $X^E$  of an extensive thermodynamic property is defined by the equation:-

$$X^E = X - X^{id}$$

where  $X$  is the experimentally measured value of  $X$  at a given temperature and pressure and  $X^{id}$  is the value of the same property if the system behaved in an ideal manner. It must be emphasised, here, that in discussing liquid mixtures in terms of excess functions we must only consider fairly low constant pressures, (of the order of 5 atmospheres or less) since at higher pressures the concept of an ideal solution is entirely meaningless.

Now 
$$g^E = g - g^{id}$$

For a binary mixture, the Gibbs Free Energy of Mixing at constant pressure is defined by the equation:-

$$g = RT (x_1 \ln x_1 \gamma_1 + x_2 \ln x_2 \gamma_2)$$

where  $x_1$  and  $x_2$  are the mole fractions of components 1 and 2, and  $\gamma_1$  and  $\gamma_2$  are the activity coefficients of components 1 and 2. For an ideal solution  $\gamma_1 = \gamma_2 = 1$ .

$$g^{id} = RT (x_1 \ln x_1 + x_2 \ln x_2)$$

$$S^{id} = - \left( \frac{\partial g^{id}}{\partial T} \right)_P = -R (x_1 \ln x_1 + x_2 \ln x_2)$$

$$h^{id} = g^{id} + TS^{id} = 0$$

$$g^E = g - RT (x_1 \ln x_1 + x_2 \ln x_2)$$

$$h^E = h$$

$$s^E = s + R (x_1 \ln x_1 + x_2 \ln x_2)$$

$$\left( \frac{\partial g^E}{\partial x_2} \right)_{T,P} = \left( \frac{\partial g}{\partial x_2} \right)_{T,P} - RT [\ln x_2 - \ln x_1]$$

$$\left( \frac{\partial^2 g^E}{\partial x_2^2} \right)_{T,P} = \left( \frac{\partial^2 g}{\partial x_2^2} \right)_{T,P} - \frac{RT}{x_1 x_2}$$

At a liquid-liquid critical solution point,

$$\left( \frac{\partial^2 g}{\partial x_2^2} \right)_{T_c, P_c} = 0 \quad \therefore \left( \frac{\partial^2 g^E}{\partial x_2^2} \right)_{T_c, P_c} = - \frac{RT}{x_1 x_2}$$

For a stable one liquid phase

$$\left( \frac{\partial^2 g}{\partial x_2^2} \right)_{T,P} > 0 \quad \therefore \left( \frac{\partial^2 g^E}{\partial x_2^2} \right)_{T,P} > \frac{RT}{x_1 x_2}$$

For two liquid phases

$$\left( \frac{\partial^2 g}{\partial x_2^2} \right)_{T,P} < 0 \quad \therefore \left( \frac{\partial^2 g^E}{\partial x_2^2} \right)_{T,P} < \frac{RT}{x_1 x_2}$$

So far, we have only obtained the conditions which give rise to a liquid-liquid critical point. No attempt has been made to define what specific conditions give rise to a U.C.S.T. or to a L.C.S.T.

If we consider a system at its critical point, then as previously shown, the following conditions must hold:-

$$g_{2x}^c = 0 \quad : \quad g_{3x}^c = 0 \quad : \quad g_{4x}^c > 0$$

If  $g$  can be represented by a Taylor Expansion in terms of  $x_2$  and  $T$  at constant pressure about its value  $g^c$  at the critical point, then the leading terms are:-

$$g = g^c + g_{2x}^c (x_2 - x_2^c) - s_{2x}^c (x_2 - x_2^c)(\delta T) - \frac{1}{2} s_{2x}^c (x_2 - x_2^c)(\delta T) + \frac{1}{24} g_{4x}^c (x_2 - x_2^c)^4 + \dots$$

In this expression  $g_{2x}^c$  and  $g_{3x}^c$  have been put equal to zero.

Now equilibrium between the two phases requires that:-

$$g_x^c' = g_x^c''$$

$$[g - (x_2 - x_2^c)g_x]^c' = [g - (x_2 - x_2^c)g_x]^c''$$

Denoting  $x_2 - x_2^c$  by  $\delta x_2$ , the equations obtained are:-

$$-s_{2x}^c (\delta T)(\delta x_2' - \delta x_2'') + \frac{1}{6} [(\delta x_2')^3 - (\delta x_2'')^3] = 0 \dots (2.5)$$

$$g_{4x}^c [(\delta x_2')^2 - (\delta x_2'')^2][(\delta x_2') - (\delta x_2'')] = 0 \dots (2.6)$$

Equation (2.6) gives:-  $\delta x_2' = -\delta x_2'' = \frac{1}{2}\Delta x_2$  where  $\Delta x_2 = \delta x_2' - \delta x_2''$

Substitution in equation (2.5):-

$$\frac{1}{6} g_{4x}^c (\delta x_2')^2 = \frac{1}{6} g_{4x}^c (\delta x_2'')^2 = s_{2x}^c (\delta T)$$

$$\text{or } \left(\frac{\partial x_2}{\partial T}\right)_P' = -\left(\frac{\partial x_2}{\partial T}\right)_P'' = \frac{12 s_{2x}^c}{g_{4x}^c \Delta x_2} \dots (2.7)$$

As  $g_{4x}^c$  is necessarily positive at a liquid-liquid critical point and  $\Delta x_2$  is negative if  $x_2'' > x_2^c > x_2'$ , the sign of  $\left(\frac{\partial x_2}{\partial T}\right)_P'$  is determined solely by the sign of  $s_{2x}^c$ .

Thus, for a U.C.S.T., where  $\left(\frac{\partial x_2}{\partial T}\right)_P'$  is positive,  $s_{2x}^c$  must be negative, and for a L.C.S.T., where  $\left(\frac{\partial x_2}{\partial T}\right)_P'$  is negative,  $s_{2x}^c$  must be positive.

Now, since  $g_{2x}^c = h_{2x}^c - Ts_{2x}^c$  and  $g_{2x}^c = 0$  at the critical point, then:-

$$h_{2x}^c = Ts_{2x}^c$$

Therefore, to summarize:-

$$\text{At a U.C.S.T. } h_{2x}^c < 0, s_{2x}^c < 0$$

$$\text{At a L.C.S.T. } h_{2x}^c > 0, s_{2x}^c > 0$$

As we have previously shown:-

$$g_{2x}^c = \frac{RT_c}{x_1 x_2} + (g_{2x}^E)^c = 0$$

$$h_{2x}^c = (h_{2x}^E)^c < 0 \text{ (U.C.S.T.) } > 0 \text{ (L.C.S.T.)}$$

$$s_{2x}^c = -\frac{R}{x_1 x_2} + (s_{2x}^E)^c < 0 \text{ (U.C.S.T.) } > 0 \text{ (L.C.S.T.)}$$

Therefore, for a U.C.S.T.

$$\left(\frac{\partial^2 g^E}{\partial x_2^2}\right)_{T_c, P_c} = -\frac{RT_c}{x_1 x_2} : \left(\frac{\partial^2 h^E}{\partial x_2^2}\right)_{T_c, P_c} < 0 : \left(\frac{\partial^2 s^E}{\partial x_2^2}\right)_{T_c, P_c} < -\frac{R}{x_1 x_2}$$

For a L.C.S.T.

$$\left(\frac{\partial^2 g^E}{\partial x_2^2}\right)_{T_c, P_c} = -\frac{RT_c}{x_1 x_2} : \left(\frac{\partial^2 h^E}{\partial x_2^2}\right)_{T_c, P_c} > 0 : \left(\frac{\partial^2 s^E}{\partial x_2^2}\right)_{T_c, P_c} > -\frac{R}{x_1 x_2}$$

If both  $h(x_2)$  and  $s(x_2)$  are smooth functions, that

is there are no points of inflexion, then:-

For a U.C.S.T.

$$g^E > 0, h^E > 0, s^E \geq 0$$

For a L.C.S.T.

$$g^E > 0, h^E \leq 0, s^E < 0$$

It must be emphasised here that the above conditions are necessary but not sufficient for liquid-liquid critical

points. They may be summed up verbally in the following way:-

A U.C.S.T. is related to conditions that produce a large positive deviation of energy or enthalpy from ideality, whereas a L.C.S.T. is associated with conditions that produce a large negative deviation of entropy from ideality. Though these conditions have been borne out by experiment, it must be emphasised here that the entropy in a U.C.S.T. and the energy in a L.C.S.T. do not play a completely insignificant part in the production of these phenomena as will be shown later.

Let us now consider the simplest class of non-ideal mixtures, namely "regular mixtures." From experimental results of the partial and total pressures of binary mixtures, it has been shown that  $g^E$  can be fitted to the following function in  $x_1$  and  $x_2$  by choosing sufficient terms.

$$g^E = x_1 x_2 [A + B(x_1 - x_2) + C(x_1 - x_2)^2 + \dots] \dots (2.8)$$

N.B. When  $x_1 = 0$ ,  $g^E = 0$ , and when  $x_2 = 0$ ,  $g^E = 0$

The simplest class of non-ideal mixtures will be when B, C, and all higher coefficients in equation (2.8) are zero, for a non-zero range of pressure and temperature. Such a mixture is called a regular mixture. For these mixtures,

$$\begin{aligned}
 g^E &= x_1 x_2 A : \quad \mu_1^E = x_2^2 A : \quad \mu_2^E = x_1^2 A \\
 h^E &= x_1 x_2 \left[ A - T \left( \frac{\partial A}{\partial T} \right)_P \right] \\
 s^E &= x_1 x_2 \left[ - \left( \frac{\partial A}{\partial T} \right)_P \right] \\
 v^E &= x_1 x_2 \left[ \left( \frac{\partial A}{\partial P} \right)_T \right]
 \end{aligned}$$

If A is assumed independent of temperature, then  $s^E = 0$  and  $g^E = h^E = A x_1 x_2$ . This restriction on A gives us the definition of a regular mixture as defined by Hildebrand,<sup>9</sup> to which more recently the term strictly regular mixture has been applied.

If  $g^E$  can be expressed by the equation:-

$$g^E = A(T) x_1 x_2$$

$$\left( \frac{\partial g^E}{\partial x_2} \right)_{T,P} = A(T) \{ 1 - 2x_2 \}$$

$$\left( \frac{\partial^2 g^E}{\partial x_2^2} \right)_{T,P} = -2A(T)$$

At a liquid-liquid critical point  $\left( \frac{\partial^2 g^E}{\partial x_2^2} \right)_{T_c, P_c} = -\frac{RT_c}{x_1 x_2}$

$$\therefore A(T_c) = \frac{RT_c}{2x_1 x_2}$$

For a regular mixture at a liquid-liquid critical point.

$$g^E = \frac{RT_c}{2} \quad , \quad \begin{aligned}
 &h^E > 0 \quad \text{and} \quad s^E > -R/2 \quad (\text{U.C.S.T.}) \\
 &h^E < 0 \quad \text{and} \quad s^E < -R/2 \quad (\text{L.C.S.T.})
 \end{aligned}$$

Therefore a regular mixture can have a U.C.S.T. if  $h^E$  is positive irrespective of the sign of  $s^E$  as long

as it is greater than  $-R/2$ . It can only show a L.C.S.T. if  $h^E$  and  $s^E$  are both negative and the latter is less than  $-R/2$ . In both cases, the phase boundary curve is symmetrical about  $x_2 = 0.5$ . It is interesting to note here that it is found experimentally that for a large number of binary systems the  $g^E(x_2)$  curve is roughly symmetrical about  $x_2$ , although there is quite often marked asymmetry in the  $h^E(x_2)$  and  $s^E(x_2)$  curves.

Thus, as a guide, we would expect a regular solution to exhibit phase separation when the excess Gibbs Free Energy of the mixture is  $T$  cal.s.mole<sup>-1</sup>. This statement is in fact substantiated by many regular solutions which show a U.C.S.T. At a U.C.S.T., the critical value of  $g^E$  can arise solely from energetic factors which affect the enthalpy of the solution, whilst not necessarily affecting its entropy. Thus strictly regular solutions ( $s^E = 0$ ) can only exhibit a U.C.S.T. On the other hand, a L.C.S.T. will be observed only if the solution has a large negative excess entropy, accompanied by a relatively small negative excess enthalpy.

Let us now view from a thermodynamic angle how a L.C.S.T. may be produced in a regular solution. (This has recently been investigated by Copp and Everett<sup>10</sup>). Consider a stable one-phase system with  $g^E > 0$ ,  $h^E < 0$  and  $s^E < 0$ , which is potentially capable of separating

into two phases on raising the temperature. Let us take any reference temperature ( $T_0$ ), where the system has a Gibbs Free Energy ( $g_0$ ) at  $x_2 = 0.5$ , corresponding to the point O in Fig. 9. As  $s^E$  is negative, then  $g^E$  increases with temperature. But, if  $c_P^E$  is positive,  $s^E$  falls with temperature so the slope of the  $g^E(T)$  curve decreases. Therefore the curvature of the  $g^E(T)$  curve will depend on the ratio  $\left(\frac{c_P^E}{s_0^E}\right)$ . From Fig. 9, we can see that it is possible to have

the following four cases on increasing the temperature:-

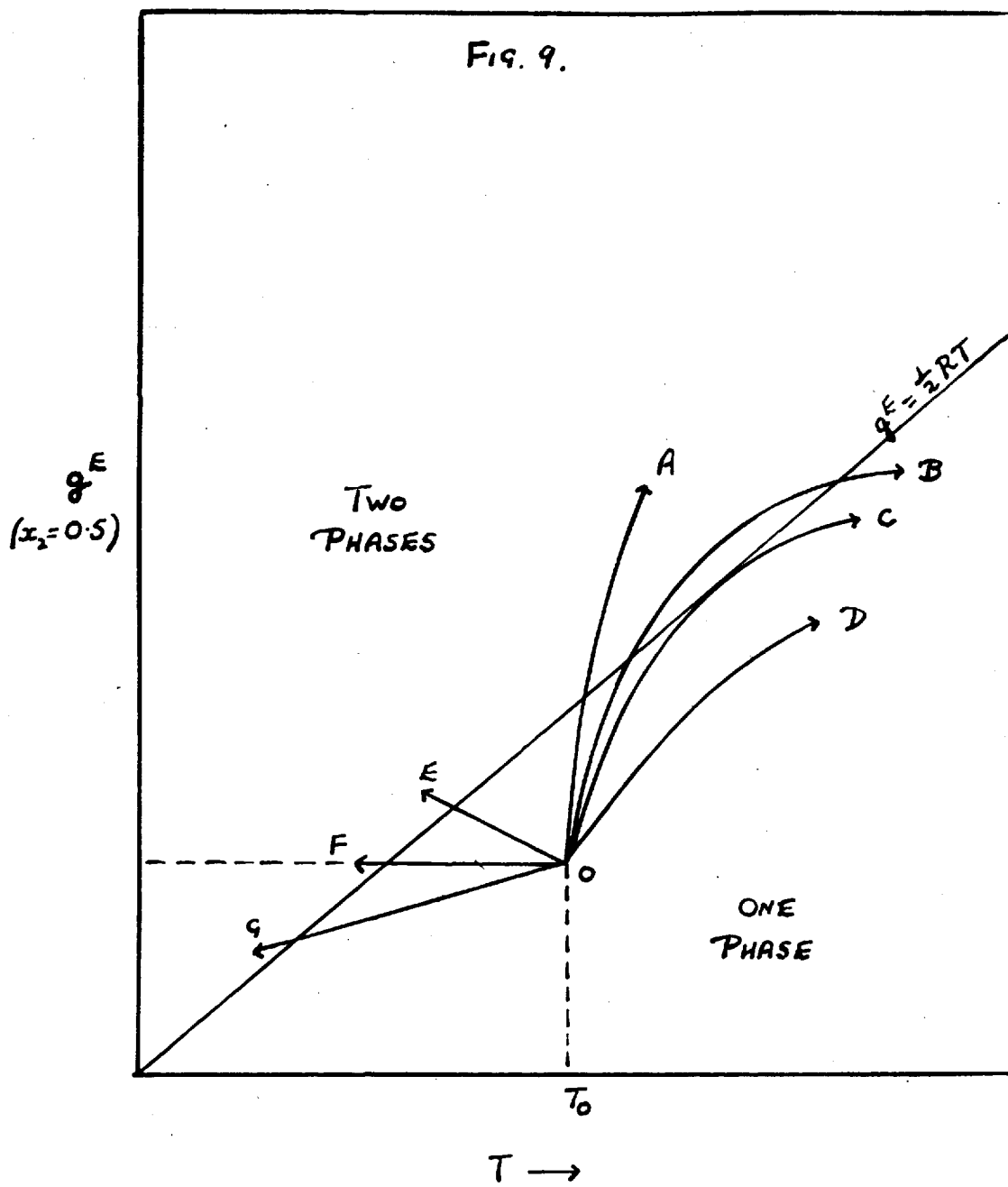
a) OA -  $c_P^E$  is very strongly positive and enables  $g^E$  to pass rapidly through the critical value of  $0.5 RT$ , and so gives rise to a L.C.S.T.

b) OB - in this case  $c_P^E$  is positive enough to give rise to a L.C.S.T., but then it does not increase rapidly enough, and so the conditions for a U.C.S.T. are reached i.e.  $g^E > 0$ ,  $h^E > 0$ ,  $s^E \ll 0$ , and we have a closed solubility loop as exemplified by the nicotine-water system.

c) OC - here, the  $g^E(T)$  curve just touches the critical line  $g^E = 0.5 RT$ . No bulk separation will occur but the solution is observed to go slightly turbid. This phenomena has been observed by Andon, Cox and Herington<sup>11</sup> in aqueous mixtures of  $\alpha$ - and  $\beta$ - picolines.

d) OD -  $c_P^E$  is not very strongly positive and





in consequence,  $g^E$  does not reach its critical value of  $0.5 RT$  and so no separation into two phases occurs.

From this recent discussion, it can be seen that lower consolute phenomena will only occur in systems that have the correct balance between  $s^E$ ,  $h^E$  and  $c_P^E$ , whereas any system at 0 having  $s^E$  greater than  $-R/2$  will separate into two liquid phases on lowering the temperature. e.g. OE, OF (corresponding to a strictly regular solution) and OG.

There are no thermodynamic restrictions on the signs and sizes of the excess heat capacity or the excess volume at a critical solution point, but in general we find that at a U.C.S.T.,  $c_P^E < 0$ ,  $v^E > 0$ , and at a L.C.S.T.,  $c_P^E > 0$ ,  $v^E < 0$  (this condition is in practice always true).

The sign of  $\left(\frac{\partial^2 v}{\partial x^2}\right)$  determines the effect of pressure on the critical temperature as:-

$$\left(\frac{\partial T_c}{\partial p}\right) = - \frac{(g_{2x}^c)_p}{(g_{2x}^c)_T} = \frac{v_{2x}^c}{s_{2x}^c}$$

At a U.C.S.T.,  $v_{2x}^c < 0$ ,  $s_{2x}^c < 0 \therefore \left(\frac{\partial T_c}{\partial p}\right)$  is positive

At a L.C.S.T.,  $v_{2x}^c > 0$ ,  $s_{2x}^c > 0 \therefore \left(\frac{\partial T_c}{\partial p}\right)$  is positive

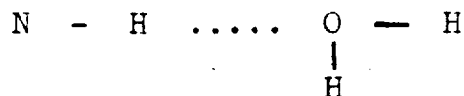
Thus increasing the pressure usually increases the critical temperature of both lower and upper consolute phenomena.

Structural Considerations for Phase Separation.

The observance of upper consolute behaviour is quite common and in general is shown by mixtures of a non-polar and polar liquid, for instance aniline or nitrobenzene with a paraffin hydrocarbon. Since the appearance of a U.C.S.T. is linked with a positive energy deviation from ideality, it is easy to explain the fact that these mixtures show a U.C.S.T. since their mean interaction energies are very different. The mean interaction energy of a polar molecule will be large because of its polarity, whereas the mean interaction energy of a non-polar molecule will be small. Therefore it is energetically difficult to dilute an assembly of polar molecules with non-polar molecules, and so the two liquids will be immiscible. However, at higher temperatures, the energy of interaction becomes less important compared with the entropy of the system and so the two liquids will mix on increasing the temperature.

The explanation of the occurrence of lower critical solution phenomena is not quite so simple. From the thermodynamic viewpoint, we have seen that these systems must have a negative excess entropy of mixing. The first types of solution which were observed to show lower critical solution points were almost ex-

clusively aqueous solutions of amines, pyridines, alcohols and alcoholic ethers and these solutions usually separated into two phases near the normal boiling point of the more volatile component. Therefore, it was at first concluded that the observance of lower consolute phenomena was linked with solutions which at low temperatures had their molecules highly orientated in certain directions by the presence of hydrogen bonds:-



As more solutions were examined, however, it was realised that the observance of lower consolute phenomena could not wholly be explained in terms of hydrogen bonding since there are quite a few solutions where hydrogen bonding is known to exist and yet they show no phase separation on heating. In these cases it may be presumed that although the excess entropy of mixing is negative, the excess heat of mixing is also negative and is in fact large enough to give a negative excess free energy of mixing resulting in an extremely stable solution. Therefore it was realised that solutions of the above type which exhibit lower consolute phenomena must have something else besides hydrogen bonding.

If we consider the solutions (a) methanol + water

(b) ethanol + water: (c) n-propanol + water and  
 (d) n-butanol + water, it was observed that at 20° C,

$$h_d^E > h_c^E > h_b^E > h_a^E$$

Now, in this series, only the n-butanol + water system shows any immiscibility behaviour and this system does in fact form a closed solubility loop. Therefore, although all these solutions are hydrogen bonded, it is not until we come to case (d) that  $h^E$  becomes of the right size to make  $g^E$  positive. A similar situation exists in aqueous mixtures of the series (1) pyridine, (2) 2-methylpyridine, (3) 3-methylpyridine, (4) 4-methylpyridine, (5) 2 : 5-dimethylpyridine, (6) 2 : 6-dimethylpyridine. In these systems, Andon, Cox and Herington<sup>11</sup> found that at 85° C,

$$h_5^E = h_4^E > h_3^E > h_2^E > h_1^E > h_6^E$$

On analysing these two sets of systems, it was suggested that the occurrence of lower consolute phenomena was related to the number of hydrocarbon groupings or segments present in the non-aqueous molecule. Thus, as we increase the size of the alcohol or pyridine molecule,  $h^E$  tends to become more positive, resulting eventually in  $g^E$  becoming positive. (2 : 6-dimethylpyridine is an exception to this rule). In the pyridine series, all the binary aqueous solutions show lower consolute behaviour, but the order of ease

of solution in water at 85° C is:-

$$(1) \gg (4) > (2) > (3) \gg (5) \approx (6)$$

Experimental evidence has shown that the excess entropy decreases with the number of hydrocarbon groupings for an aqueous series, and, as would be expected, the excess specific heat tends to increase as well. Both these factors, as long as  $c_p^E$  does not become too large, tend to make  $g^E$  more positive and increase its value with respect to temperature. Mitchell and Wynne-Jones<sup>12</sup> have predicted from their results for mixtures of methanol + ethanol and ethanol + n-propanol that the excess entropies for the aqueous alcohol systems will be roughly constant whereas Andon, Cox and Herington<sup>11</sup> have shown that  $s^E$  for the pyridine series at 85° C, decreases as follows:-

$$s_1^E > s_4^E > s_3^E > s_2^E > s_5^E > s_6^E$$

In their paper they attribute the decrease in the excess entropy to the increasing basicity of the pyridine homologues, resulting in a more hydrogen bonded solution, but there is also a case for arguing that the decrease in excess entropy could be linked with the number of hydrocarbon groupings present in the pyridine molecule.

From this discussion, we should expect that the addition of hydrocarbon groupings to the alcohol or

pyridine molecule would increase the value of  $h^E$  and hence  $c_p^E$ , whilst in general they would decrease  $s^E$ . These conditions will tend to decrease the lower critical solution temperature and also give rise to closed solubility loops where  $h^E$  has to change from negative to positive.

Therefore, to recapitulate, it appears that the appearance of lower consolute behaviour in aqueous media is closely related to the following important factors:-

a) Association between the two components usually by a hydrogen bonding mechanism resulting in a large negative value for  $s^E$ .

b) Heat, entropy and heat capacity effects arising from the interaction of the inert hydrocarbon grouping of the second component with the water structure.

These mixtures will thus be more fully understood when a more fundamental investigation of effects (a) and (b) has been made.

Speculative attempts have been made by other workers to try to explain the role<sup>e</sup> played by the relative orientations of the molecules at a L.C.S.T. Hirschfelder, Stevenson and Eyring<sup>13</sup>, whilst agreeing that a L.C.S.T. was due to an interaction such as hydrogen bonding which interfered with the free rota-

tion of the molecules, suggested that in the systems discussed previously, at least one component was free to rotate, so seriously limiting the effect of hydrogen bonding. Therefore it seems quite likely that the longer range London forces between the inert hydrocarbon groupings and the water molecules may play a very essential role in making these systems mix at low temperatures. However, both these effects must be weighted in such a way as to enable the molecules to adopt orientations of low energy, these favourable alignments being broken on raising the temperature resulting in immiscibility at a L.C.S.T. Barker and Fock<sup>14</sup> have attempted to explain the occurrence of a closed solubility loop and a U.C.S.T. on models based upon a lattice picture, each molecule occupying a single site in a z- co-ordinated lattice. They have shown that where we have a model, in which the contacts and interaction energies correspond to the effect of an active group of one molecule polarising the other molecule and so interacting strongly with it, a closed co-existence curve is predicted, whereas with a model in which each component carries a hydroxyl or similar group, only an upper consolute temperature is predicted.

There is however a completely different class of systems which exhibit lower consolute phenomena in which the appearance of a L.C.S.T. is not linked to any



difference in molecular energies or to any specific forces of attraction or mutual orientations. Kuenen and Robson found in 1899 that ethanol, n-propanol and n-butanol are completely miscible with ethane at  $25^{\circ}$  C, but that each of these systems forms two liquid phases over a few degrees close to the gas-liquid critical point of pure ethane ( $T^c = 32^{\circ}$  C). The (p, T, x) surface and the (p, T) and (T, x) projections are shown in Figures 10 (a), (b), and (c). It can be seen that the range of immiscibility is small. The projections are bounded below by the liquid-liquid critical point and above by a gas-liquid critical end point at which the gas phase and the liquid phase rich in ethane become identical. If we study the (p, T, x) surface for this type of system we see that at temperatures below the L.C.S.T., there exists a homogeneous liquid phase but at the L.C.S.T., the single liquid phase separates critically into two liquid phases. [point P in Fig. 10 (a)]. The dashed line  $C_2P$  lies between y and z and represents the locus of the liquid-liquid critical point. At the critical point of pure ethane  $C_1$ , another dashed line  $C_1O$  appears which represents the locus of the gas-liquid critical point of ethane rich mixtures. On increasing the temperature, the points y and z recede from each other while x and y come closer together. At the upper critical end point

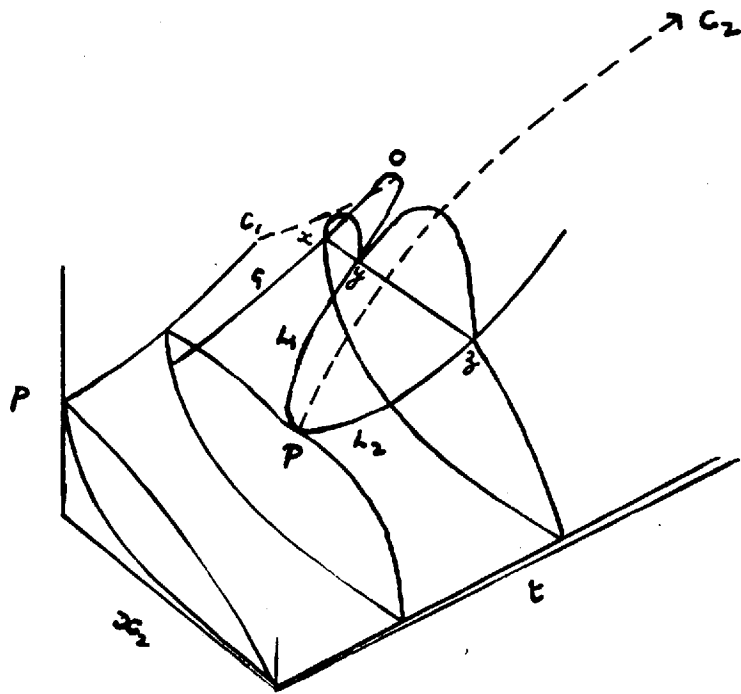


FIG. 10(a)

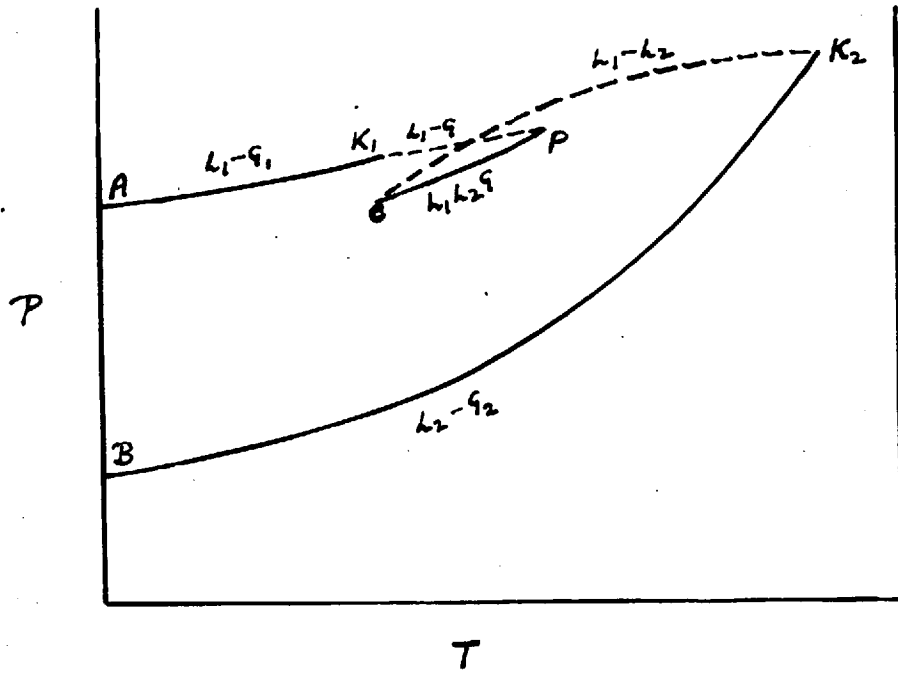


FIG. 10(b)

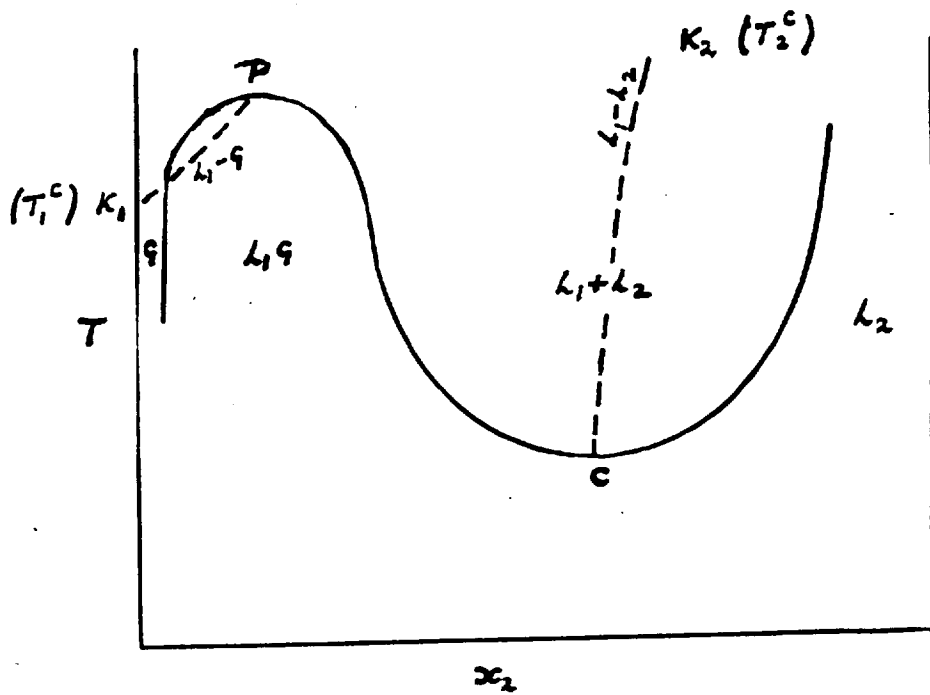


FIG. 10(c).

(U.C.E.P.), represented by O in Fig. 10 (a), the dashed line  $C_1O$  terminates. This feature is peculiar to these type of systems since in all other systems exhibiting a L.C.S.T. in the form of a closed solubility loop, it is the locus of the liquid-liquid critical point P [represented by  $C_2P$  on Fig. 10 (a)] which vanishes. In this class of system, the less dense liquid phase takes over the role of the gas phase, i.e. it acts as a superfluid phase.

If we look at the (p, T) projection for this type of system, we see that  $AK_1$  and  $BK_2$  represent the normal vapour pressure curves of the volatile and involatile components respectively. If the two liquids were miscible at all temperatures, a single line ( $K_1K_2$ ) would extend from  $K_1$  to  $K_2$  which corresponds to the gas-liquid critical pressures and temperatures of all intermediate mixtures of the two components. However, at C, the liquids become immiscible and remain so up to P. Thus the line CP represents the simultaneous coexistence of  $L_1$ ,  $L_2$  and G. The dotted lines  $K_1P$  ( $L_1 - G$ ) and  $CK_2$  ( $L_1 - L_2$ ) represent respectively the critical line for the ethane rich compositions where the system is miscible and the critical line of the liquid-liquid immiscibility which ends and the critical point of component 2 ( $K_2$ ). This latter line is in fact a measure of the way in which a L.C.S.T. increases with increasing pressure.

A variety of similar systems have come to light since the original type was discovered by Kuenen and Robson. In each case, the gas-liquid critical points of the pure components are widely separated and the three phase line is confined to a short region near the gas-liquid critical point of the more volatile component.

Examples of systems where both critical end points have been located are:-

- Carbon Dioxide ( $T^c = 31^\circ\text{C}$ ) + Nitrobenzene<sup>15</sup> (Liquids immiscible between  $30^\circ\text{C} - 40^\circ\text{C}$ )
- Carbon Dioxide + o-Nitrophenol<sup>16</sup> (Liquids immiscible between  $26^\circ\text{C} - 40^\circ\text{C}$ )
- Ethylene ( $T^c = 9^\circ\text{C}$ ) + p-Dichlorobenzene<sup>17</sup> (Liquids immiscible between  $26^\circ\text{C} - 26.5^\circ\text{C}$ )
- Ethane ( $T^c = 32^\circ\text{C}$ ) + 1, 3, 5 - Trichlorobenzene<sup>18</sup> (Liquids immiscible between  $40.3^\circ\text{C} - 46.8^\circ\text{C}$ )

Many other systems look as though they behave similarly from the partial data already reported. e.g. Propane ( $T^c = 97^\circ\text{C}$ ) has been found to show a L.C.S.T. near its own gas-liquid critical point with a large number of long chain organic acids and esters.<sup>19</sup>

In all these systems, the two components are of widely different chemical type, but it now looks as though this chemical difference is not an essential feature of this type of system since Freeman and Rowlinson<sup>3</sup>

have found that this type of immiscibility can occur with systems of similar chemical type - for instance, a pair of hydrocarbons if their chain length and hence their gas-liquid critical points are sufficiently different. They found that although liquid propane is miscible with a series of hydrocarbons up to 37 carbon atoms at all temperatures, liquid ethane ( $T^c = 32^\circ \text{C}$ ) is immiscible with the following hydrocarbons in the range stated:-

- 1) 5-n-butyleicosane ( $\text{C}_{24}\text{H}_{50}$ ) - Liquids immiscible between  $28^\circ \text{C} - 33^\circ \text{C}$ .
- 2) 11-cyclohexylmethylheneicosane ( $\text{C}_{28}\text{H}_{56}$ ) - Liquids immiscible between  $13^\circ \text{C} - 33^\circ \text{C}$ .
- 3) squalene ( $\text{C}_{30}\text{H}_{50}$ ) - Liquids immiscible between  $4^\circ \text{C} - 33^\circ \text{C}$ .
- 4) squalane ( $\text{C}_{30}\text{H}_{62}$ ) - Liquids immiscible between  $23^\circ \text{C} - 34^\circ \text{C}$ .
- 5) 11-n-decyldocosane ( $\text{C}_{32}\text{H}_{66}$ ) - Liquids immiscible between  $11^\circ \text{C} - 33^\circ \text{C}$ .

Freeman and Rowlinson<sup>4</sup> and Baker, Brown, Gee, Rowlinson, Stubley and Yeadon<sup>28</sup>, have also found that lower critical solution phenomena is exhibited by non-polar hydrocarbon polymers in hydrocarbon solvents. For instance, polyisobutene with a molecular weight of  $10^{6.2}$  shows a lower critical solution point at  $25^\circ \text{C}$  with n-pentane, the range of

immiscibility being from  $75^{\circ}$  C to an upper critical end point at  $199^{\circ}$  C.

There are quite a few systems which would probably belong to this class if the less volatile liquid phase did not freeze before the L.C.S.T. is reached. One of the first systems of this kind to be discovered was by Scheffer<sup>16</sup> and his colleagues, namely carbon dioxide + m-chloronitrobenzene. The (p, T, x) surface and the (p, T) and (T, x) projections are shown in Figures 11 (a), (b), (c) and (d). This type of system has a non-variant line R - Q on the (p, T, x) surface which is the quadruple axis. On this axis, the four phases (solid I, liquid I, liquid II and gas) coexist in equilibrium.  $T_2$  is the triple point of component 2. This type of behaviour usually occurs where the melting point of the less volatile component is fairly high. For instance, Freeman and Rowlinson<sup>3</sup> found that the systems:-

Liquid ethane + n-octadecylcyclohexane ( $C_{24}H_{48}$ ).

M. Pt. =  $40^{\circ}$  C. Q. Pt. =  $17^{\circ}$  C.

Liquid ethane + 18-ethylpentatriacontane ( $C_{37}H_{76}$ ).

M. Pt. =  $28^{\circ}$  C. Q. Pt. =  $15^{\circ}$  C.

(M. Pt. = Melting Point : Q. Pt. = Quadruple Point).

show this behaviour, and it can be seen that the melting point of the involatile hydrocarbon is fairly high compared with the previous five that showed L.C.S.T.'s

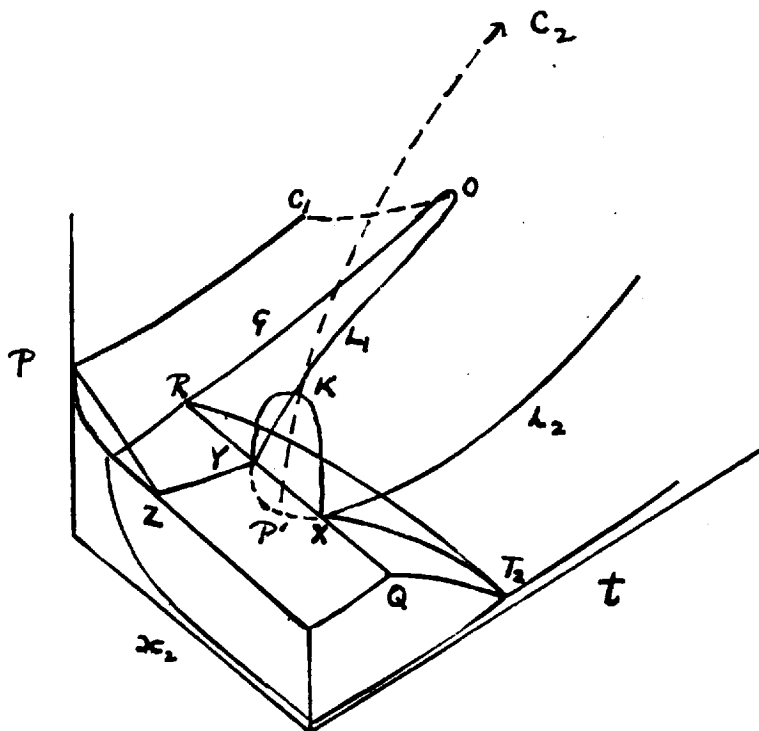


Fig. 11 (a).



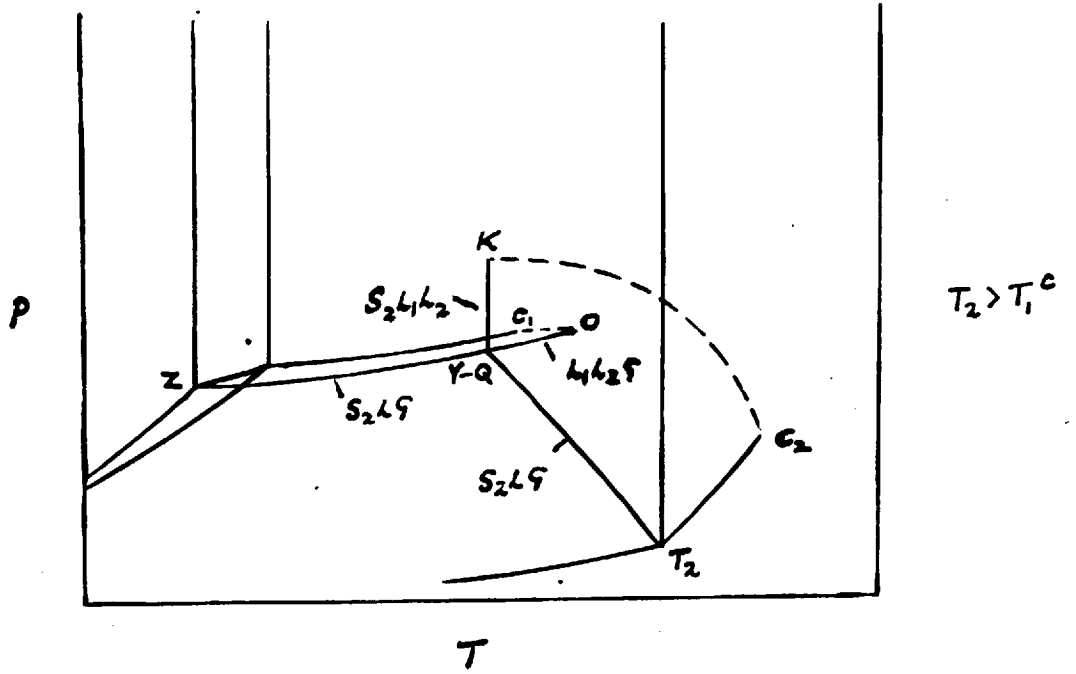


FIG. 11 (b).

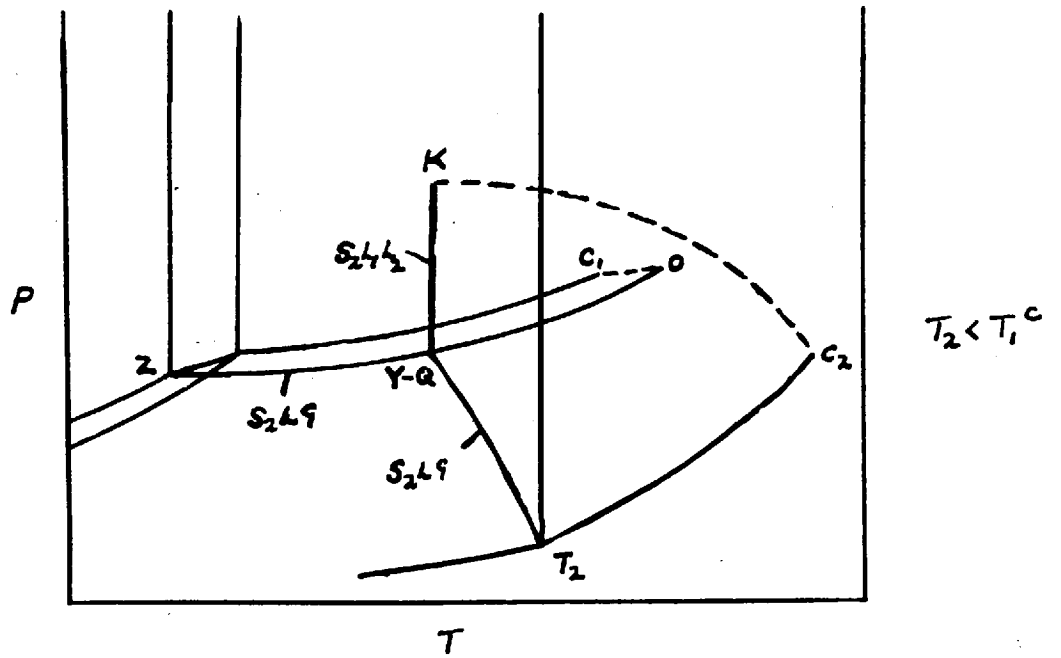


FIG. 11. (c)

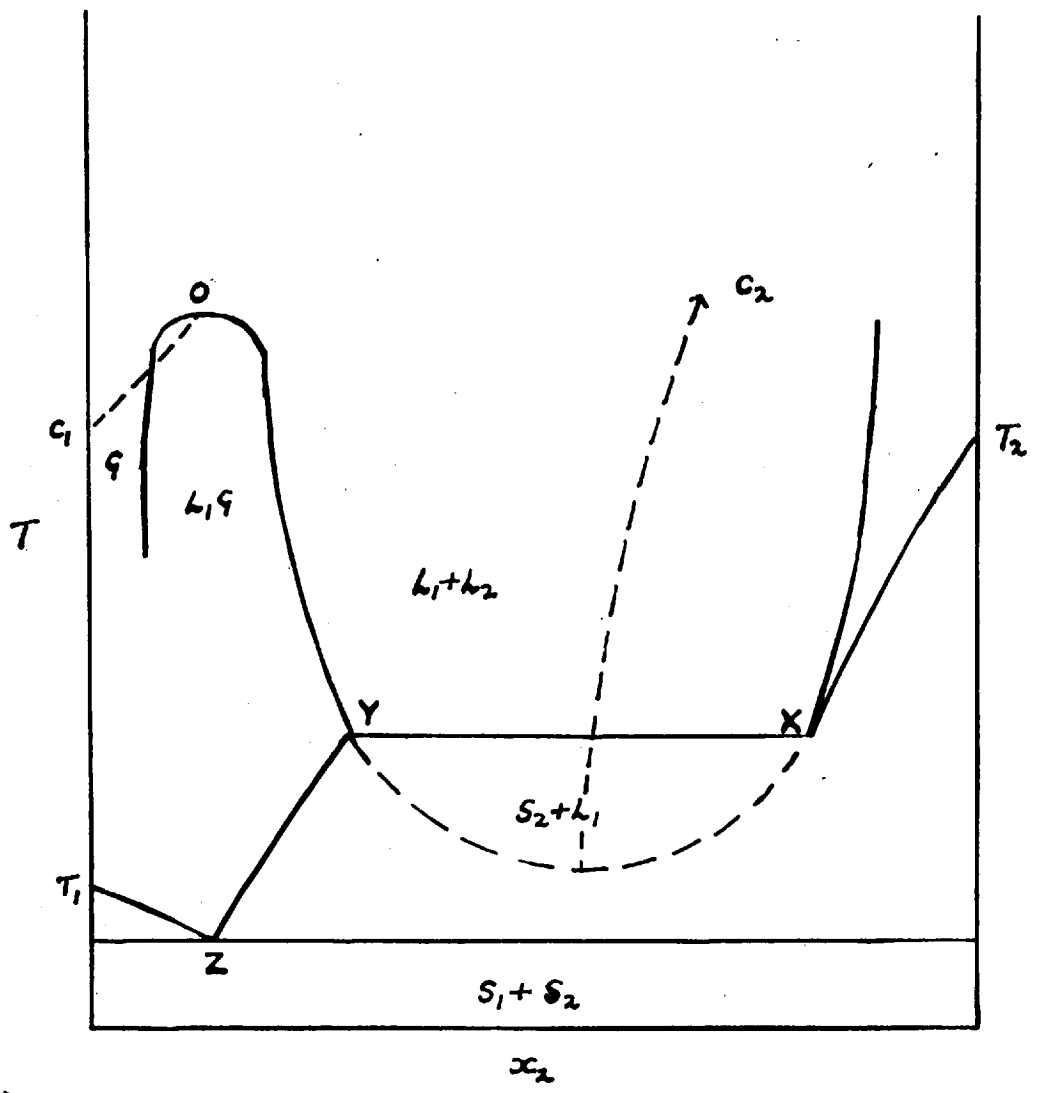


FIG. 11(d).

with liquid ethane, where the highest melting point was  $1^{\circ}$  C.

The two (p, T) projections shown correspond to the cases where the triple point of the pure involatile component is either below or above the gas-liquid critical point of the volatile component. The system ethylene ( $T^c = 9^{\circ}$  C) + naphthalene (M. Pt. =  $80^{\circ}$  C)<sup>19</sup> is an example of the (p, T) projection shown in Fig. 11 (b) where the melting point of the involatile component is above the gas-liquid critical point of the volatile component.

In all these systems, it appears that it must be the approach of the volatile component to its gas-liquid critical point where we get rapid fluctuations in density and other thermodynamic properties that give rise to separation into two liquid phases.

CHAPTER III.EXPERIMENTAL.Materials.

The methane used in all the phase boundary measurements was supplied in a cylinder from the National Coal Board. Analysis of a small sample using the mass-spectrograph of the Department of Chemistry, University of Manchester showed that the chief impurities were  $C_2$  and  $C_3$  hydrocarbons and a little nitrogen. (1.14 moles%  $C_2$  hydrocarbons/nitrogen; 0.29 moles%  $C_3$  hydrocarbons).

The methane was purified by distillation using a slightly modified version of the column designed by Clusius and Riccobini<sup>20</sup>, shown in Fig. 13a. Bulbs A and B were opened to the high vacuum line and evacuated to a pressure of  $10^{-5}$  mm. of mercury. Nitrogen was now admitted to bulb B to a pressure of one atmosphere. The Dewar vessel was then filled with liquid oxygen and methane condensed into bulb A direct from the cylinder until the bulb was three-quarters full. (This was about 100 mls. of impure methane). Bulb B was re-evacuated to  $10^{-5}$  mm. of mercury and the methane refluxed under a 15 watt heat supply. At periodic intervals during the refluxing of the methane, bulb A was opened to the vacuum pump in order to remove the more volatile materials. After the first third of the impure sample had

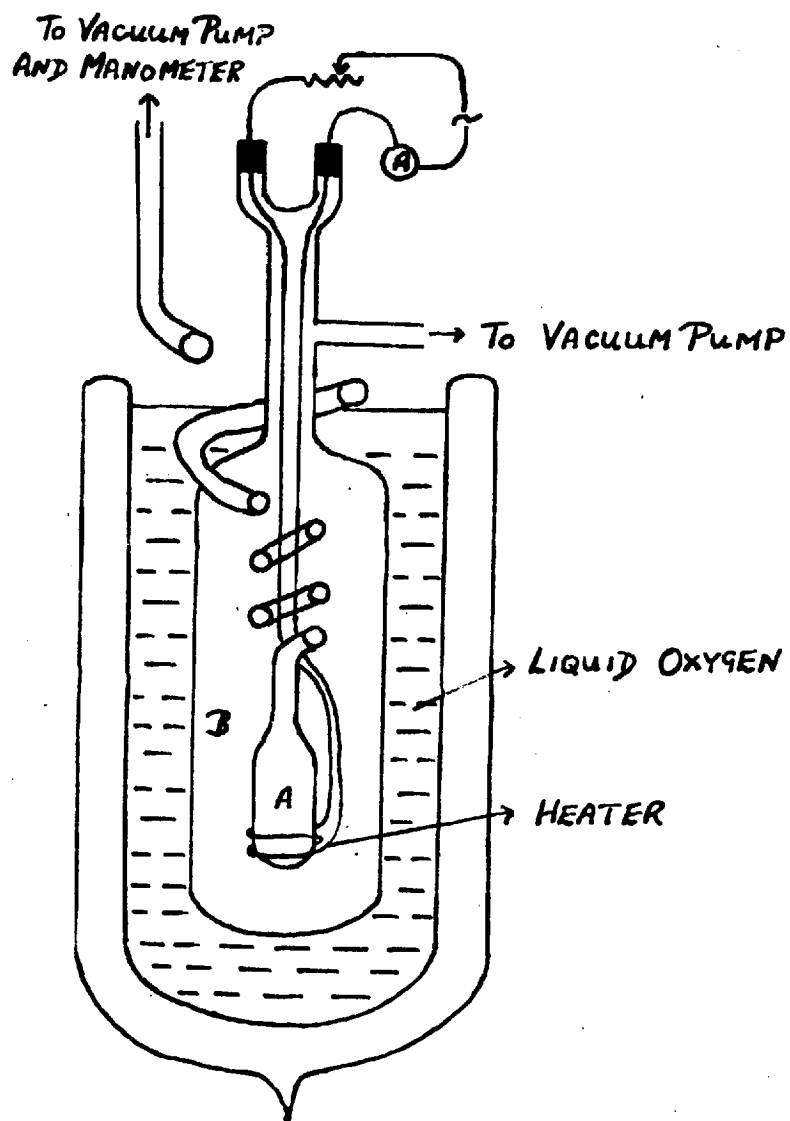


FIG. 13 (a).

been taken off, the next third was condensed into a cooling finger surrounded by liquid nitrogen and then allowed to evaporate into pyrex storage bulbs which had previously been evacuated to  $10^{-5}$  mm. of mercury pressure. 30 litres ( $\sim 1\frac{1}{4}$  moles) of purified methane at one atmosphere pressure were collected. The residue in bulb A was allowed to evaporate into the atmosphere. The gas-liquid critical point of the purified sample was determined, and the value obtained ( $190.3^{\circ}$  K) agreed with the value determined experimentally for a sample obtained from the National Chemical Laboratory, which had a quoted purity of 99.98 moles%.

The following hydrocarbons (Table 1) were supplied by the National Chemical Laboratory and were used without any further purification.

Table 1.

Hydrocarbon	Purity Moles %.	Hydrocarbon	Purity Moles %.
C <sub>4</sub> 1, 3-butadiene	99.91	C <sub>6</sub> 2, 2-dimethylbutane	99.99
		2, 3-dimethylbutane	99.74
C <sub>5</sub> n-pentane	99.98	methycyclopentane	99.99
isopentane	100.00	hex-1-ene	99.99
neopentane	99.98		
pent-1-ene	100.00	C <sub>7</sub> n-heptane	99.94
isoprene	99.99	2, 4-dimethylpen- tane	99.70
		toluene	99.96
C <sub>6</sub> n-hexane	99.81		
2-methylpen- tane	99.82	C <sub>8</sub> 2, 3, 4-trimeth- ylpentane	99.70

1, 3-butadiene and neopentane were supplied at atmospheric pressure in 500 ml. bulbs fitted with break-seals. The other fourteen hydrocarbons were supplied as 5 ml. liquid samples fitted with breakseals and sealed off under vacuo.

The 2-methylhexane was supplied in a 5 ml. glass breakseal by the American Petroleum Institute. Its purity was quoted at 99.88% and it was used as obtained.

The 3-methylpentane, 2, 2-dimethylpentane and 2, 2, 4-trimethylpentane were supplied by the British Petroleum Company in glass ampoules sealed in vacuo. The purity of these samples was quoted as 99% or better. They

were cooled under a Dewar vessel containing a mixture of methanol and solid carbon dioxide and evacuated for a short while and then were used without any further purification.

Cyclopentene, pent-1-yne and hex-1-yne were supplied as 15 ml. samples in sealed bottles by Messrs. L. Light and Co. Ltd. The cyclopentene sample had a quoted purity of 99% or better and was treated in a similar way to the samples obtained from the British Petroleum Company. The two acetylenes were distilled in air through a  $1\frac{1}{2}$  ft. silvered fractionating column packed with glass beads and the main middle fraction of about 8 ml. collected. The normal boiling points of these samples were:-

pent-1-yne	40.2° C	(+0.18° C)
hex-1-yne	71.4° C	(71.33° C)

The figures in brackets represent the values quoted in the American Petroleum Institute Tables<sup>21</sup> for the normal boiling points of these compounds. The fractions collected were treated in the same way as the samples from the British Petroleum Company.

The sample of cyclohexene had an unknown source. Its boiling point was quoted as 83° C/765 mm. (82.98/760 mm.<sup>21</sup>) and on analysing a sample by means of a gas chromatogram, no impurities were observed. The



sample was cooled and evacuated under a methanol/solid carbon dioxide mixture and used without any further purification.

Preparation of Experimental Sealed Tubes and the High Vacuum Technique.

The binary mixtures were prepared in sealed tubes under high vacuum conditions. A length of heavy walled capillary tubing (internal diameter 2 mm., external diameter 8 mm.) was ~~th~~<sup>o</sup>roughly cleaned in permanganic acid cleaning mixture and washed with distilled water. It was sealed symmetrically at one end, a glass loop being incorporated into the seal in order to facilitate the transfer of a tube to and from the cryostat. The open end was sealed to a B 7 cone. The tube was then constricted so that the internal measurements of the resulting sealed tube would be approximately 2 x 120 mm. Finally it was annealed at a temperature of 550° C. This process was necessary to remove most of the thermal strain from the glass, since in studying mixtures near the gas-liquid critical point of methane, pressures of the order of 40 atmospheres are experienced and so the glass will be subjected to large mechanical stress.

The next part of the practical work involved the preparation of a mixture of known composition. Though the volume occupied by the liquid mixture was not

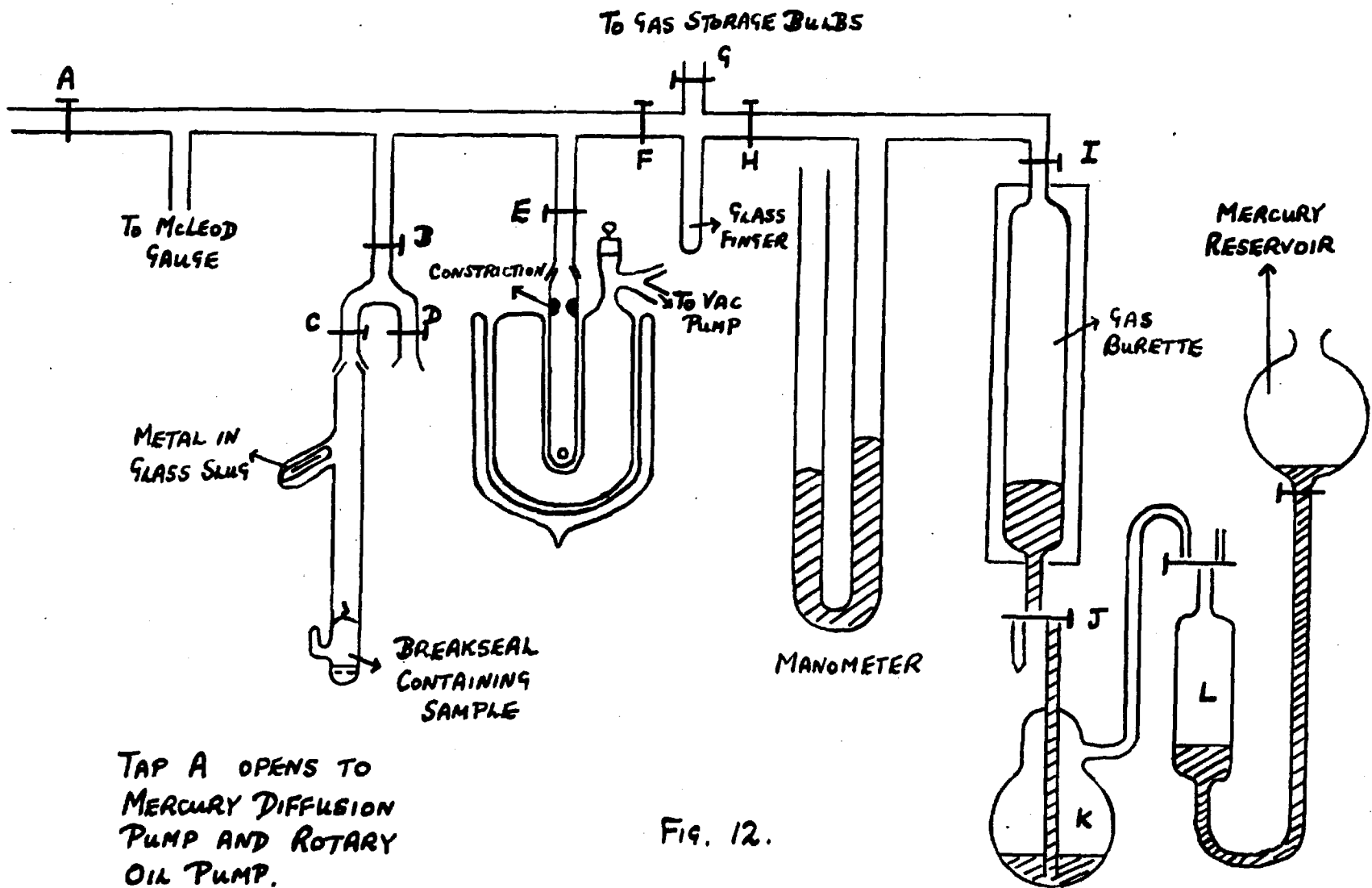
critical, the tubes were arranged to be approximately three-quarters full at a temperature within ten degrees of the gas-liquid critical point of pure methane. This procedure was adopted since although it was impossible to remove the vapour phase, it was essential to keep it to a practical minimum so that there were no serious effects on the calculated values of the weight fractions. When a tube was filled with a liquid mixture it was necessary to ensure that:-

a) There was sufficient material present so that on warming the mixture in the cryostat to  $200^{\circ}$  K it did not all evaporate into the gaseous phase.

b) There was not too much material present so that when heated to  $200^{\circ}$  K the liquid mixture did not expand and completely fill the tube.

The gases (methane, neopentane and 1, 3-butadiene) were measured out in a 100 ml. gas burette (Fig. 12.). The burette was maintained at  $25^{\circ}$  C by a water jacket, through which water was constantly circulated by means of a Stewart-Turner centrifugal pump from a thermostat controlled by a mercury-toluene regulator and an electronic relay. The gas burette was calibrated before being joined to the vacuum line. One of the connections of the bottom tap (tap J in Fig. 12.) was drawn out into a fine jet and the burette evacuated with the jet under clean triple-distilled mercury. After the mercury had

completely filled the gas-burette, including the upper tap I, the lower tap was closed and the burette thermostatted at 25° C, by means of the circulated pumped water. The upper tap was then closed and all traces of mercury removed from above it. The burette was clamped in an accurate vertical orientation using a plumb line. The upper tap was opened and mercury run out through the jet into a weighed container until the bottom of the mercury meniscus corresponded with a convenient mark on the scale of the gas burette. The container was reweighed and the volume above the meniscus calculated from the density of mercury at 25° C. Calibrations were repeated for a given volume until a reproducibility of 0.01 ml. or better was obtained. The calibrations are given in Table 2. They include the key of the upper tap and were made with atmospheric pressure above the surface of the mercury. The gas burette was now joined to the vacuum line in the accurate vertical orientation in which the calibrations had been made.



TAP A OPENS TO  
MERCURY DIFFUSION  
PUMP AND ROTARY  
OIL PUMP.

FIG. 12.

Table 2.

Mark	Volume (mls.)
10	10.551
20	20.534
30	30.584
40	40.599
50	50.610
60	60.635
70	70.660
80	80.741
90	90.784
100	100.803

Twenty-four mixtures of hydrocarbons with liquid methane were investigated. In twenty-two cases the hydrocarbons were liquid at room temperature. Samples of these liquids were accurately weighed out in small glass containers of approximately 0.5 ml. capacity fitted with breakseal tips and a B 7 cone. The glass containers were cleaned with permanganic acid cleaning mixture, washed with distilled water and thoroughly dried in an oven. They were then weighed accurately in air on a micro-analytical balance reading to  $1 \times 10^{-4}$  gm. The temperature of the air was noted. They were now filled with distilled water of measured temperature to a convenient mark for sealing off, and the container reweighed. They were then redried in the oven and attached in turn to the vacuum line by

means of the B 7 cone. The pure hydrocarbons were now connected to the vacuum line. In the cases <sup>R</sup>where they were obtained as samples fitted with breakseal tips, the sample was connected to a special glass fitting designed with a small side pocket containing a metal-in-glass slug. (Fig. 12.). This assembly was joined to the vacuum line via a B 7 socket below tap C. The smaller container which was to contain the liquid sample was joined below tap D. The vacuum line was evacuated with taps B, C and D open. Tap B was then closed and the metal-in-glass slug raised in its side arm using a magnet, and allowed to fall on to the fine glass tip of the large pure hydrocarbon sample. The small container was now filled with a suitable quantity of liquid by condensation in vacuo under liquid nitrogen. Taps C and D were closed again and the small container sealed off under vacuum at the afore-mentioned mark. The B 7 cone end of this sample was detached from the vacuum line, cleaned completely free of high-vacuum silicone grease by using trichloroethane and dried in the oven. The container and B 7 cone were reweighed, and the weight of the sample calculated from the difference in weight between the final and initial weighings, allowance being made for the buoyancy factor by calculating the weight of air present from the density of water and air at their

respective temperatures. This procedure was repeated with varying quantities of liquid in the glass containers. By this method, the mass of any sample of hydrocarbon could be estimated to  $2 \times 10^{-4}$  gm. or better.

Quantities of neopentane and 1, 3-butadiene were measured using the gas burette. It was very difficult to condense completely either of these hydrocarbons into capillary tubing since they both had very high melting points and extremely short normal liquid ranges. The procedure adopted for these two gaseous hydrocarbons was to measure the pressure, volume and temperature of the gases before and after condensation into the tube. The level of the gas burette was set to a calibrated mark under atmospheric pressure. The line was then completely evacuated, together with the section below tap C where the gaseous hydrocarbon, supplied in the form of a one litre bulb fitted with a breakseal, was attached. Tap A was turned off and the breakseal broken, so that the burette was filled with gas. With the gas burette thermostatted at  $25^{\circ}\text{C}$ , the difference in height between the two manometer surfaces was read to 0.05 mm. using a cathetometer. As one surface of the manometer was open to atmospheric pressure, it was necessary to measure atmospheric pressure to an accuracy of 0.05 mm. using a Fortin

Barometer. A correction was applied to allow for the small difference in temperature between the two manometers. An experimental tube was not<sup>w</sup> connected to the line by a B 7 cone and socket junction below tap E, and the line completely re-evacuated, tap I having been closed. Tap A was closed again and tap I opened. The hydrocarbon was condensed into the tube under liquid nitrogen. When sufficient hydrocarbon had been condensed into the tube tap E was closed and the mercury level in the gas burette raised level with the top of the bore of tap I by means of a Toepfler pump. (Parts K and L in Fig. 12.). The pressure of the residual gaseous hydrocarbon was measured using the cathetometer and Fortin Barometer and the temperature of the vacuum line read using a thermometer placed in mercury next to the manometer. The residual volume, namely that enclosed by taps A, B, E, G and I was measured by expanding quantities of methane, whose pressure, volume and temperature had been previously measured, into this volume and then re-reading the pressure and temperature of the line.

From the virial expansion for a gas:-

$$\frac{pV_m}{RT} = 1 + \frac{Bp}{RT}$$

$$\text{or } pV_m = RT + Bp$$

Now  $V_m (= \frac{V}{n})$  is the molar volume, if the quantities



R and B are in molar units

$$n = \frac{pV}{RT+Bp}$$

From this expression, n - the number of moles of gas present can easily be calculated from experimental data if the values of B are known at the temperature concerned.

In the case of methane and neopentane, the values of the 2nd Virial Coefficient can be determined.

For methane, the values of B of Michels and Nederbragt<sup>22</sup> were plotted against  $T^{-2}$  and values at temperatures between 15° C and 25° C determined by interpolating from the graph. The value of -43.4 cc. mole<sup>-1</sup> was used for the 2nd Virial Coefficient of methane at 25° C.

A similar procedure was employed to obtain the 2nd Virial Coefficient of neopentane between 15° C and 25° C from the data of Hamann and Lambert<sup>23</sup>. The value of -873 cc. mole<sup>-1</sup> was used for the 2nd Virial Coefficient of neopentane at 25° C.

No accurate values for the 2nd Virial Coefficient of 1, 3-butadiene have been recorded in the literature. The number of moles of gas present in this case was estimated using the equation of Berthelot:-

$$\frac{pV}{nRT} = 1 + \frac{9}{128} \frac{pT^c}{p^c T} \left[ 1 - \frac{6(T^c)^2}{T^2} \right]$$

using the values  $p^c = 42.7$  atms,  $T^c = 425^\circ$  K from the

American Petroleum Institute Tables<sup>21</sup>. The advantages of this equation over the perfect gas equation, and its approach to the virial expansion have been discussed by Lambert, Roberts, Rowlinson and Wilkinson<sup>24</sup>.

The compositions obtained from these equations and recorded in the tables in the next chapter are probably accurate to 0.2% or better.

Methane can be completely condensed into a tube using the 'pump-down' trap, shown schematically in Fig. 12. The inner glass container and the Dewar vessel were completely filled with liquid nitrogen. The inner container was connected to a rotary oil vacuum pump. The pump was now started and after carefully controlling the initial boiling off of the nitrogen, the leak to air was sealed by a metal clip and the stopper inserted in the neck. When about two-thirds of the nitrogen had been pumped off, the stopper was removed and the inner container refilled to its original level. By repeating this process several times, and allowing the liquid nitrogen to be subjected to continuous pumping, the nitrogen can be solidified at its triple point of  $63^{\circ}$  K.

To prepare a tube, the heavier hydrocarbon was first completely distilled into the tube under liquid nitrogen from either the small glass breakseal containers or by the method previously described for gaseous

hydrocarbons. The quantity of methane required was measured out in the gas burette at 25° C and its pressure recorded to 0.05 mm. using the cathetometer and Fortin Barometer as previously described. It was then expanded into the rest of the line enclosed by the tube, manometer and breakseal container, the position of high vacuum having been marked on the manometer. The 'pump-down' trap was now slowly raised so that the tube became submerged in the finger. The rate of condensation of methane was noted on the manometer, and the level of the pump-down trap raised when condensation ceased. When all the methane had been condensed, as indicated by the return of the mercury level in the manometer to the mark indicating high vacuum, the level of the mercury in the gas burette was raised to the top of tap 1. The pump-down trap was finally raised to a point just below the constriction as shown in Fig. 12 and the tube sealed off carefully in order to introduce the minimum of strain. The tube was stored under liquid nitrogen until ready for use.

#### Measurement of Phase Behaviour of Liquids.

A cryostat (Fig. 13b) was designed to operate over a temperature range extending from 113° K to 200° K. It consisted of a brass disc,  $\frac{1}{16}$  " thick and  $2\frac{3}{4}$  " in diameter, supported just off centre by a 1 ft. length

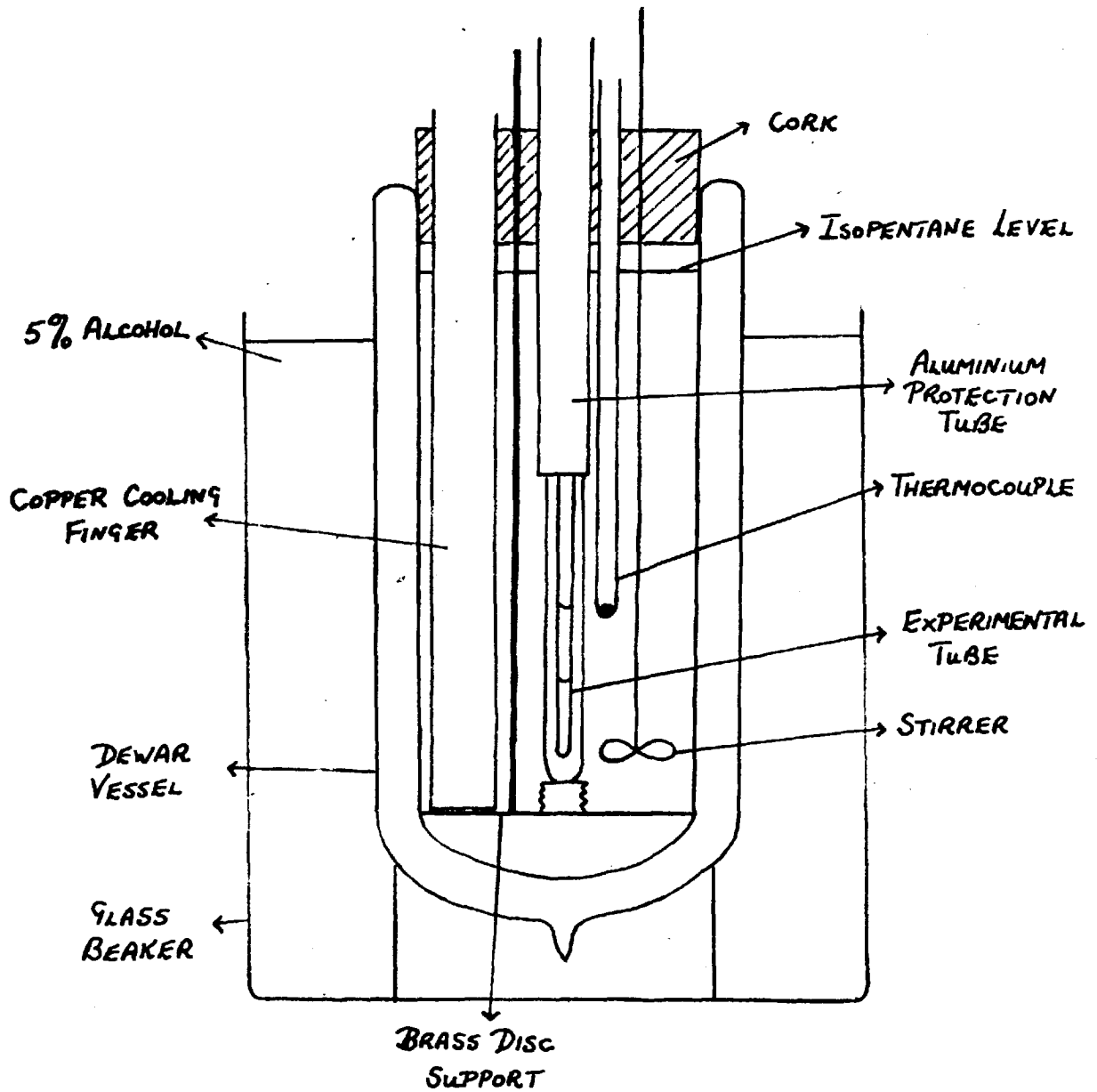


FIG. 13 (b).

of  $\frac{1}{4}$  " diameter brass rod. The disc rested on the base of a Dewar vessel of 1 litre capacity and was supported at the top through a large cork which fitted into the neck of the Dewar vessel.

The experimental tubes were located in an aluminium tube of outside diameter  $\frac{11}{16}$  ". This tube passed through the upper cork and was positioned so that it could be screwed down to a short screw knob soldered on to the brass disc. The aluminium tube was placed near to the front of the Dewar vessel so that when it was raised, the experimental tube could be easily seen through a 1 " clear strip in the silver Dewar vessel. The whole Dewar vessel was illuminated from the rear by a 40 watt tubular bulb.

The Dewar vessel was filled with isopentane which had a boiling range of  $27^{\circ}$  C to  $30^{\circ}$  C. It was then placed on a cork ring support in a 10 litre beaker which was filled with a 5% alcohol solution. The purpose of surrounding the Dewar vessel with aqueous alcohol was to prevent the outside surface of the vessel frosting up and so hindering observation of the tubes.

The cryostat could be cooled to any temperature in the range  $110^{\circ}$  K to  $200^{\circ}$  K by filling the copper cooling finger with liquid nitrogen. The cooling finger rested on the brass disc and was supported in the cork. During

the cooling of the cryostat, the level of the isopentane was maintained just below the base of the cork.

Temperature gradients within the cryostat were reduced to a minimum by rapid circulation of the cold isopentane using a stirrer driven by an electric motor fitted above the cryostat. The stirrer consisted of one set of four paddle blades and dipped into the Dewar vessel to within  $\frac{1}{2}$ " of the brass disc.

The temperature was measured by a thermocouple placed in a glass tube situated alongside the experimental tube. The proximity of the thermocouple to an experimental tube together with the rapid stirring ensured that the temperature recorded and the temperature of the experimental tube were very close. The thermocouple consisted of four copper-constantan junctions connected in series. The reference junction was surrounded by a Dewar vessel containing finely crushed ice, prepared by freezing distilled water. The purity of the ice prepared in this manner was such as to ensure that the melting point was reproducible to  $0.01^{\circ}$  C. The E.M.F. was measured using a Tinsley Vernier Potentiometer and a tangent mirror galvanometer. The potentiometer was capable of measuring to 1 microvolt and it was observed that a change of 1 microvolt in the E.M.F. produced a deflection of 3mm. on a scale

placed about a metre away from the galvanometer. However, since the temperature of phase separation could only be measured to the nearest  $0.1^{\circ}$  K, it was only necessary to be able to measure the E.M.F. to an accuracy of 10 microvolts.

The thermocouple was calibrated against the triple points of five pure hydrocarbons, namely n-butane, n-pentane, n-heptane, toluene and trans but-2-ene, all supplied by the National Chemical Laboratory and against the triple point of pure carbon dioxide, prepared from commercial solid carbon dioxide. The latter was purified by drying over phosphorus pentoxide, followed by sublimation in vacuo. The samples were all sealed using standard high vacuum technique in thin-walled glass tubes of similar external dimensions to the experimental tubes. After being frozen in liquid nitrogen, these tubes were quickly transferred to the cryostat, which had previously been cooled to a temperature below the triple point of the sample. The tube was observed at intervals and when the film of solid coating the walls of the tube collapsed, with the formation of a liquid meniscus on top of the main body of the solid, the E.M.F. between the junctions was noted.

The triple point temperature of the ~~absolutely~~ pure hydrocarbons were taken as quoted by the American Petroleum Institute tables<sup>21</sup>. The purity of the actual

hydrocarbons used are quoted in Table 3, and a calculation of the depression of the triple point as a result of this quoted molar purity was less than  $0.02^{\circ}$  K in all five cases.

Ambrose<sup>25</sup> has determined the triple point of carbon dioxide prepared by the method just described above, and has shown<sup>ow</sup> that it is reproducible to  $0.002^{\circ}$  K.

The standard triple point temperatures and the corresponding E.M.F.'s observed are listed in Table 3 below, together with the purity of the five hydrocarbons in moles %.

Table 3.

Triple Point Substance	Purity	Standard Temp. $^{\circ}$ C.	E.M.F. between junctions in millivolts
Carbon dioxide		-56.603	$8.25_5 \pm 0.01$
n-heptane	99.94	-90.59	$12.61 \pm 0.01$
toluene	99.96	-94.99	$13.12_5 \pm 0.01$
trans but-2-ene	99.98	-105.55	$14.36_5 \pm 0.01$
n-pentane	99.98	-129.67	$16.95 \pm 0.01$
n-butane	99.97	-138.33	$17.77 \pm 0.01$

The difference in temperature between the measuring and hot junctions  $\Delta T$ , (which is also numerically equal to the temperature of the measuring junction in  $^{\circ}$ C) and



the corresponding E.M.F.,  $E$  measured on the potentiometer was fitted to the following polynomial:-

$$\Delta T = 6.6636E - 1.096 \times 10^{-2} E^2 + 4.164 \times 10^{-3} E^3$$

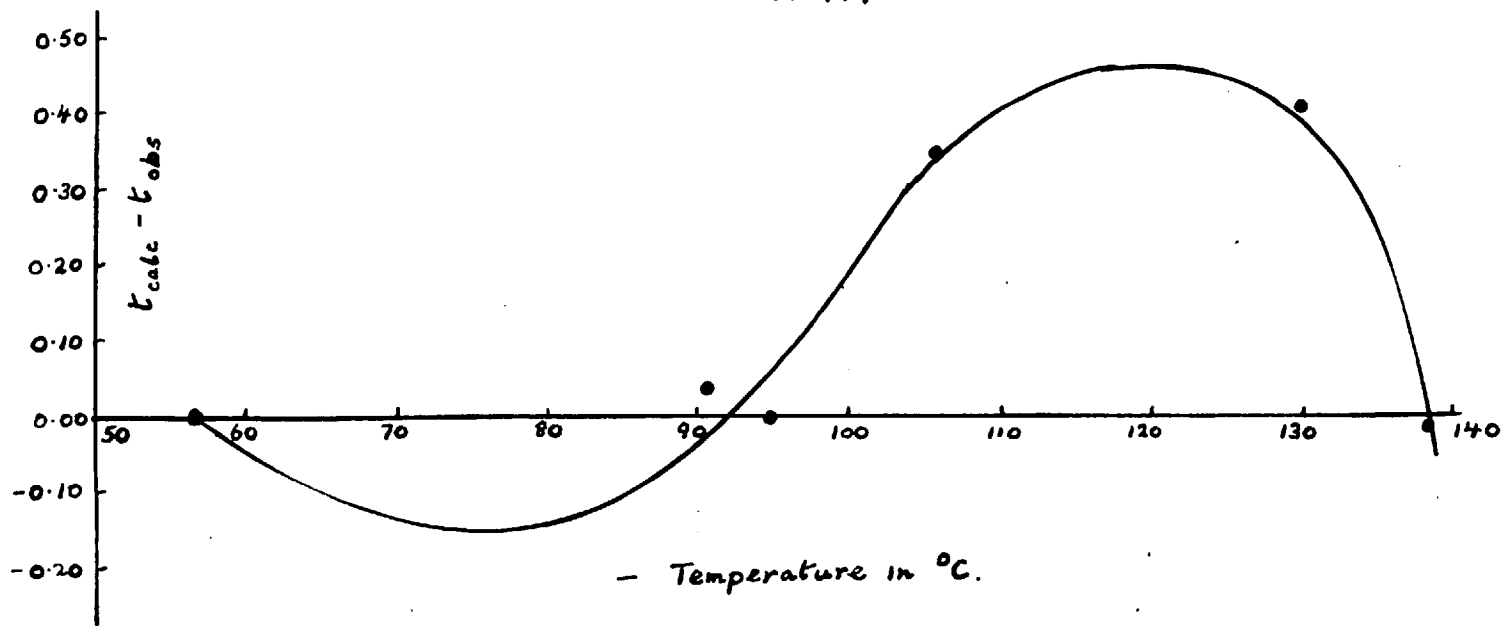
where  $E$  is in millivolts,  $\Delta T$  in  $^{\circ}\text{C}$ .

Using the above equation and the observed experimental data, a correction curve was drawn over the whole range of temperature required i.e.  $113^{\circ}\text{K}$  to  $200^{\circ}\text{K}$ . This correction curve is shown in Fig. 14.

The temperature of the measuring junction in  $^{\circ}\text{C}$  was available from the measured E.M.F. using the above polynomial and the correction curve. It was converted into  $^{\circ}\text{K}$  by taking a temperature of  $-273.15^{\circ}\text{C}$  as absolute zero. Within the range  $113^{\circ}\text{K}$  to  $200^{\circ}\text{K}$ , this temperature scale probably coincided with the absolute scale to  $\pm 0.1^{\circ}\text{K}$ .

The main source of heat leak into the cryostat was through the air above the surface of the isopentane and through the attachments dipping into the cryostat. The natural rate of warming of the cryostat was  $0.7$  deg.  $\text{min.}^{-1}$  at  $130^{\circ}\text{K}$  and  $0.4$  deg.  $\text{min.}^{-1}$  at  $220^{\circ}\text{K}$ . Detailed observation of an experimental tube, followed by temperature measurement could easily be made within  $10$  seconds, that is at temperature intervals of about  $0.1^{\circ}\text{K}$  at  $130^{\circ}\text{K}$  and  $0.07^{\circ}\text{K}$  at  $220^{\circ}\text{C}$ . Therefore, since the cryostat reproduced temperatures of  $0.1^{\circ}\text{K}$  quite adequately, no further attempts were made to

Fig. 14.



decrease the rate of warming.

When the tubes were being filled on the vacuum line, moisture from the atmosphere readily condensed on the outer walls of the tubes. This was removed by inserting the tubes quickly in acetone and then returning them back to the liquid nitrogen. This process was repeated for about four more times for each tube, after which a tube was virtually cleaned of moisture. The frozen acetone layer was removed by rapidly dipping the tubes in isopentane for a couple of times. The tubes were then stored until ready for measuring in a large Dewar vessel, which was kept continuously topped up with liquid nitrogen.

In order to take an experimental measurement, the cryostat was first cooled to  $200^{\circ}$  K. An experimental tube was then inserted by means of its wire holder down the aluminium tube, which had previously been screwed down firmly. The tube was then left for a few minutes to acquire temperature equilibrium. The reason for adopting this procedure for the tubes was to test their ability to withstand the pressures encountered at this temperature. When the tube had reached equilibrium, the cryostat was cooled for a further four or five degrees and the aluminium tube raised so that the tube could be observed. The procedure then adopted depended on the following three types of behaviour shown:-

a) If only one liquid phase was observed, the tube was warmed for a further few degrees until the temperature reached  $200^{\circ}$  K. If no separation of the liquid phase occurred, it was concluded that the contents were miscible in all proportions up to  $200^{\circ}$  K.

b) If two liquid phases were observed, the cryostat was cooled steadily. In the cases where the two liquid phases disappeared into one liquid phase, the temperature at which this occurred was noted roughly. The cryostat was then cooled to about ten degrees below this temperature and the tube quickly removed, inverted, and then replaced in the cryostat. This process was carried out in an attempt to ensure that there was a homogeneous, single liquid phase present in the tube. The cryostat was then allowed to warm at its natural rate until separation of the single liquid phase into two liquid phases was observed. This process was observed fairly easily as the liquid showed a brown turbidity around the region where separation was occurring. The E.M.F. at which the onset of this turbidity arose was noted. This experimental process was repeated until a reproducibility in the E.M.F. of 10 microvolts was recorded.

In the case where separation into two liquid phases occurred on cooling, a similar procedure was adopted except that the tube was removed and inverted

at about ten degrees above the phase separation temperature, and then the cryostat cooled slowly until the onset of turbidity was observed when the E.M.F. was noted. This system - methane+hex-1-ene was actually measured in the cryostat described in part II of this thesis for measuring the volumes of methane+hydrocarbon mixtures.

c) In the third case, it was found that on cooling the two liquid phases, the lower or less volatile phase solidified. Here, the E.M.F. at which the solid phase melted to give two liquid phases was observed, and the process repeated until the E.M.F. for this solid-liquid transition was obtained to a reproducibility of 10 microvolts.

CHAPTER IV.Results and Discussion.

Twenty four hydrocarbon mixtures with liquid methane were studied from the melting point of isopentane ( $113^{\circ}$  K) to a temperature of  $200^{\circ}$  K, which is ten degrees above the gas-liquid critical point of pure methane ( $190.3^{\circ}$  K). The type of phase behaviour exhibited by these systems fell into the following three classes:-

(a) Complete Miscibility.

In this case, the mixtures showed only two phases namely solid + vapour or liquid + vapour over the complete temperature range studied.

(b) Limited Immiscibility.

The term 'limited immiscibility' is used to denote the case where the mixture is completely miscible only from its solid-liquid boundary up to a temperature where it separates into two liquid phases.

(c) Absolute Immiscibility.

Here, we have a system where there is no temperature between the solid-liquid boundary and the gas-liquid critical curve of the mixture where the pair of liquids studied are completely

miscible.

It should be pointed out here that the terms used to denote the type of phase behaviour exhibited by these mixtures are by no means established, but in the case of (b) and (c), the words 'limited' and 'absolute' are chosen to describe the range of immiscibility since they correspond to a similar use of these terms in studying the phenomena of azeotropy.

Table 4 (Parts A-Y) shows the compositions, type of phase behaviour observed, temperature of phase separation and temperature of the quadruple point where applicable. In the cases where complete miscibility was observed, three tubes having weight fractions of the heavier hydrocarbon ( $w_2$ ) between 0.0 and 0.8 were observed. Where 'limited immiscibility' was observed, five or six tubes having weight fractions ( $w_2$ ) between 0.0 and 0.8 of the heavier hydrocarbon were prepared. Finally, for 'absolute immiscibility', in general three tubes having a weight fraction ( $w_2$ ) between 0.0 and 0.8 were taken and the temperature of the quadruple point noted. The one exception was the system methane + n-heptane which has been studied simultaneously by Kohn.<sup>5</sup> The phase diagram for this system was observed over the whole of the composition range.

Table 4.

A) Methane + 1, 3-butadiene (4a)

Weight fraction ( $w_2$ )	Type of Phase Behaviour
0.227	Complete Miscibility
0.432	
0.594	

B) Methane + n-pentane (5a)

Weight fraction ( $w_2$ )	Type of Phase Behaviour
0.204	Complete Miscibility
0.412	
0.624	

C) Methane + isopentane (5b)

Weight fraction ( $w_2$ )	Type of Phase Behaviour
0.204	Complete Miscibility
0.504	
0.660	

D) Methane + neopentane (5c)

Weight fraction ( $w_2$ )	Type of Phase Behaviour
0.259	Complete Miscibility
0.418	
0.706	



E) Methane + pent-1-ene (5d)

Weight fraction ( $w_2$ )	Type of Phase Behaviour
0.279	Complete Miscibility
0.291	
0.435	
0.578	
0.668	

F) Methane + isoprene (5e)

Weight fraction ( $w_2$ )	Type of Phase Behaviour	Temperature of Quadruple Point ( $^{\circ}\text{K}$ )
0.162	Absolute Immiscibility	119.8
0.439		119.8
0.523		119.8

G) Methane + cyclopentene (5f)

Weight fraction ( $w_2$ )	Type of Phase Behaviour	Temperature of Quadruple Point ( $^{\circ}\text{K}$ )
0.257	Absolute Immiscibility	126.9
0.527		126.9
0.613		126.9

H) Methane + pent-1-yne (5g)

Weight fraction ( $w_2$ )	Type of Phase Behaviour	Temperature of Quadruple Point ( $^{\circ}\text{K}$ )
0.154	Absolute Immiscibility	159.9
0.309		159.8
0.517		159.7

J) Methane + n-hexane (6a)

Weight fraction ( $w_2$ )	Type of Phase Behaviour	Temperature of Phase Separation ( $^{\circ}\text{K}$ )
0.141	Limited Immiscibility	183.25
0.204		182.83
0.273		182.56
0.354		182.67
0.435		183.02
0.538		183.50
0.624		184.15
0.723		185.05

K) Methane + 2-methylpentane (6b)

Weight fraction ( $w_2$ )	Type of Phase Behaviour	Temperature of Phase Separation ( $^{\circ}\text{K}$ )
0.150	Limited Immiscibility	194.87
0.238		194.71
0.355		194.71
0.421		194.79
0.517		194.79
0.620		194.87

## L) Methane + 3-methylpentane (6c)

Weight fraction ( $w_2$ )	Type of Phase Behaviour	Temperature of Phase Separation ( $^{\circ}\text{K}$ )
0.135	Limited Immiscibility	189.91
0.230		189.10
0.342		188.54
0.424		188.62
0.528		188.78
0.624		188.78

## M) Methane + 2, 2-dimethylbutane (6d)

Weight fraction ( $w_2$ )	Type of Phase Behaviour
0.219	Complete Miscibility
0.440	
0.518	

## N) Methane + 2, 3-dimethylbutane (6e)

Weight fraction ( $w_2$ )	Type of Phase Behaviour	Temperature of Phase Separation ( $^{\circ}\text{K}$ )
0.287	Limited Immiscibility	195.5
0.419		195.5
0.501		195.5

## O) Methane + methyl cyclopentane (6f)

Weight fraction ( $w_2$ )	Type of Phase Behaviour	Temperature of Quadruple Point ( $^{\circ}\text{K}$ )
0.219	Absolute Immiscibility	122.6 $^{\circ}$
0.440		122.6 $^{\circ}$
0.518		122.5 $^{\circ}$

## P) Methane + hex-1-ene (6g)

Weight fraction ( $w_2$ )	Type of Phase Behaviour	Temperature of phase separation ( $^{\circ}\text{K}$ )
0.267	Limited Immiscibility (U.C.S.T.)	133.40
0.420		133.81
0.547		133.71
0.741		132.75
0.142	Limited Immiscibility (L.C.S.T.)	180.53
0.233		179.95
0.315		179.62
0.408		179.77
0.511		179.95
0.598		180.27

## Q) Methane + cyclohexene (6h)

Weight fraction ( $w_2$ )	Type of Phase Behaviour	Temperature of Quadruple Point ( $^{\circ}\text{K}$ )
0.231	Absolute Immiscibility	153.8
0.418		153.6
0.616		153.7

## R) Methane + hex-1-yne (6i)

Weight fraction ( $w_2$ )	Type of Phase Behaviour	Temperature of Quadruple Point ( $^{\circ}\text{K}$ )
0.262	Absolute Immiscibility	134.7
0.328		134.8
0.621		134.8

## S) Methane + n-heptane (7a)

Weight fraction ( $w_2$ )	Type of Phase Behaviour	Temperature of solid-liquid Equilibrium ( $^{\circ}\text{K}$ )
0.000	Absolute Immiscibility	90.7
0.068		169.4
0.161		169.1
0.211		169.7
0.284		169.8
0.359		169.5
0.423		169.5
0.535		169.7
0.628		169.8
0.722		169.7
0.840		169.8
0.903		173.0
1.000		182.6

## T) Methane + 2-methylhexane (7b)

Weight fraction ( $w_2$ )	Type of Phase Behaviour	Temperature of Quadruple Point ( $^{\circ}\text{K}$ )
0.233	Absolute Immiscibility	139.7
0.409		139.8
0.593		139.9

## U) Methane + 2, 2-dimethylpentane (7c)

Weight fraction ( $w_2$ )	Type of Phase Behaviour	Temperature of Phase Separation ( $^{\circ}\text{K}$ )
0.176	Limited Immiscibility	184.63
0.256		184.39
0.322		184.56
0.432		184.63
0.513		184.80
0.672		185.05

## V) Methane + 2, 4-dimethylpentane (7d)

Weight fraction ( $w_2$ )	Type of Phase Behaviour	Temperature of Phase Separation ( $^{\circ}\text{K}$ )
0.113	Limited Immiscibility	183.57
0.212		182.59
0.332		182.51
0.428		182.59
0.520		182.76
0.619		183.00

## W) Methane + toluene (7e)

Weight fraction ( $w_2$ )	Type of Phase Behaviour	Temperature of Quadruple Point ( $^{\circ}\text{K}$ )
0.278	Absolute Immiscibility	171.6
0.413		171.6
0.530		171.7

## X) Methane + 2, 2, 4-trimethylpentane (8a)

Weight fraction ( $w_2$ )	Type of Phase Behaviour	Temperature of Phase Separation ( $^{\circ}\text{K}$ )
0.165	Limited Immiscibility	172.22
0.266		171.79
0.350		171.87
0.422		171.87
0.520		171.96
0.586		172.05

## Y) Methane + 2, 3, 4-trimethylpentane (8b)

Weight fraction ( $w_2$ )	Type of Phase Behaviour	Temperature of Quadruple Point ( $^{\circ}\text{K}$ )
0.193	Absolute Immiscibility	146.6
0.298		146.6
0.524		146.6

Figures 15, 16, 17, 18 and 19 show the T, w projections

FIG. 15.

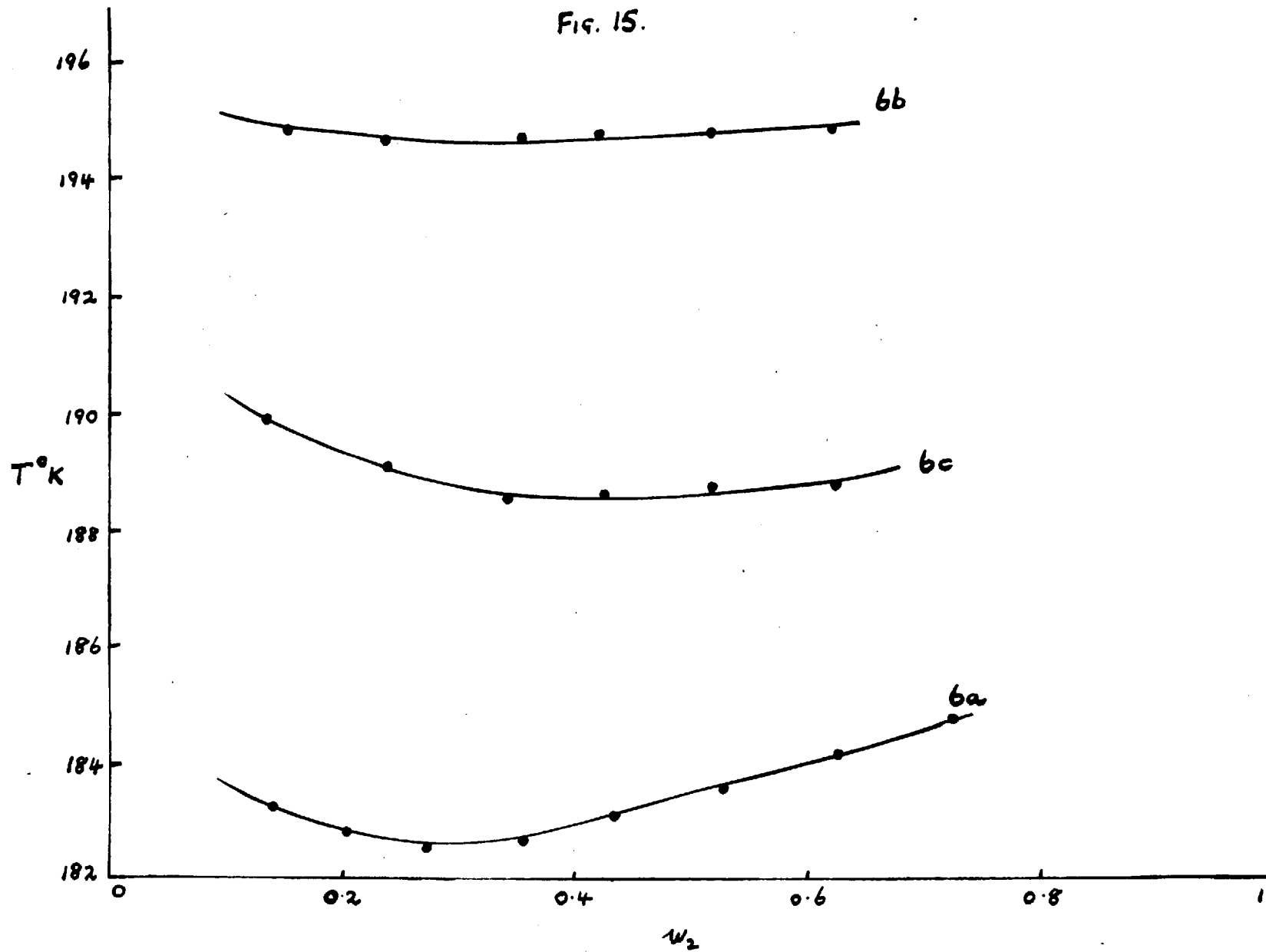
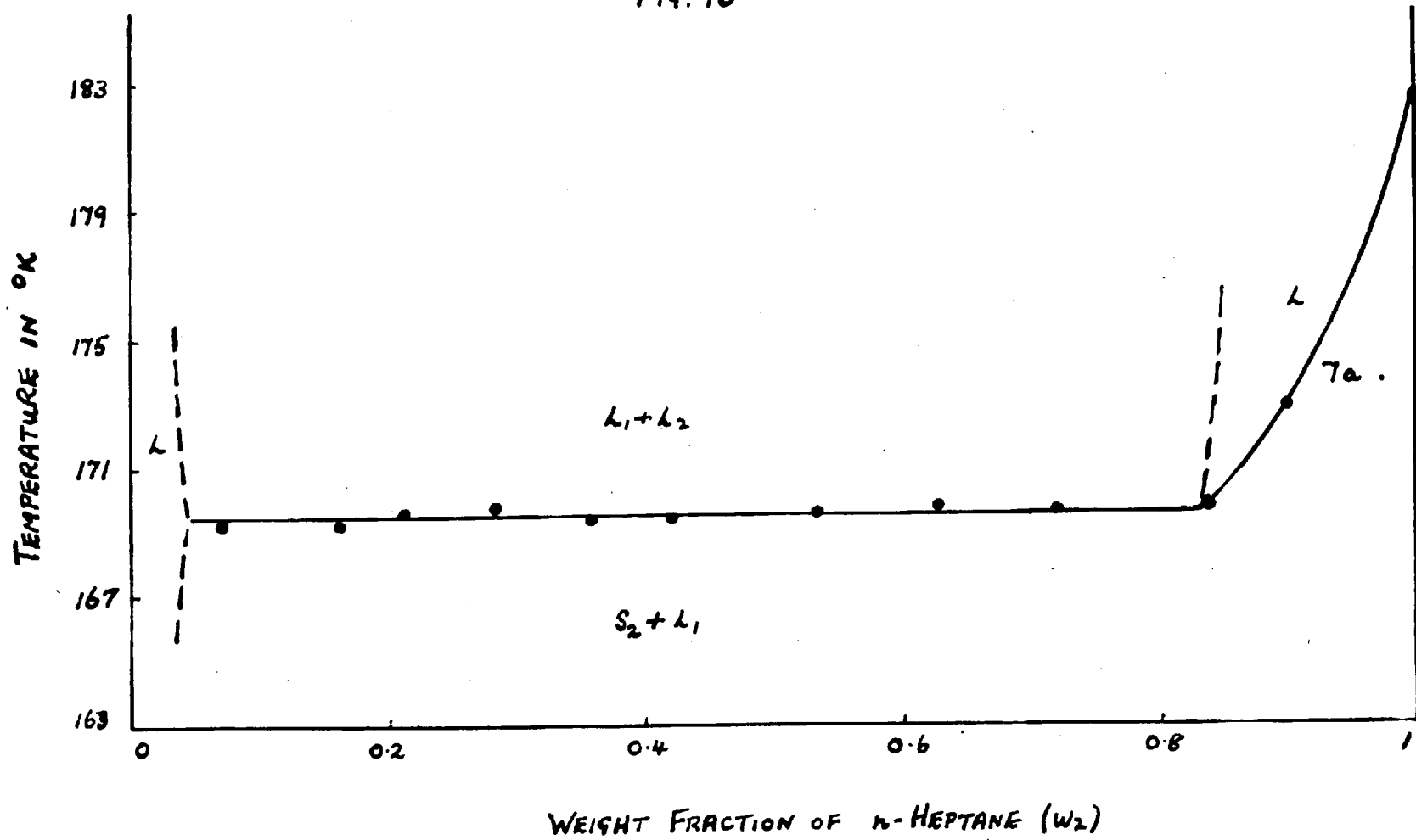




Fig. 16



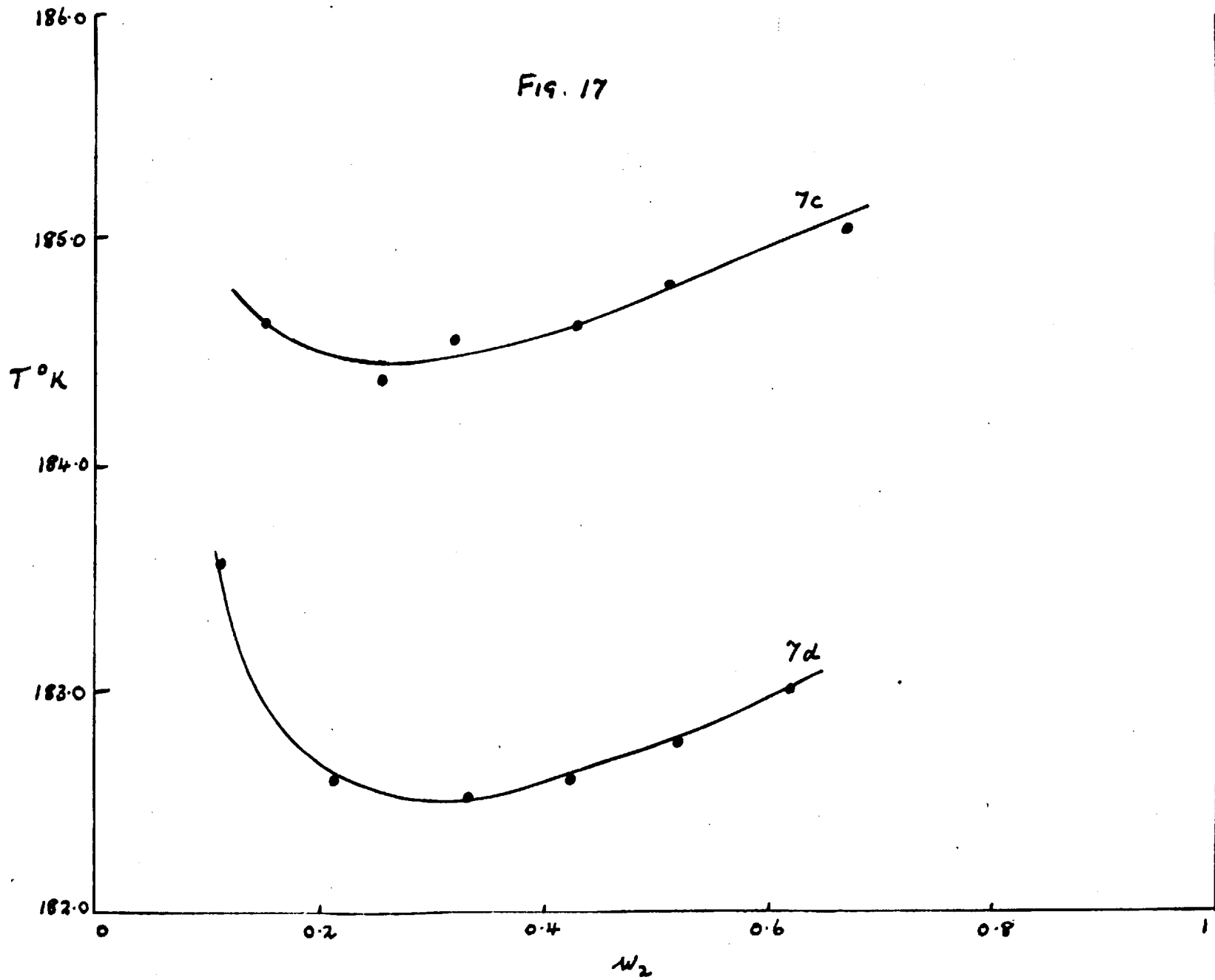
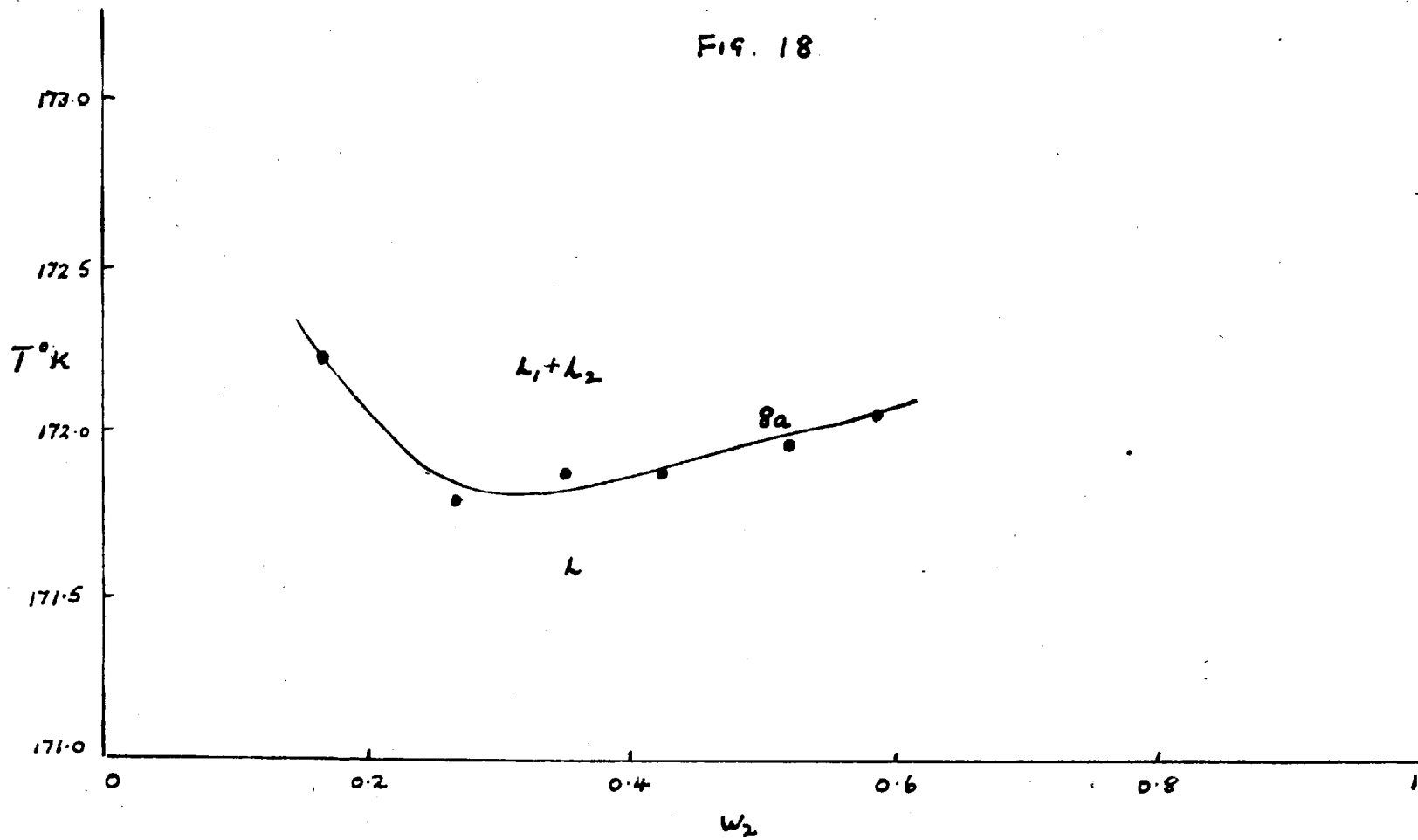


FIG. 18



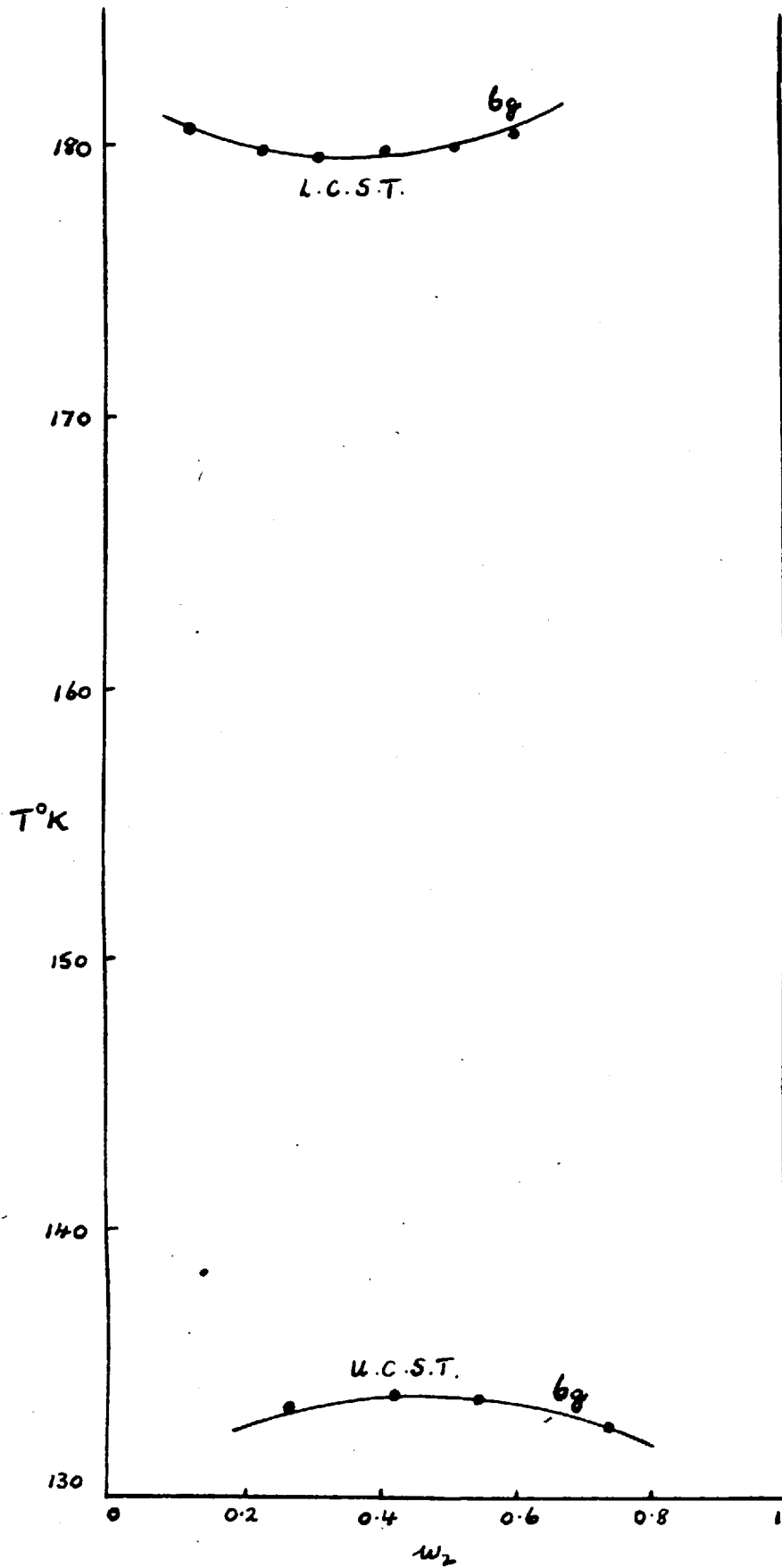


Fig. 19

for the systems 6a, 6b and 6c; 7a; 7c and 7d; 8a and 8b.  
From these graphs, the temperature and composition of the

Table 5A.

Hydrocarbon	Melting Point (°K)	Quadruple Point (°K)	L.C.S.T. (°K)	w <sub>2</sub> <sup>c</sup>
isoprene (5e)	127.2	119.8	-	-
cyclopentene (5f)	138.1	126.9	-	-
pent-1-yne (5g)	167.5	159.8	-	-
n-hexane (6a)	177.8	-	182.6	0.30
2-methylpentane (6b)	119.5	-	194.7	0.29
3-methylpentane (6c)	-	-	188.5	0.33
2, 3-dimethylbutane (6e)	144.6	-	195.5	-
methyl cyclopentane (6f)	130.7	122.6	-	-
hex-1-ene (6g)	133.3	-	179.6	0.32
cyclohexene (6h)	169.6	153.7	-	-
hex-1-yne (6i)	141.3	134.8	-	-
n-heptane (7a)	182.5	169.6	-	-
2-methylhexane (7b)	154.9	139.8	-	-
2, 2-dimethylpen- tane (7c)	149.3	-	184.4	0.27
2, 4-dimethylpen- tane (7d)	153.9	-	182.5	0.28
toluene (7e)	178.2	171.6	-	-
2, 2, 4-trimethylpen- tane (8a)	165.8	-	171.8	0.27
2, 3, 4-trimethylpen- tane (8b)	163.9	146.6	-	-

N.B. Methane (Melting Point = 90.7°K, T<sup>c</sup> = 190.3° K)

lower critical solution point was determined and in the case of the system methane + hex-1-ene (6g) the temperature and composition of the upper critical solution point was also determined. Table 5 lists these values, together with the quadruplepoint temperatures and the melting points of the pure involatile hydrocarbon.

Table 5B.

Hydrocarbon	Melting Point	U.C.S.T. ( $^{\circ}$ K)	$w_2^c$
hex-1-ene	133.3	133.8	0.43

In general, the results obtained show that the type of immiscibility shown here is very similar to that found by Kuenen and Robson where we have two components of very different molecular size and energies of interaction. The immiscibility observed in certain pairs seems to have been due to the approach of methane to its own gas-liquid critical point and the (T,x) projections correspond to the type previously discussed for ethane + ethanol. Similarly, it is reasonable to deduce that the (p,T,x) surface and the (p,T) projection would be of a similar type to those for ethane + ethanol.

The (T,w) projection for the system methane + n-heptane was studied in full in order to confirm the results obtained very recently by Kehr.<sup>5</sup> There is very

good agreement between his and our results on the temperature of the quadruple point as shown in Table 6, but there is a slight discrepancy as to the compositions over which this invariant line extends.

Table 6.

Quadruple Point of methane + n-heptane

	Temperature °K	Pressure	Weight Fraction of CH <sub>4</sub> in Liquid Phases
Kohn	169.6	23.0	0.227 ~1
Present work	169.6	-	0.17 0.93

The system methane + hex-1-ene is very interesting since we have the lower critical solution point occurring within 12° of the gas-liquid critical point of pure methane with a U.C.S.T. some 46° lower. This is the first simple binary system to show this behaviour, although it has recently been reported for polyethylene in several hydrocarbon solvents<sup>7</sup>, and for the system polyisobutene + benzene, where Krigbaum and Flory<sup>26</sup> found a U.C.S.T. between 17° C and 23° C and Freeman and Rowlinson<sup>4</sup> a L.C.S.T. between 150° and 170° C. More recently Patterson<sup>27</sup> and Myrat<sup>29</sup> have found the L.C.S.T. for the systems polystyrene + methyl acetate and polystyrene + cyclohexane which had previously been shown to have

U.C.S.T.'s at lower temperatures by Jenckel and Keller<sup>30</sup> and Schultz and Flory<sup>31</sup> respectively. As the U.C.S.T. occurs at a much lower temperature than the L.C.S.T., fluctuations in pressure, volume and other thermodynamic quantities will be small and so it can be concluded that it is the difference in molecular energies due to the presence of the olefinic bond that produces two liquid phases which coalesce on warming. The appearance of a U.C.S.T. at temperatures well below the gas-liquid critical point of pure methane was looked for in the system methane + pent-1-ene, but no separation had occurred on cooling to 113° K.

The type of phase diagram shown by each pair, solute + methane, depends upon the following factors:-

- 1) The miscibility of the liquids.
- 2) The temperature of the melting point of the solute.

If the miscibility is low and the melting point is low, the system will give us 'limited miscibility', whereas if the miscibility is low and the melting point high we get 'absolute miscibility'. In certain systems, which show absolute miscibility, it is possible to deduce where the L.C.S.T. might be if solidification did not intervene. Thus, where the quadruple point is considerably below the melting point of the pure solute (e.g. 2, 3, 4-trimethylpentane), it is probable that the L.C.S.T.



would be only a few degrees below the quadruple point. When the melting point and the quadruple point are close together as with the system methane + pent-1-yne, then there is no metastable L.C.S.T. near the quadruple point. Recently van Hest and Diepen have reported that for the system methane + naphthalene, there will never be a metastable L.C.S.T., that is, the liquids would always be immiscible even if solidification did not intervene. On the (p,T,x) surface for this type of system, it means that the line  $C_2KP$  of Fig. 11 (a), would rise at low temperatures and would probably be still rising at the point K at which it cuts the solid boundary.

From tables 4 and 5 it is possible to draw the following conclusions:-

- 1). Where we have a simple normal straight chain paraffin hydrocarbon, the solubility in methane decreases with increasing number of carbon atoms in the solute.

e.g. Solubility decreases as we go from 5a - 6a - 7a.

This behaviour is also found in the comparable branched paraffin isomers e.g. Solubility decreases 5b - 6b - 7b and 5c - 6c - 7c.

- 2) A comparison of 6a, 6b, 6c, 6d and 6e together with 7a, 7b, 7c and 7d shows that miscibility increases with chain-branching. Each branch-

point raises the L.C.S.T. by  $5^{\circ}$  -  $10^{\circ}$  in the hexanes and by more in the heptanes.

- 3) A comparison of 6a, 6g and 6i shows that miscibility decreases down the scale -ane, -ene and -yne. In fact, from 5a, 5d, 5e and 5g, it can be seen that any increase in unsaturation tends to decrease the solubility in liquid methane.
- 4) A comparison of 6a and 6f shows that the presence of a saturated ring tends to reduce the miscibility with liquid methane.
- 5) Miscibility is also reduced by the presence of an aromatic ring e.g. 7a and 7e. This fact is in agreement with the known thermodynamic properties of more conventional mixtures.<sup>32</sup>

These conclusions listed above extend and confirm those previously drawn for seven hydrocarbons in liquid ethane.

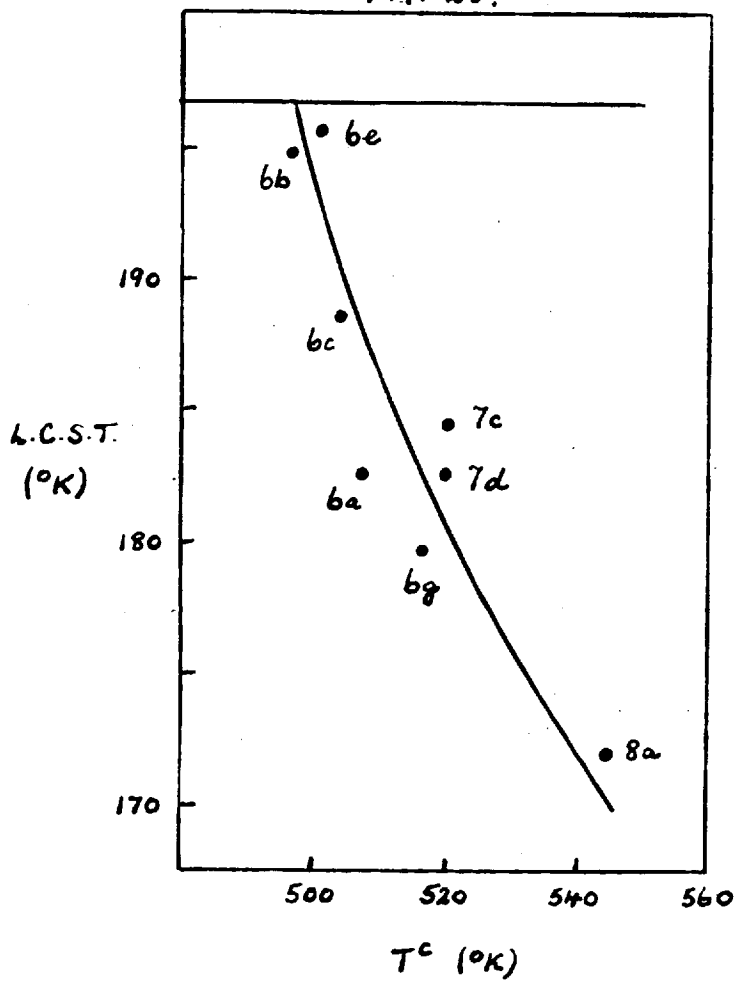
An attempt to draw quantitative conclusions from the results presented here is not quite so easy. Earlier on in the theory of immiscibility, we have discussed the factors that combine to produce a L.C.S.T. of this type. It occurs when the solute is a molecularly dense liquid of strong intermolecular forces and the solvent is a liquid of low molecular density and weak intermolecular forces, which is obviously fulfilled by a solvent that

is approaching its gas-liquid critical point.

We have now taken the gas-liquid critical temperature of the solute to be a measure of the mean interaction energy minimum of the potential between two molecules of solute. If we plot the value of the L.C.S.T. found for the eight systems showing limited immiscibility against the gas-liquid critical temperature of the solute, we obtain the graph shown in Fig. 20. It can be seen that all eight hydrocarbons (seven are paraffins and the other is an olefin) can be fitted within reason to the curve shown. The partial information about the L.C.S.T. of other solutes does not contradict this correlation except that it is found that isoprene and the acetylenes have an unexpected low solubility in liquid methane. From Fig. 20, it is reasonable to infer that the upper limit of  $197^{\circ}$  K is the highest temperature at which immiscibility can occur with hydrocarbon solutes in liquid methane, which is  $7^{\circ}$  above the gas-liquid critical point of pure methane. From this correlation, it seems possible to conclude that any hydrocarbon which has a gas-liquid critical point below  $495^{\circ}$  K will be completely miscible with pure methane in all proportions over the whole of the liquid range of mixtures.

We have also tried to correlate the values of the L.C.S.T. for the eight immiscible mixtures with Hildebrand's solubility parameter  $\delta$  for the solute at  $25^{\circ}$  C.

Fig. 20.



Now  $\delta$  is defined by the equation:-

$$\delta = \left(\frac{\Delta e}{v}\right)^{\frac{1}{2}}$$

To a first approximation,  $\Delta e = \Delta h - RT$

$$\delta = \left(\frac{\Delta h - RT}{v}\right)^{\frac{1}{2}}$$

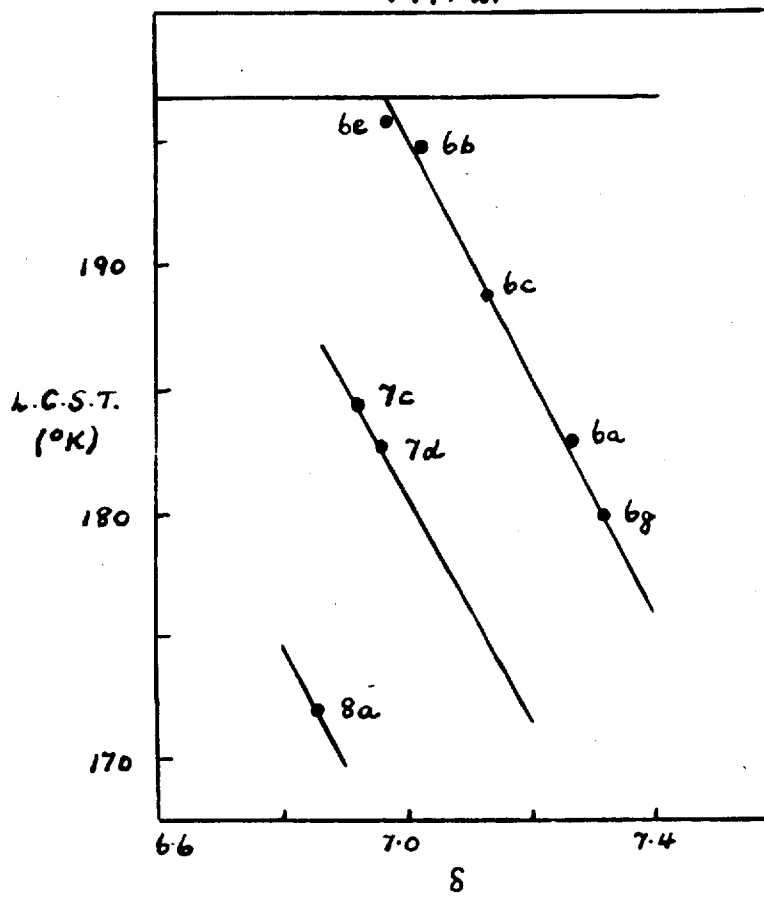
where  $\Delta h$  = Latent Heat of Evaporation per mole of solute and  $v$  = Molar Volume of solute.

The values for  $\Delta h$  and  $v$  are taken from the American Petroleum Institute Tables.<sup>21</sup> The values of  $\delta$ , together with the values for the gas-liquid critical points of the pure solute and the values of the L.C. S.T. s are listed in Table 7.

Fig. 21 shows that if we correlate  $(T_L^C)$  against  $\delta$ , we get a good straight line for the  $C_6$  hydrocarbons, but that the  $C_7$  and  $C_8$  hydrocarbons lie on different lines. The line for the  $C_8$  hydrocarbon has been plotted by taking the partial information drawn from the quadruple point of the system 2, 3, 4-trimethylpentane into account.

From Figs. 20 and 21, it can be seen that whereas Hildebrand's solubility parameter, comprising of a size and energy effect, splits the hydrocarbons into specific lines for  $C_6$ ,  $C_7$  and  $C_8$  solutes, the gas-liquid critical temperature of the solute correlates both  $C_6$ ,  $C_7$  and  $C_8$  solutes. This seems to suggest that the molecular property which has most influence on the L.C.S.T. and

FIG. 21



determines whether we get miscibility or immiscibility is the mean maximum depth of the potential energy ( $\epsilon^*$ ) of the mixture (see Fig. 22)

Table 7.

Hydrocarbon	$\delta$	$T^c$ ( $^{\circ}\text{K}$ )	L.C.S.T. ( $^{\circ}\text{K}$ )
n-hexane	7.27	507.9	182.6
2-methylpentane	7.02	497.9	194.7
3-methylpentane	7.13	504.7	188.5
2, 2-dimethylbutane	6.71	489.4	
2, 3-dimethylbutane	6.97	500.3	195.5
hex-1-ene	7.32	516.7	179.6
n-heptane	7.43	540.2	
2-methylhexane	7.21	531.1	
2, 2-dimethylpentane	6.92	520.9	184.4
2, 4-dimethylpentane	6.96	520.3	182.5
2, 2, 4-trimethylpentane	6.85	544.1	171.8
2, 3, 4-trimethylpentane	7.26	568.0	

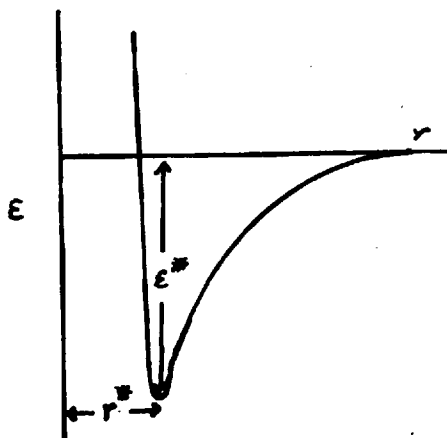


Fig. 22

and not the entropy of the solution as determined by the ratio of the sizes of solute and solvent, though this must necessarily have the size and sign required for producing a L.C.S.T.

Very recently, Everett and Mumm<sup>33</sup> have applied the Miller-Guggenheim<sup>34</sup> equations to mixtures of hydrocarbons, especially to the system hexane + n-hexadecane, which has been studied in great detail by McGlashan and his co-workers.<sup>35</sup> They find very good agreement with the experimental results and from their results they predict that there should be lower consolute behaviour in hydrocarbon mixtures when  $r$  (the ratio of the molar volume of the solute to that of the solvent) is of the order of 8 to 10. This result agrees well with the occurrence of L.C.S.T. in mixtures of hydrocarbons with liquid ethane, but it is not in good agreement with the present results for hydrocarbons in liquid methane where immiscibility occurs with methane + n-hexane when  $r = 1.9$  at the L.C.S.T. It must be pointed out that here  $r = \text{Molar Volume of n-hexane} / \text{Molar Volume of methane}$ , and is not obtained by taking the segments  $\text{CH}_3-$  and  $-\text{CH}_2-\text{CH}_2-$  or  $\text{CH}_3-$  and  $-\text{CH}_2-$  as is done in many cases. This may account for the anomaly in the liquid methane series, since methane is a unique molecule in the paraffin hydrocarbon series having only a  $\text{CH}_3-$  and a  $-\text{H}$  segment.

An attempt was made to correlate the critical



composition values with the values predicted by treating the system as a polymer solution, to which the Flory-Huggins expression was applicable:-

$$\frac{\Delta\mu_1}{RT} = \ln \phi_1 + \left(1 - \frac{1}{r}\right)\phi_2 + \chi \phi_2^2$$

where  $\phi_1, \phi_2$  are the volume fractions of components 1 and 2 respectively and  $\chi$  is the Flory-Huggins interaction parameter. Applying the conditions that at a liquid-liquid critical point:-

$$\left(\frac{\partial \Delta\mu_1}{\partial \phi_1}\right)_{T,P} = 0 \quad \text{and} \quad \left(\frac{\partial^2 \Delta\mu_1}{\partial \phi_1^2}\right)_{T,P} = 0$$

then  $\phi_2^c = \frac{1}{1+r}^{1/2}$  where  $\phi_2^c = \frac{rx_2^c}{x_1^c + rx_2^c}$

or  $x_2^c = \frac{1}{1+r}^{1/2}$

Table 8 shows the results obtained for three systems with  $r = \frac{v_2}{v_1}$  (r being calculated from the values in the American Petroleum Institute Tables.<sup>21</sup>)

Table 8.

Hydrocarbon (2)	$x_2^c$ observed	$x_2^c$ calculated
n-hexane	0.07	0.27
2, 2-dimethylpentane	0.07	0.24
2, 2, 4-trimethylpentane	0.05	0.18

These results confirm, I think, that it is impossible to treat methane + hydrocarbon systems in the same way as polymer solutions, even though when we go to ethane + hydrocarbon systems some measure of agreement is found.

PART II.

THERMODYNAMIC PROPERTIES OF THE SYSTEMS:-

- 1) METHANE + 2-METHYLPENTANE.
- 2) METHANE + ISOPENTANE.

CHAPTER I.INTRODUCTION.

Recently, quite a good deal of attention has been paid to the miscibility of long chain non-polar hydrocarbons solutes in non-polar hydrocarbon solvents. This type of system has been discussed in Part I of this thesis, and includes the behaviour of non-polar hydrocarbon polymers in non-polar hydrocarbon solvents<sup>4</sup> as well as the ~~more~~ simpler class of systems where non-polar hydrocarbons have been mixed using liquid propane, liquid ethane or liquid methane as solvent.

In certain of these systems, it has been found that given the right difference in chain length and intermolecular energies, two hydrocarbons will exhibit lower critical solution behaviour and the lower critical solution temperature usually lies quite close to the gas-liquid critical point of the solvent. As we have mentioned earlier, however, this class of lower consolute behaviour is not compatible with the earlier class of systems that showed lower consolute behaviour and at the moment, the molecular properties of the two components that lead to it are not fully understood.

Recently, a systematic study of the thermodynamic properties of the system polyisobutene + n-pentane has been made<sup>28</sup>, and Patterson and his co-workers<sup>36</sup> have

measured the heats of mixing of various polyisobutene + n-alkane systems.

One of the chief intentions behind the systematic study of the miscibility of hydrocarbons in liquid methane, described in Part I of this thesis, was to find a suitable system which exhibited lower consolute phenomena on which a systematic study of the thermodynamic properties could be made, since in using liquid methane as solvent we have the simplest class of system of this type. In these systems, where immiscibility occurs at quite high pressures, (of the order of 40 atmospheres for methane rich mixtures), it was necessary to study the thermodynamic properties at temperatures quite far removed from the L.C.S.T., but it was hoped that the molecular interactions which lead to lower consolute behaviour of this type would not have been frozen out at temperatures, where the pressures are below 10 atmospheres.

The system chosen for thermodynamic study was methane + 2-methylpentane. This system has a L.C.S.T. at  $194.7^{\circ}$  K, which is quite high, but it has the advantage that 2-methylpentane has a very low melting point ( $119.5^{\circ}$  K) and so the thermodynamic properties of liquid 2-methylpentane can easily be studied experimentally without the disadvantage of extrapolating a long way into the super-cooled liquid range (e.g. if the system methane

+ n-hexane had been chosen, where the L.C.S.T. is at  $182.6^{\circ}$  K, we would have to have extrapolated some  $60^{\circ}$  or so to obtain the volume of super-cooled liquid hexane). We have studied the volume behaviour of the system methane + 2-methylpentane from  $115^{\circ}$  K to  $155^{\circ}$  K and vapour pressure measurements have been made at the triple point of krypton.

In an attempt to access the effect of hydrocarbon groupings on the miscibility of hydrocarbons in liquid methane, the volume behaviour of the system methane + isopentane has also been studied in the temperature range  $115^{\circ}$  K to  $155^{\circ}$  K.

CHAPTER II.THEORY.Theories of Simple Solutions.

The theoretical study of liquid mixtures is very useful for providing information about the intermolecular forces between unlike molecules. The usual point of departure in discussing the thermodynamic properties of a liquid mixture has been Raoult's Law, which states that the partial vapour pressure of each component in a liquid mixture is proportional to its mole fraction, assuming that the vapours behave as perfect gases. Thus for component 1:-

$$p_1 = p_1^{\circ} x_1$$

where  $p_1$  is the partial vapour pressure and  $p_1^{\circ}$  the vapour pressure of pure component 1. Such a solution is termed an ideal solution. An alternative definition for an ideal solution which follows quite simply from Raoult's Law, is given by the equation:-

$$\mu_1 = \mu_1^{\circ} + RT \ln x_1$$

where  $\mu_1$  is the chemical potential of component 1 in the solution and  $\mu_1^{\circ}$  is the chemical potential of the pure liquid component 1, both being at temperature  $T$  and a prescribed pressure.

The Gibbs Free Energy ( $g$ ) per mole of binary liquid

mixture at constant temperature and pressure is given by:-

$$g = x_1 \mu_1 + x_2 \mu_2$$

$$= x_1 \mu_1^0 + x_2 \mu_2^0 + RT (x_1 \ln x_1 + x_2 \ln x_2)$$

Therefore the Gibbs Free Energy of mixing per mole for an ideal solution ( $g^{id}$ ) is given by:-

$$g^{id} = RT (x_1 \ln x_1 + x_2 \ln x_2)$$

Now since  $h = -T^2 \left( \frac{\partial g/T}{\partial T} \right)_p$  ;  $s = - \left( \frac{\partial g}{\partial T} \right)_p$  and  $v = \left( \frac{\partial g}{\partial p} \right)_T$

it follows that:-

$$h^{id} = 0 \quad ; \quad v^{id} = 0$$

$$s^{id} = -R (x_1 \ln x_1 + x_2 \ln x_2)$$

The departure of the observed mixing functions from their ideal values are termed the excess mixing functions, denoted by the superscript E. These functions have been discussed in Part I of this thesis, and are listed again here for convenience. For a mole of mixture at constant temperature and pressure:-

$$g^E = g^{obs} - RT (x_1 \ln x_1 + x_2 \ln x_2)$$

$$h^E = h^{obs}$$

$$s^E = s^{obs} + R (x_1 \ln x_1 + x_2 \ln x_2)$$

$$v^E = v^{obs} - x_1 v_1^0 - x_2 v_2^0$$



All theories of solution assume that the partition function  $Q$  for a system can be written in the form:-

$$Q = Q_{int} \cdot Q_{trans}$$

where  $Q = \sum e^{-E_i/kT}$

$Q_{trans}$  is the translational partition function due to position and  $Q_{int}$  is the partition function associated with other degrees of freedom such as the internal vibrations and rotations of the molecules. The above expression is however, only valid for molecules of near spherical symmetry.

If we now assume that when a mixture is formed,  $Q_{int}$  remains unchanged, then theoretical interest only centres on the quantity  $Q_{trans}$ . For a classical system:-

$$Q_{trans} = \left( \frac{2\pi m kT}{h^2} \right)^{3N/2} \cdot Q_{config}$$

where  $Q_{config} = \frac{1}{N!} \int \dots \int e^{-u/kT} dr_1 \dots dr_N \dots$  (2.1)

and is called the configurational partition function.

$$\begin{aligned} \therefore Q &= Q_{int} \cdot \left( \frac{2\pi m kT}{h^2} \right)^{3N/2} \cdot Q_{config} \\ &= Q_0 \cdot Q_{config} \end{aligned}$$

The Helmholtz Free Energy ( $F$ ) is given statistically by:-

$$F = -kT \ln Q \quad \dots \quad (2.2)$$

$$\therefore F = -kT \ln Q_0 - kT \ln Q_{\text{config}}$$

or

$$F = F_0 + F_{\text{config}}$$

It is therefore with the determination of  $Q_{\text{config}}$  from the intermolecular parameters of the mixture that most theories of solution are concerned.

The initial attempts to correlate thermodynamic properties of liquid mixtures with intermolecular parameters were made using a lattice model for the liquid mixture, since in the early days of solution theory, the vast majority of experimental evidence suggested that the liquid state had many properties in common with the solid state. Guggenheim<sup>37</sup> expressed the excess thermodynamic properties of liquid mixtures in terms of a lattice partition function, the intermolecular energies in this function being obtained by treating the particles at rest on their lattice sites. The lattice was taken as rigid and no attempt was made to allow for any change in intermolecular distance on mixing, i.e.  $v^E = 0$ . This model only predicted small negative excess entropies with  $g^E > 0$  and  $h^E > 0$  ( $g^E \approx h^E$ ) for molecules of the same size, whereas experimental evidence on the simplest mixtures suggested that  $Ts^E \approx h^E$  and that  $s^E$  could be positive or negative. The chief success of

this model was the prediction of the combinatorial factor for polymer solutions by Flory<sup>38</sup> and Huggins<sup>39</sup>.

The next step in the theory of liquids was made by Lennard-Jones and Devonshire<sup>40</sup>. They employed the so-called cell model of the liquid state and achieved a fair measure of success in applying it to the pure liquid state and to multicomponent systems.

The most recent theories of simple solutions have made use of the following two ideas:-

- 1) The potential energy of the system is the sum of all the pair interactions.
- 2) The theorem of corresponding states as formulated by Pitzer<sup>41</sup>.

Pitzer showed that if the intermolecular energy of a pair of molecules ( $u$ ) and a distance ( $r$ ) can be expressed in the form

$$u = \epsilon \phi \left( \frac{r}{\sigma} \right)$$

where  $\phi$  is a universal function and  $\epsilon$  and  $\sigma$  are scalar parameters characteristic of the interacting molecules, then the configurational contribution to the thermodynamic properties can be expressed in terms of  $\frac{kT}{\epsilon}$  and  $\frac{r}{\sigma}$ .

This is one of the main reasons why most theories of liquid mixtures make use of the Lennard-Jones potential for the interaction energy between molecules.

$$\begin{aligned} \text{i.e. } u(r) &= 4\epsilon^* \left[ \left( \frac{\sigma^*}{r} \right)^{12} - \left( \frac{\sigma^*}{r} \right)^6 \right] \\ &= \epsilon^* \left[ \left( \frac{r^*}{r} \right)^{12} - 2 \left( \frac{r^*}{r} \right)^6 \right] \end{aligned}$$

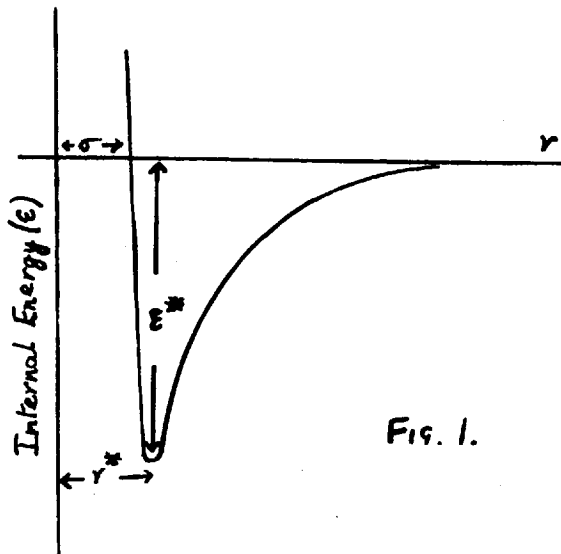


FIG. 1.

The theorem of corresponding states means that if there are  $N$  molecules of component 1 and  $N$  molecules of component 2, the configurational energy of the first system can be expressed in terms of the second by

$$\frac{u_1[\dots r_i \dots]}{kT} = \frac{u_2[\dots r_i \left( \frac{\sigma_{22}}{\sigma_{11}} \right) \dots]}{k(T\epsilon_{22}/\epsilon_{11})} \dots (2.3)$$

where  $\epsilon$  and  $\sigma$  are an energy and distance respectively.

Putting (2.3) into (2.1) leads to

$$Q_1(V, T) = \left( \frac{\sigma_{11}}{\sigma_{22}} \right)^{3N} Q_2 \left( \frac{V\sigma_{22}^3}{\sigma_{11}^3}, T \frac{\epsilon_{22}}{\epsilon_{11}} \right) \dots (2.4)$$

From (2.4) and (2.2) we get

$$F_1(V, T) = \left( \frac{\epsilon_{11}}{\epsilon_{22}} \right) F_2 \left[ V \left( \frac{\sigma_{22}}{\sigma_{11}} \right)^3, T \left( \frac{\epsilon_{22}}{\epsilon_{11}} \right) \right] - 3NkT \ln \left( \frac{\sigma_{11}}{\sigma_{22}} \right)$$

and the corresponding expression for G is

$$G_1(P, T) = \left( \frac{\epsilon_{11}}{\epsilon_{22}} \right) G_2 \left[ P \left( \frac{\sigma_{11}}{\sigma_{22}} \right)^3 / \frac{\epsilon_{22}}{\epsilon_{11}}, T \left( \frac{\epsilon_{22}}{\epsilon_{11}} \right) \right] - 3NkT \ln \left( \frac{\sigma_{11}}{\sigma_{22}} \right)$$

In 1951, Longuet-Higgins<sup>42</sup> first applied the principle of corresponding states to his theory of conformal solutions. The remarkable feature of this theory was its lack of appeal to any model of the liquid state. He showed that if the right reference substance was chosen (the reference substance is usually chosen for convenience to be one of the pure substances of which the binary mixture is composed) and only first order terms in the statistical expression were considered, then the thermodynamic properties of the mixture could be expressed in terms of the thermodynamic properties of the substance.

The main disadvantage of the theory of conformal solutions as postulated by Longuet-Higgins was that it gave the same sign to all the excess mixing functions

$$\text{i.e. } g^E > 0, h^E > 0, s^E > 0 \text{ or } g^E < 0, h^E < 0, s^E < 0$$

whereas many simple systems show excess mixing functions that are not of the same sign [e.g. the system  $C(CH_3)_4 + CCl_4$  has  $g^E > 0$ ,  $h^E > 0$  but  $s^E < 0$ ,  $v^E < 0$  at  $0^\circ C$ ]. Many

authors recently have tried to improve conformal solution theory by introducing second order terms into the conformal perturbation. Unfortunately, however, these new terms cannot be entirely expressed in terms of the thermodynamic functions of the reference substance and in consequence further assumptions have to be made to avoid these non-thermodynamic terms. Most recently, the theory has been taken to a fairly high degree of accuracy by Prigogine<sup>43</sup>, Scott<sup>44</sup> and Byers-Brown<sup>45</sup> in their random and semi-random treatments of liquid mixtures. These latter refinements produce the right variations in the signs of the excess functions but it is ultimately left to experiment to determine which theory fits the facts best.

It is important to emphasise here that all the previous mentioned theories of solutions have so far been found only to apply satisfactorily to liquid mixtures where the two components are approximately of the same size i.e.  $r_{12}^* = r_{11}^* = r_{22}^*$ . They also assume the usual combining rules for the intermolecular energies and distances:-

$$\epsilon_{12}^* = (\epsilon_{11}^* \cdot \epsilon_{22}^*)^{1/2}$$

$$r_{12}^* = \frac{1}{2} (r_{11}^* + r_{22}^*)$$

#### Solution Theory for Molecules of Different Sizes.

Quite a good deal of interest has centred recently

on solutions of non-electrolytes where the two components of the mixture differ in size. The easiest class of system for this kind of study is, of course, hydrocarbon systems where the two components are made up of similar individual units. McGlashan and his co-workers<sup>35</sup> have recently studied the thermodynamic mixing properties of the system n-hexane + n-hexadecane. They have applied the lattice theory<sup>37</sup> to their results using the following three processes.

- 1) Mixing at constant pressure.

$$g^E = g(T, P) - x_1 g_1^{\circ}(T, P) - x_2 g_2^{\circ}(T, P) - g^{id}$$

- 2) Mixing with zero volume change.

$$F^E = F(T, \bar{V}) - x_1 F_1^{\circ}(T, V_1) - x_2 F_2^{\circ}(T, V_2) - F^{id}$$

$$\text{where } \bar{V} = x_1 V_1 + x_2 V_2$$

- 3) Mixing at constant volume per element.

$$F^E = F(T, \bar{r} V^*) - x_1 F_1^{\circ}(T, r_1 V^*) - x_2 F_2^{\circ}(T, r_2 V^*) - F^{id}$$

where  $V^*$  is some chosen volume per mole of element and  $\bar{r}$  is defined by

$$\bar{r} = x_1 r_1 + x_2 r_2$$

They find that process 3) fits the results best which is to be expected in view of the more refined treatment. Everett and Mumm<sup>33</sup> have recently however found good agreement between experiment and theory when they applied the Miller-Guggenheim equation to McGlashan's

results. This has been discussed briefly in Part I of this thesis.

A more recent treatment of solutions of chain molecules of different sizes has been developed by Prigogine and his co-workers<sup>46</sup>. This theory is based on a principle of corresponding states treatment applied to this type of solution. In the theory, the chain molecule is considered in terms of its inter and intramolecular degrees of freedom, which arise from the strong short range valency forces between segments of one molecule and the much weaker intermolecular van der Waals forces between neighbouring molecules. Thus the energy of the system is divided into two mutually independent contributions, one depending only on the internal co-ordinates and the other on the external co-ordinates. Hence the partition function  $Q$  reduces to a product of two independent factors:-

$$Q = Q_{int}(T) \cdot Q_{ext}(T, V)$$

The theory as developed by Prigogine, Trappeniers, Mathot and Bellemans is essentially a model for calculating  $Q_{ext}(T, V)$ . They consider a one component liquid phase containing  $N$  homogeneous straight chain  $r$ -mers and assume that each  $r$ -mer can be treated as a set of  $r$ -point centres, (called segments or elements) each of which is subjected to central forces exerted by elements



of neighbouring molecules. The potential between two segments of different r-mers is therefore of the form:-

$$\epsilon(r) = \epsilon_r \phi^* \left( \frac{r}{\sigma_r} \right)$$

where  $\epsilon_r$  and  $\sigma_r$  are now parameters characteristic of a particular r-mer. The total energy is assumed equal to the pairwise contribution of the segments. The theory assumes that the distances between the segments is such that the mean distance between two neighbouring segments is always the same, whether they belong to the same r-mer or different molecules. They use a quasi-crystalline lattice, where each segment occupies a single lattice point. Using the lattice parameter  $a$  (nearest neighbour distance) and co-ordination number  $z$ , they express the potential energy contribution to the external partition function as:-

$$Q = g \psi^N \exp(-E_0/kT)$$

$$\text{where } E_0 \text{ (lattice energy)} = \sum \epsilon_{ij}(a)$$

$g$  is the combinatorial factor, equal to the number of different possible arrangements of molecules on sites of the quasi-crystalline lattice for a given value of  $E_0$ .

and  $\psi^N$  is the cell partition function.

This treatment leads to the thermodynamic properties of mixing being expressed in terms of a reduced temper-

ature  $T^*$ , volume  $V^*$  and pressure  $p^*$  and the cell partition function  $\Psi^*$ , where:-

$$T^* = \frac{c_r kT}{q_r \epsilon_r} \quad : \quad V^* = \frac{V}{Nr \sigma_r^3} \quad : \quad P^* = \frac{r \sigma_r^3}{q_r \epsilon_r} \cdot P$$

In these expressions,  $q_r$  is defined by the equation  $q_r^2 = rz - 2r + 2$  and  $c_r$  is the number of external degrees of freedom of a molecule.

Application of the theory of molecules of different sizes to systems showing a L.C.S.T. of the type mentioned in Part I of this thesis.

The first systematic study of the thermodynamic mixing functions of systems showing a L.C.S.T. was made on the system polyisobutene + n-pentane by Baker, Brown, Gee, Rowlinson, Stubley and Yeadon. They treated the problem using polymer theory based on the Flory-Huggins Equation:-

$$(\mu_1 - \mu_1^0)/RT = \ln \phi_1 + \phi_2(1-r^{-1}) + \chi \phi_2^2$$

where  $r$  is the ratio of the molar volumes of solute and solvent respectively and  $\chi$  is the Flory-Huggins parameter. They analysed two samples of polyisobutene having mean molecular weights of 1,170 (I) and 62,000 (II). Polymer I dissolves in n-pentane at room temperature with a small positive heat and entropy of mixing which is given approximately by the Flory-Huggins equation.

At higher temperatures, the heat and entropy become negative, and the solution shows a L.C.S.T. With a polymer of longer chain length, the region of negative heats and entropies moves further away from the gas-liquid critical point of the solvent and Polymer II shows a L.C.S.T. at room temperature. It is found that systems which show a L.C.S.T. cannot be rationalised in terms of the Flory-Huggins equation unless some qualifications about the parameter  $\chi$  <sup>are</sup> ~~is~~ made, since the equation predicts positive heats of mixing and the heat of mixing of polymer II + n-pentane is small and negative at all concentrations. If, however,  $\chi$  is assumed to vary both with temperature and composition, polymer systems that show a L.C.S.T. can be rationalised, since for polymer II + n-pentane  $\chi T$  is approximately constant from 25° C. to 65° C.

The volumes of mixing of both polymers I and II in n-pentane were found to be negative. This is in agreement with the known facts for systems showing a L.C.S.T. However, a negative volume of mixing is not necessarily related to the occurrence of a L.C.S.T. since simple systems such as n-hexane + n-hexadecane have a negative volume of mixing, but no L.C.S.T. has yet been found. It is therefore likely that any two aliphatic hydrocarbons of widely different chain lengths

will contract on mixing since there is a reduction in the mean molecular volume when a molecule of light component is transferred from a liquid of very low internal energy to a mixture of much higher internal energy. Thus one can conclude that whenever hydrocarbons of different sizes are mixed there is a negative volume of mixing, the size of this negative volume of mixing depending upon the difference in size of the two components. However for a L.C.S.T., the heat and entropies of mixing are necessarily negative as well and this is not true for all solutions of hydrocarbons of different sizes.

More recently, polymer systems that show a L.C.S.T. have been explained on a more quantitative basis by Patterson and his co-workers<sup>36</sup>. They have used the Prigogine Theory of r-mer solutions outlined previously and have analysed the results of Freeman and Rowlinson<sup>4</sup> for systems showing a L.C.S.T. as well as their own results on the heats of mixing various polyisobutene + n-alkane systems.

Using the Prigogine Theory, Patterson and his co-workers obtained the following expressions for the L.C.S.T. and the heat of mixing.

$$\frac{T_c}{r_A} = \frac{R}{2B} \quad \text{where } B \text{ is a constant} \quad \dots(2.5)$$

$$\frac{\Delta H_m}{(N_A r_A + N_B r_B) \phi_A \phi_B / N} = A - B \left( \frac{T}{r_A^2} \right) \dots (2.6)$$

where A and B are constants, B being the same constant as in equation (2.5).

Using  $r_A = (n + 1)/2$  where n is number of carbon atoms in the chain of the solvent, they found good agreement with Freeman and Rowlinson's results for the systems polyisobutene + n-pentane, polyisobutene + n-hexane, polyisobutene + n-heptane and polyisobutene + n-octane. They also found that the Prigogine's Theory fitted the experimental heats of mixing quite well, giving a good temperature dependence for the polymer-solvent interactions and enabling one to correlate parameters obtained for different members of a homologous solvent series.

CHAPTER III.EXPERIMENTAL.Materials.

The methane used in the volume and vapour pressure measurements was supplied by the L'Air Liquide Company of Belgium. It had a quoted purity of 99.95 moles%, the impurities being nitrogen and water vapour. It was condensed from the cylinder into the Clusius and Riccobini column described in the first part of this thesis and refluxed and distilled as previously described. 20 litres at one atmosphere pressure of purified methane were stored in pyrex storage bulbs. No check was made on the purity of the distilled sample in view of its high initial purity. The only other check on its purity was that in the experimental measurements, no difficulty was found in condensing the purified gas completely into a glass finger under liquid nitrogen subjected to continuous pumping.

The krypton used as the cryostatting solid in the vapour pressure measurements was supplied by the British Oxygen Company. It was stated to be spectroscopically pure having a quoted purity of 99 moles%, the only impurity being 1 mole% of xenon. 15 litres of impure krypton were purified on a column designed by Saville<sup>47</sup>

in Oxford. This column was based on a design suggested by Coulson and Herington<sup>48</sup>. The column, shown in Fig. 2, consists of an inner bulb of approximate volume 55 mls., which was joined to a glass column filled with pyrex glass rings. The column was surrounded by a silvered container which could be filled with hydrogen or left evacuated. The lower half of the silvered container and the inner bulb were both surrounded by a large glass vacuum jacket and the whole apparatus fitted into a large Dewar vessel having an unsilvered strip. Heat to the inner bulb was supplied by a small heating coil of 6 ohm resistance to which a maximum current of 0.6 amps was applied. The heating coil was sealed inside the glass bulb using tungsten seals and it rested very close to the bottom of the bulb. The krypton was condensed from glass cylinders into a glass finger cooled under liquid nitrogen. The Dewar vessel was then filled with liquid nitrogen until the nitrogen level just reached the top of the inner bulb. Krypton was now allowed to condense in under approximately one atmosphere pressure, hydrogen being carefully added to the silvered container to promote more rapid condensation. When almost all the krypton had been condensed in, the heater was switched on and hydrogen carefully removed from the silvered container so that the pressure of krypton in the inner bulb was kept at roughly one

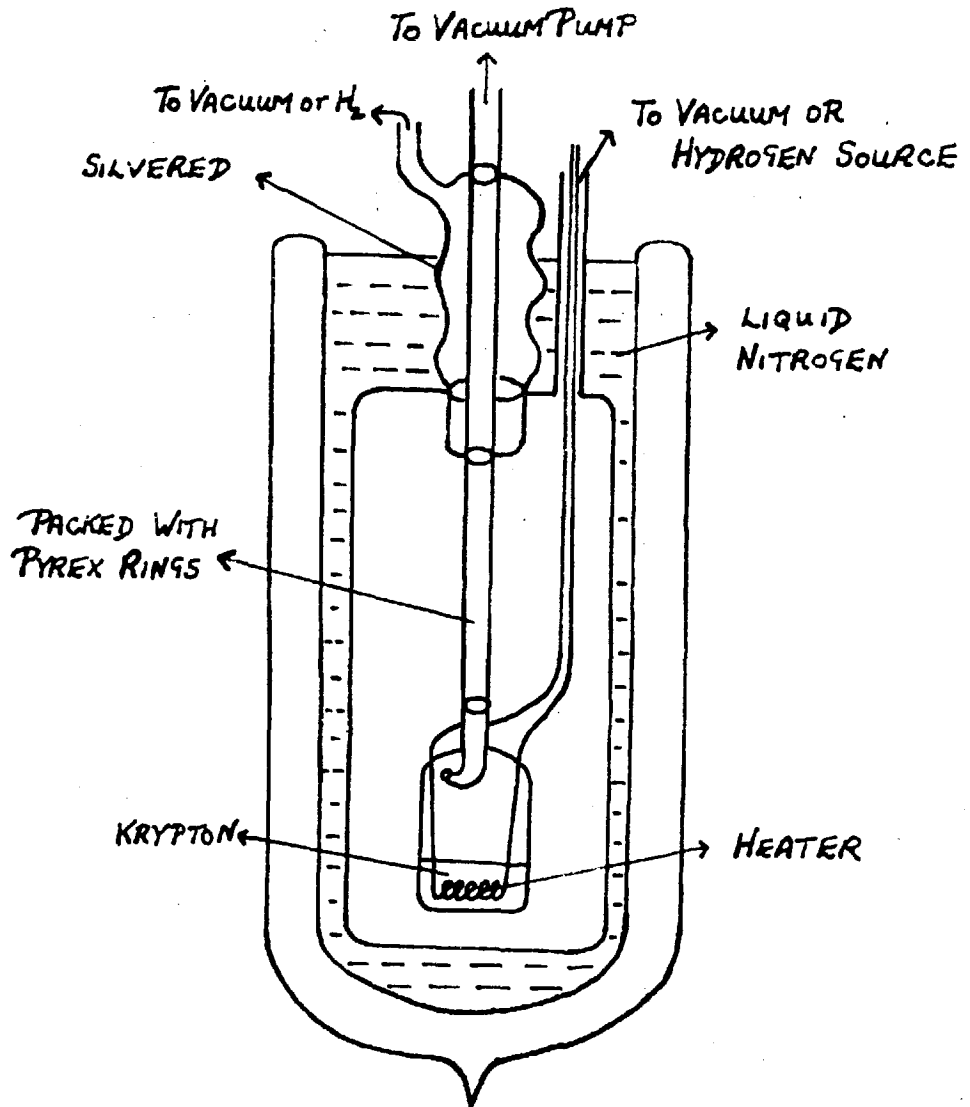


FIG. 2.



atmosphere. This process was needed in the case of krypton in order to prevent solidification and blockage of the column, since krypton melts at a pressure of 548 mm. The Dewar vessel was now completely filled with liquid nitrogen and the krypton allowed to reflux. A small needle valve was opened to allow the krypton vapour to be pumped away at a reflux ratio of  $\frac{1}{15}$ . Since xenon was the chief impurity, only a small sample of vapour was taken off initially before the main fraction was condensed in vacuo under liquid nitrogen into a glass vessel. This main fraction was now expanded into two 5 litre pyrex storage bulbs and 10 litres of purified krypton at 50 cms pressure were collected. The purity of this sample was not tested. The only check was the value obtained for the vapour pressure of pure methane under the melting krypton and the observed steadiness of this pressure over 2 hours while the krypton melted.

The isopentane and 2-methyl pentane used in the volume and vapour pressure measurements was supplied by the National Chemical Laboratory in 5 ml. glass breakseals sealed in vacuo. The purities quoted were 100.00 moles % and 99.82 moles % respectively.

#### Volume Measurements.

Volume measurements were made on pure methane,

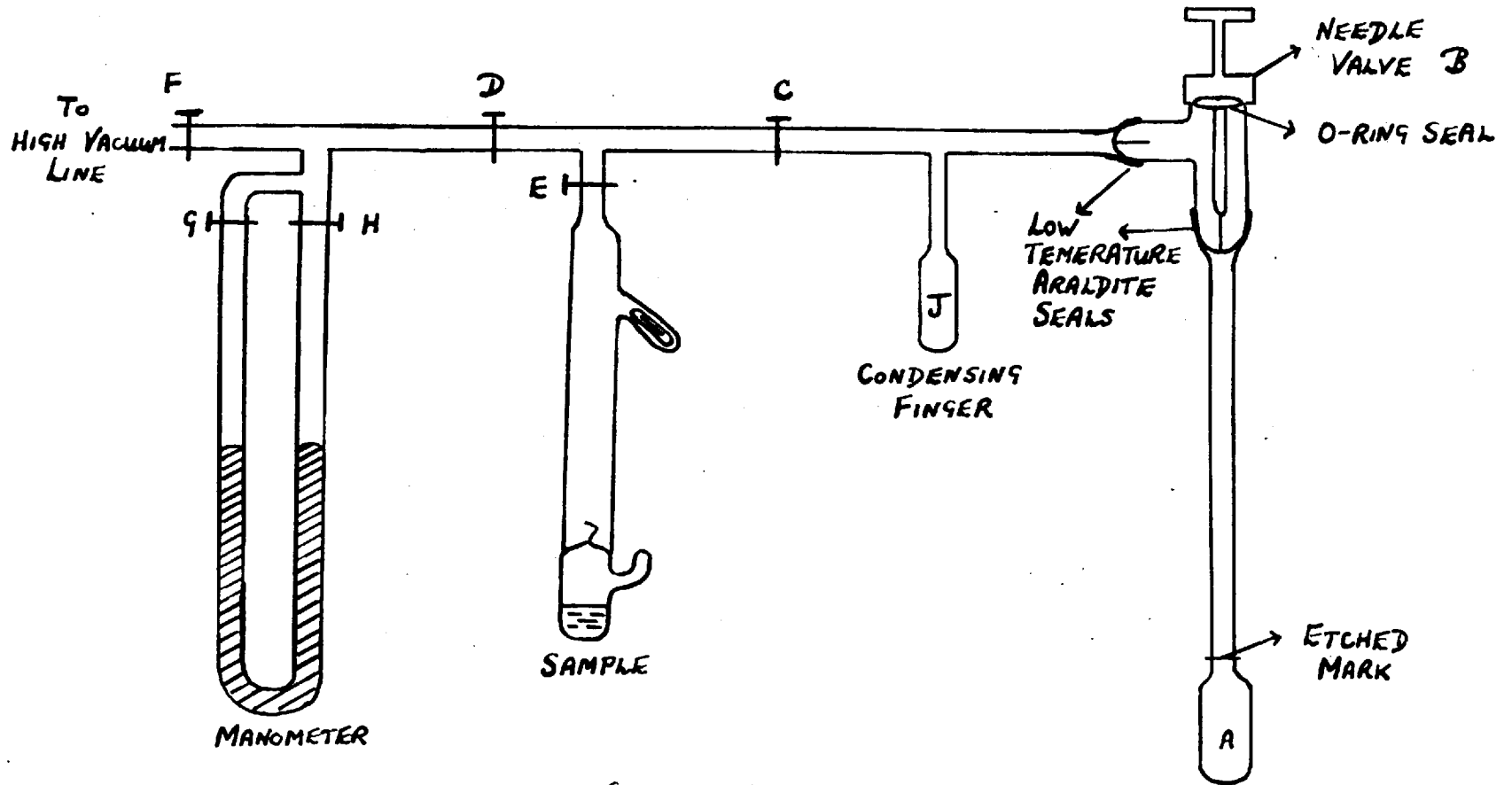
pure isopentane, pure 2-methylpentane and mixtures of methane + isopentane and methane + 2-methylpentane over the temperature range  $115^{\circ}$  K to  $155^{\circ}$  K.

#### Details of High Vacuum Apparatus.

The apparatus is shown in outline in Figure 3. The liquids were contained in a small glass bulb A of approximately 0.6 ml. capacity to which was fitted a 15 cm. length of 1 mm. precision bore glass capillary tubing. The capillary tubing and bulb dipped into the cryostat as shown. An etched mark was affixed to the lower end of the capillary tubing about 1 cm. above the bulb. The upper end of the capillary tubing was joined to a B 7 socket and connected to the vacuum line by means of the metal valve B fitted with an O-ring seal. The glass to metal seals were made using low temperature araldite.

Samples of 2-methylpentane or isopentane were joined below tap E and distilled into bulb A under liquid nitrogen in vacuo, the breakseal tip being broken in a manner previously described. Taps C, D and E were high vacuum greaseless taps fitted with neoprene diaphragms. It was found necessary to use greaseless taps in this section since both isopentane and 2-methylpentane were found to absorb into the standard greases. Pure methane was completely condensed into the glass

Fig. 3.



C, D, E are GREASELESS TAPS

condensing finger J using the 'pump-down' trap previously mentioned in Part I of this thesis. With the methane in the condensing finger, tap C was shut off and the metal valve B opened, the methane being allowed to expand into bulb A. It must be pointed out here that before this process was started, the cryostat had been cooled to the melting point of isopentane. When all the methane possible had been condensed into bulb A, the metal valve B was shut, and the remaining methane allowed to expand into the volume enclosed by taps B, C, D, E, F and G, tap H being opened to the manometer. The pressure shown on the manometer was read to 0.05 mm. using a cathetometer, the temperature of the methane being recorded.

The samples of isopentane and 2-methylpentane were prepared in glass tubes fitted with breakseal tips. The procedure used to obtain the weight of these samples to  $2 \times 10^4$  gm. has been described in Part I of this thesis. Pure methane was measured out in a gas burette surrounded by circulating water at  $25^{\circ}$  C. The burette was calibrated at  $25^{\circ}$  C, using the procedure previously described. The calibrations are shown in Table 1.

The volume enclosed by taps B, C, D, E, F and G which was kept as small as possible using capillary tubing, was measured as a function of the position of the mercury meniscus level below tap H by condensing small

Table 1.

Nominal Value of Mark (ml.)	Measured Value (ml.)
10	10.487
20	20.470
30	30.520
40	40.535
50	50.546
60	60.571
70	70.596
80	80.677
90	90.720
100	100.739

quantities of methane into the glass finger J, the pressure, volume and temperature of these quantities having previously been measured. These quantities of methane were then allowed to expand into the volume enclosed by the above taps, and the pressure, temperature and difference between the mercury level below tap H at vacuum and with methane present measured. It was thus possible to estimate the number of moles of methane which were left in the volume between taps B and C after the main bulb of the methane had been expanded into the bulb A. In all these measurements the number of moles of gas present was calculated from the expression:-

$$n = \frac{pV}{RT+Bp}$$

the appropriate values of B for methane being obtained

from the data of Michels and Nederbraght<sup>22</sup>.

The bulb A and capillary tube were calibrated by filling it with appropriate quantities of mercury, thermostating it at 30° C and then measuring the difference in height between the mercury meniscus and the etched mark using a cathetometer, the weight of mercury present having been previously determined to  $2 \times 10^{-4}$  gm. Allowing for a correction for the shape of the mercury meniscus, the results obtained are shown in Table 2. ( $\Delta h$  denotes difference between the mercury meniscus height and the height of the fixed mark).

Table 2.

$\Delta h$ (cm.)	V (mls.)
-0.103	0.6061
0.151	0.6081
7.469	0.6658
11.849	0.7004

These results were fitted to the equation:-

$$V = 0.6069 + 7.889 \times 10^{-3} \Delta h \dots (3.1)$$

using the method of least squares. From this equation the total volume of liquid in bulb A and the capillary could be determined, allowance being made for the shape of the liquid meniscus and the contraction of the glass on cooling.

The total volume of bulb A and capillary below the metal valve B was measured by filling it with water. Using this and the volume occupied by the liquid sample calculated from equation (3.1) a correction was applied for the number of moles of methane present in the vapour phase, the vapour phase being assumed to be pure methane. The volume occupied by the vapour was treated as two parts, one being at room temperature and the other at the temperature of the cryostat, the appropriate virial coefficients being used to calculate 'n' in each case.

#### The cryostat.

The cryostat is shown schematically in Fig. 4a. The bulb A and 1 mm. precision bore capillary tubing, in which the volume measurements were made, fitted inside a  $\frac{3}{4}$ " diameter cylindrical hole 7" long. This cylindrical hole was cut out of a solid copper cylindrical block of dimensions  $7\frac{1}{2}$ " long by 2" diameter. The copper block was supported from above by two stainless steel rods. The bulb A, capillary tubing and fixed mark could be observed by means of a  $\frac{3}{16}$ " slit 7" long cut out at both front and back of the copper block.

The copper block was surrounded by a silvered Dewar vessel which had a clear strip in it in order that the capillary tubing and bulb could be observed. Cooling

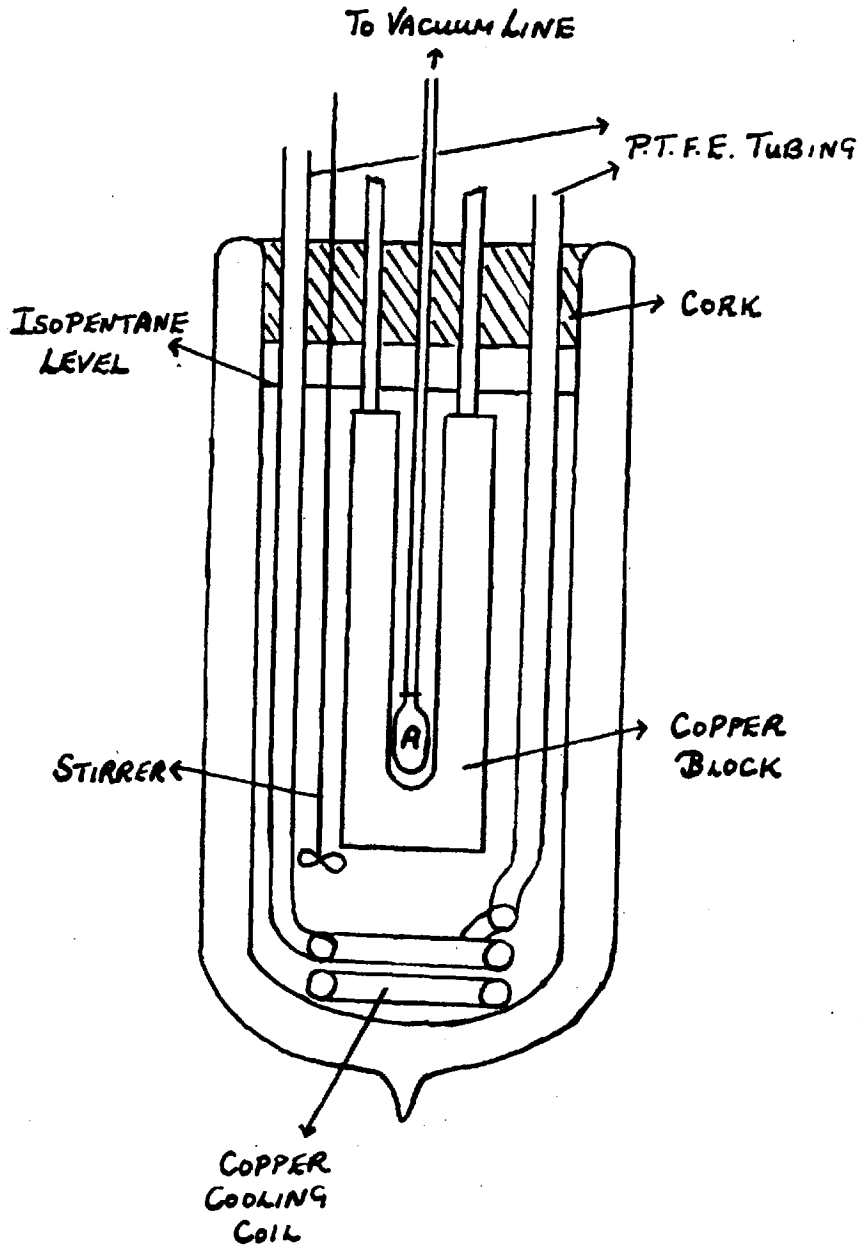


FIG. 4 (a).



was effected by means of a copper coil resting on the base of the Dewar vessel. The copper coil was connected to a 5 gallon metal Dewar vessel of liquid nitrogen placed outside the apparatus by means of P.T.F.E. tubing. The other end of the copper coil also had P.T.F.E. tubing connected to it and was used as a blow off for nitrogen. The Dewar vessel was now filled with isopentane, and liquid nitrogen from the metal Dewar syphoned through the copper coil, the level of the isopentane being maintained at approximately 1" above the copper block. Using this procedure, the isopentane and contents of the Dewar vessel could be cooled quite rapidly to the melting point of isopentane.

The isopentane was stirred by a stainless steel metal stirrer having four pair of blades. The stirrer was situated just below the copper block as shown and was driven by an electric motor. The apparatus was illuminated from behind by a 40 watt tubular lamp.

The temperature of bulb A and the capillary tubing was measured by four copper-constantan thermocouples connected in series. The reference junction was surrounded by pure crushed melting ice contained in a dewar. The ice was prepared from distilled water and its melting point was reproducible to  $0.01^{\circ}$  C. The measuring junction was situated on either side of bulb A inside the copper block. The E.M.F. was measured using

the Tinsley vernier potentiometer, tangent mirror galvanometer and scale described in Part I of this thesis, which was capable of reading to 1 microvolt.

The thermocouple was calibrated over the temperature range  $110^{\circ}$  K to  $155^{\circ}$  K using the procedure previously described for the thermocouple in the first part of this thesis. The hydrocarbons whose triple points were used in this case were isopentane, 2-methylpentane, n-butane, n-pentane and 2, 4-dimethylpentane. These hydrocarbons were obtained from the National Chemical Laboratory and had the purities quoted in Table 3. The samples were sealed in glass tubes in vacuo and placed down the centre of the copper block next to the thermocouple. The E.M.F. at which the onset of melting occurred was noted and the values obtained are recorded in Table 3.

Table 3.

Hydrocarbon	Purity (moles <sup>%</sup> )	Triple Point ( $^{\circ}$ C)	E.M.F. observed (millivolts)
isopentane	100.00	-159.90	20.50 $\pm$ 0.01
2-methylpentane	99.82	-153.60	19.91 $\pm$ 0.01
n-butane	99.97	-138.32	18.44 $\pm$ 0.01
n-pentane	99.98	-129.83	17.59 $\pm$ 0.01
2,4-dimethylpentane	99.70	-119.17	16.49 $\pm$ 0.01

The values for the triple points were obtained from the American Petroleum Institute tables<sup>21</sup>.

The difference in temperature between the reference and measuring junctions,  $\Delta T$ , which is numerically equal to the temperature of the measuring junction in  $^{\circ}\text{C}$ , was fitted to the following polynomial in  $E$ , the measured E.M.F.

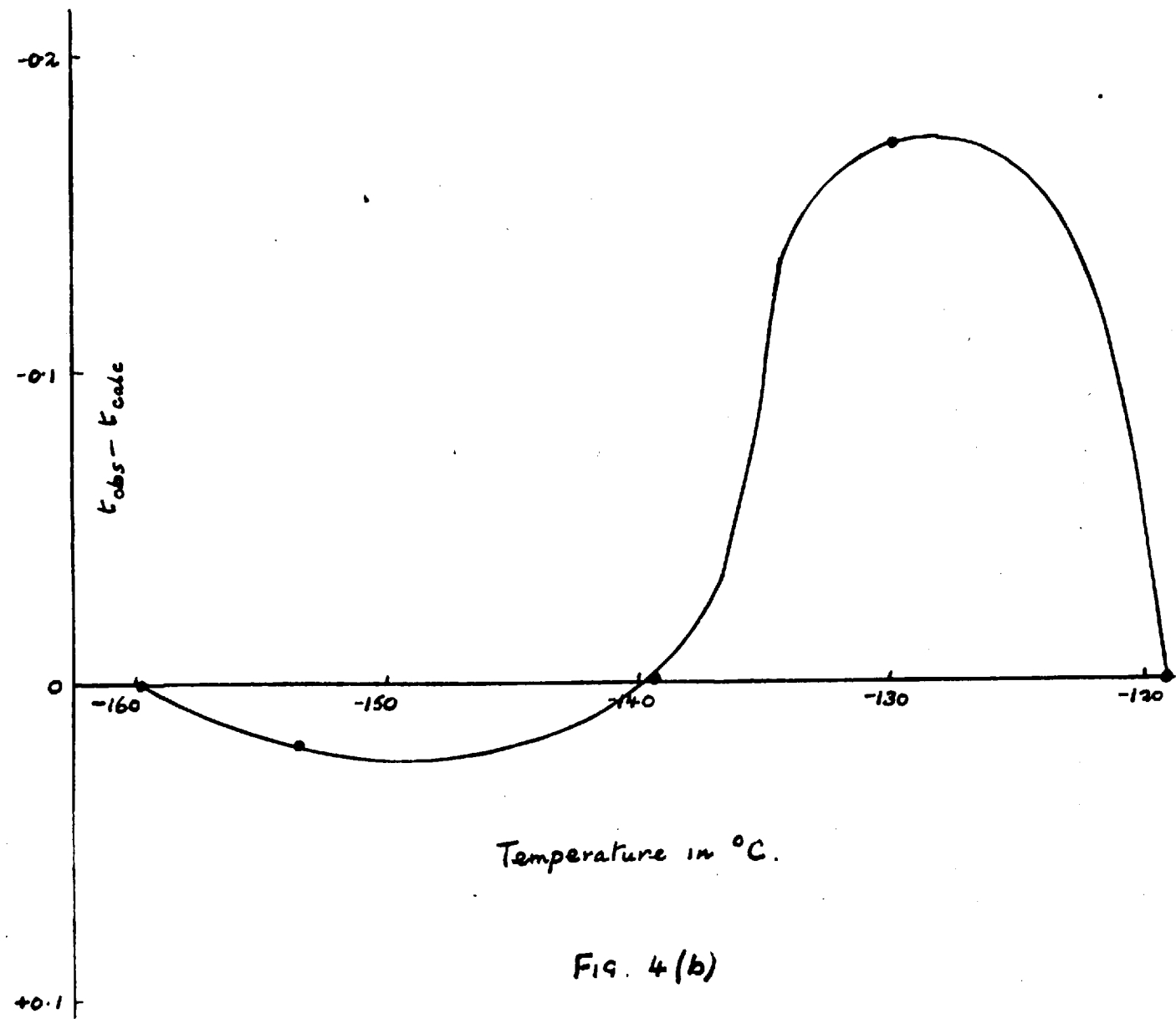
$$\Delta T = 5.245 E + 1.0189 \times 10^{-1} E^2 + 1.1099 \times 10^{-3} E^3 \dots(3.2)$$

where  $E$  is in millivolts.

From these results a correction curve was plotted over the temperature range used and it is shown in Fig. 4b. Using equation (3.2) and the correction curve, the temperature of the measuring junction in  $^{\circ}\text{C}$ , which corresponded to a given E.M.F., could be calculated. It was converted to  $^{\circ}\text{K}$  assuming the temperature of absolute zero was  $-273.15^{\circ}\text{C}$ .

The main source of heat to the cryostat was through the surface of the isopentane and through the fittings dipping into the Dewar vessel. The natural rate of warming was  $0.4^{\circ}/\text{min}$ . at  $115^{\circ}\text{K}$  and  $0.5^{\circ}\text{K}$  at  $155^{\circ}\text{K}$ . The lower value at the lower temperature is due to the presence of solid isopentane at this temperature. The natural rate of warming allowed the temperature to be easily read to  $0.02^{\circ}\text{K}$ .

The procedure adopted to measure the volumes of



Temperature in °C.

FIG. 4 (b)

pure methane, pure isopentane, pure 2-methylpentane was as follows:-

Bulb A was filled with an appropriate amount of liquid with the cryostat at the melting point of isopentane. The quantity of liquid present was such that the liquid meniscus was within 1 cm. of the fixed mark. The cryostat was now allowed to warm naturally and the position of the liquid meniscus read using a cathetometer at a temperature of approximately  $115^{\circ}$  K. This procedure was repeated at approximately  $2^{\circ}$  intervals corresponding to a change of 0.20 millivolts on the potentiometer, until the temperature of the isopentane bath had reached almost  $155^{\circ}$  K. Finally the reading of the fixed mark was taken. The whole procedure was repeated over the whole temperature range until the reading of the liquid meniscus could be reproduced to 0.2 mm. or better. This gave the volumes of the pure substances to 0.03% or better.

In the case of mixtures of methane + isopentane and methane + 2-methylpentane, the following procedure was adopted:-

Bulb A was filled with a suitable quantity of both components and the cryostat allowed to warm to  $155^{\circ}$  K. It was then kept at this temperature for about 2-3 hours in order to mix the components. The cryostat was now cooled to  $115^{\circ}$  K again to allow the liquid in the

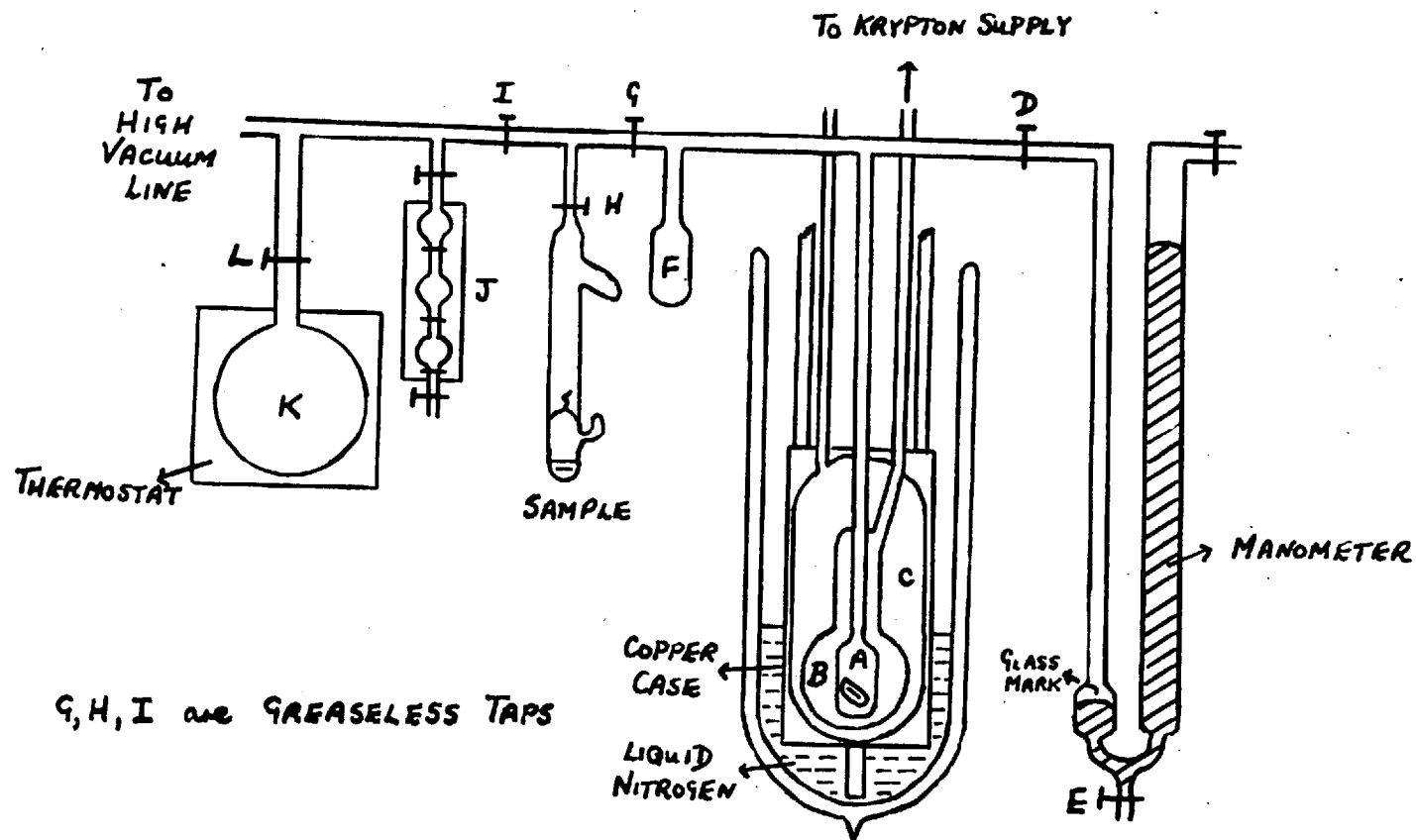


FIG. 5.

capillary which was mainly methane to be mixed with the liquid in the bulb. The cryostat was then warmed to  $155^{\circ}$  K for another two or three hours. It was finally re-cooled to the melting point of isopentane and the readings of the liquid meniscus taken using the procedure described for the pure substances.

#### Vapour pressure measurements.

The vapour pressure of pure methane and of mixtures of methane + 2-methylpentane were made at the triple point of krypton.

#### Details of the Apparatus.

The apparatus is shown schematically in Fig. 5. The pure liquid or liquid mixture under examination was contained in bulb A, which had a volume of about 2 mls. Bulb A was surrounded by a bulb B which contained the solid krypton, and bulb B in turn was surrounded by a larger bulb C which was either evacuated or contained a small pressure of nitrogen for the purpose of better thermal conduction. The inner bulb A contained a small stirrer of soft iron in glass which could be activated by a strong external magnet. The whole glass assembly fitted inside a hollow copper container which was supported from above by three stainless steel tubes. A 4 " length of solid copper rod of  $\frac{1}{4}$  " diameter was affixed

to the base of the copper container. The level of liquid nitrogen in the surrounding Dewar vessel was adjusted in such a way that sufficient cooling was provided to the cryostat by means of this copper rod. A 1700 ohm heater of manganin wire was wound onto the outside of the copper container and it was wired in such a way as to provide heat to the cryostat ranging from 0 - 40 watts.

The mercury manometer was made of 2 cm. internal diameter precision bore glass tubing. The left hand limb of the manometer was designed so that the enclosed gas space between the liquid mixture in bulb A and the mercury level in the left hand limb was kept as small as possible. It therefore consisted of 1 mm. capillary tubing joined to the 2 cm. precision bore tubing, a glass marker being incorporated as shown in order to fix the volume of gas. The mercury level in the manometer could be adjusted by applying a pressure of nitrogen to the mercury contained in a reservoir below tap E. The mercury used in these vapor<sup>u</sup> pressure measurements was prepared by distilling triple distilled mercury into the reservoir under vacuo. The right hand limb of the manometer was of sufficient length that pressures up to 120 cms. could be measured.

The experimental values of the pressure were obtained as a height of mercury. These were corrected



as follows:-

- 1) For capillary depression in each limb from the tables of Kistemaker<sup>49</sup>.
- 2) To standard gravity and 0° C using the expression:-

$$h_o = h_i \frac{\rho_i}{\rho_o} \cdot \frac{g_i}{g_o}$$

where at Imperial College,  $g/g_o = 1.00058$  and

$\frac{\rho_i}{\rho_o} = 1 - \alpha t$ ,  $t$  being the temperature of the mercury in °C and  $\alpha$  the coefficient of expansion of mercury.

The bulb K was calibrated at 25° C to the nearest 0.2 ml. by weighing it empty and full of distilled water. The value obtained was  $1176.6 \pm 0.1$  ml. It was mounted in a large water thermostat which contained constantly circulating water at 25° C. The thermostat was controlled by a mercury regulator and electronic relay.

The glass line connecting the inner bulb A, the tap G and the manometer was made of 1 mm. capillary tubing. The actual volume of this dead space was determined by using known quantities of methane measured out in the calibrated bulb J.

#### Experimental Procedure.

This is described for a liquid mixture of methane + 2-methylpentane. In the case of pure methane a similar procedure was adopted except that no exact quantities were required provided there was both liquid and vapour

present in bulb A.

An accurately weighed sample (prepared and weighed using the method described in Part I of this thesis) of 2-methylpentane was joined to the vacuum line below tap H and the line then completely evacuated. The fine glass tip of the glass breakseal was then broken with taps I and D closed using the method previously described and the 2-methylpentane condensed into bulb A under liquid nitrogen. Krypton from the storage bulbs was now condensed into bulb B under liquid nitrogen, a small quantity<sup>etc</sup> of gaseous nitrogen having previously been admitted to bulb C. When all the krypton had been condensed in, the tap below the storage bulbs was closed and the krypton melted using the heater. This procedure was adopted to ensure all the solid krypton was at the bottom of bulb B. A suitable quantity of methane was measured out in bulb K and its pressure noted. It was then completely condensed into the glass finger F using the 'pump-down' trap of solid nitrogen described earlier. The methane was now allowed to expand<sup>into</sup> bulb A with the krypton at a temperature about  $10^{\circ}$  above its melting point. The mixture was now stirred using the external magnet. This procedure of allowing the mixture to warm to about  $125^{\circ}$  K was adopted since 2-methylpentane melts at  $119.6^{\circ}$  K and it was found that the small glass magnetic stirrer got stuck in the

solid 2-methylpentane. The krypton was now cooled below its triple point by adding more liquid nitrogen to the Dewar vessel. It was then allowed to warm up steadily until the krypton just began to melt. This point could easily be detected in the case of krypton since it has a large triple point pressure of 548 mms. The nitrogen present in bulb C was now pumped away and the cryostatting melting krypton kept at constant temperature by adjusting the liquid nitrogen level on the copper rod, a check on the temperature distribution on the copper container being made by means of thermocouples placed at the top and bottom of the container. When the monometer became steady, the mercury level in the left hand limb was raised slightly until it just touched the glass marker. The difference in height between the two mercury levels in the manometer was now read using a cathetometer. In the case of pure methane, two cathetometers had to be used as the vapour pressure of methane at the triple point of krypton was approximately 106 cms. The two cathetometers were related to each other by using fixed marks on the right hand limb of the manometer.

The number of moles of methane present was calculated from the expression:-

$$n = \frac{pV}{RT + Bp}$$

using the values of the second virial coefficient of methane previously mentioned<sup>22</sup>. Allowance was made for the number of moles of methane present in the vapour phase between the liquid mixture and the manometer. This dead space volume was treated as being at room temperature.

### Calculation of the excess free energy.

Consider a binary liquid mixture of two components 1 and 2. For the liquid phase:-

$$\mu_1(\text{liq}, p, x_1) = \mu_1^\circ(\text{liq}, p^*) + RT \ln x_1 \gamma_1 + (p - p^*) v_1^\circ \dots (3.3)$$

$$\mu_2(\text{liq}, p, x_2) = \mu_2^\circ(\text{liq}, p^*) + RT \ln x_2 \gamma_2 + (p - p^*) v_2^\circ \dots (3.4)$$

where  $p$  is a small but arbitrary pressure.

For the gas phase:-

$$\begin{aligned} \mu_1(\text{gas}, p, y_1) = & \mu_1^\circ(\text{gas}, p^*) + RT \ln \left( \frac{p y_1}{p^*} \right) \\ & + (p - p^*) B_{11} + 2p (\delta B)_{12} y_2^2 \dots (3.5) \end{aligned}$$

$$\begin{aligned} \mu_2(\text{gas}, p, y_2) = & \mu_2^\circ(\text{gas}, p^*) + RT \ln \left( \frac{p y_2}{p^*} \right) \\ & + (p - p^*) B_{22} + 2p (\delta B)_{12} y_1^2 \dots (3.6) \end{aligned}$$

where  $y$  denotes the mole fraction in the gas phase, and  $B_{11}$ ,  $B_{22}$  and  $B_{12}$  are the second virial coefficient for the interactions of the pairs of molecules 1-1, 2-2 and 1-2.

$$(\delta B)_{12} = B_{12} - \frac{1}{2} B_{11} - \frac{1}{2} B_{22}$$

The arbitrary pressure is now put equal to  $p_1^\circ$ , the vapour pressure of pure 1 in equations (3.3) and (3.5) and to  $p_2^\circ$  in equations (3.4) and (3.6).

Equating  $\mu_1$  and  $\mu_2$  in each phase, we get:-

$$\begin{aligned} \mu_1^\circ(\text{liq}, p_1^\circ) + RT \ln x_1 \gamma_1 + (p - p_1^\circ) v_1^\circ \\ = \mu_1^\circ(\text{gas}, p_1^\circ) + RT \ln \left( \frac{p y_1}{p_1^\circ} \right) + (p - p_1^\circ) \beta_{11} + 2p (\delta B)_{12} y_2^2 \end{aligned} \quad (3.7)$$

$$\begin{aligned} \mu_2^\circ(\text{liq}, p_2^\circ) + RT \ln x_2 \gamma_2 + (p - p_1^\circ) v_2^\circ \\ = \mu_2^\circ(\text{gas}, p_2^\circ) + RT \ln \left( \frac{p y_2}{p_2^\circ} \right) + (p - p_2^\circ) \beta_{22} + 2p (\delta B)_{12} y_1^2 \end{aligned} \quad (3.8)$$

Since:-

$$\mu_1^\circ(\text{liq}, p_1^\circ) = \mu_1^\circ(\text{gas}, p_1^\circ) \text{ and } \mu_2^\circ(\text{liq}, p_2^\circ) = \mu_2^\circ(\text{gas}, p_2^\circ)$$

then

$$\begin{aligned} RT \ln p = RT \ln \left( \frac{x_1 \gamma_1 p_1^\circ}{y_1} \right) + (p - p_1^\circ) (v_1^\circ - \beta_{11}) - 2p (\delta B)_{12} y_2^2 \\ = RT \ln \left( \frac{x_2 \gamma_2 p_2^\circ}{y_2} \right) + (p - p_2^\circ) (v_2^\circ - \beta_{22}) - 2p (\delta B)_{12} y_1^2 \end{aligned}$$

whence

$$\begin{aligned} p = x_1 \gamma_1 p_1^\circ \exp \left[ \frac{(p - p_1^\circ) (v_1^\circ - \beta_{11}) - 2p (\delta B)_{12} y_2^2}{RT} \right] \\ + x_2 \gamma_2 p_2^\circ \exp \left[ \frac{(p - p_2^\circ) (v_2^\circ - \beta_{22}) - 2p (\delta B)_{12} y_1^2}{RT} \right] \end{aligned} \quad \dots (3.9)$$

For the system methane + 2-methylpentane, the following assumptions are justifiably made

- 1) Since  $p_2^0$  is of the order of  $10^{-4}$  mm., then the second term in equation (3.9) is negligibly small.
- 2) The vapour phase is pure methane i.e.  $y_1 = 1$  and  $y_2 = 0$

Equation (3.9) reduces to

$$p = x_1 \gamma_1 p_1^0 \exp \left[ \frac{(p-p_1^0)(v_1^0 - B_{11})}{RT} \right]$$

or  $RT \ln \gamma_1 = RT \ln \left( \frac{p}{p_1^0 x_1} \right) - (p-p_1^0)(v_1^0 - B_{11}) \dots (3.10)$

Hence  $\ln \gamma_1$  can be calculated.

If we now assume that the activity coefficients are of the form:-

$$\ln \gamma_1 = a_1 x_2 + b_1 x_2^2 + c_1 x_2^3 + \dots$$

$$\ln \gamma_2 = a_2 x_1 + b_2 x_1^2 + c_2 x_1^3 + \dots$$

Then applying the Gibbs-Duhem Equation:-

$$x_1 \frac{d \ln \gamma_1}{dx_2} + x_2 \frac{d \ln \gamma_2}{dx_2} = 0$$

we get:-

$$a_1 = a_2 = 0$$

$$b_2 = b_1 + \frac{3c_1}{2}$$

$$c_2 = -c_1$$

Then  $\ln \gamma_2$  may be determined, and  $g^E$  found using the expression:-

$$g^E = RT (x_1 \ln \gamma_1 + x_2 \ln \gamma_2)$$

CHAPTER IV.RESULTS AND DISCUSSION.The Volume Measurements.

Experimental volume measurements were made on pure methane, pure 2-methylpentane and pure isopentane over the temperature range  $115^{\circ}$  K to  $155^{\circ}$  K. Table 4 lists the results obtained for the molar volume of three samples of pure methane and Fig. 6 shows the variation of molar volume of methane obtained by taking the average value of the three samples, with temperature. In Fig. 6, the results obtained here are compared with those of Keyes, Taylor and Smith<sup>50</sup> and Bloomer and Parent<sup>51</sup> in this temperature range. The deviation from the results of Keyes and co-workers varies from a minimum of 0.4% to a maximum of 0.9%. It is, however, worthwhile pointing out here that the value of the molar volume of pure methane at  $90.7^{\circ}$  K obtained by Mathot, Staveley, Young and Parsonage<sup>51</sup> differs from that deduced from the results of Keyes and co-workers, using the method of first and second differences, by + 0.7%.

Table 5 lists the experimental values for the molar volumes of pure 2-methylpentane and pure isopentane, whilst Figs. 7 and 8 show the variation of molar volume with temperature for these two hydrocarbons.

The results for the volume per mole of liquid mixture against the mole fraction of 2-methylpentane or isopentane ( $x_2$ ) for seven liquid mixtures of the system methane + 2-methylpentane and five liquid mixtures of the system methane + isopentane are listed in Tables 6 - 10. The variation of the volume per mole of liquid mixture against temperature for each of the mixtures is shown in Figs. 9 - 20.

From the graphs, the quantity  $v^E$  (the excess volume per mole of mixture) was calculated using the relation

$$v^E = v - x_1 v_1^0 - x_2 v_2^0$$

where  $v_1^0$  and  $v_2^0$  are the molar volumes of the pure substances

$x_1$  and  $x_2$  are the mole fractions of components 1 and 2 respectively

$v$  is the volume per mole of liquid mixture.

Values of  $v^E$  were obtained at nine different temperatures, namely 115° K, 120° K, 130° K, 140° K, 145° K, 150° K and 155° K. The results obtained are listed in Tables 11 - 15. Fig. 21 shows the variation of  $v^E$  with mole fraction  $x_2$  for the system methane + 2-methylpentane and Fig. 22 shows the  $v^E - x_2$  graph for the system methane + isopentane, curves being drawn at the nine different temperatures.



The Vapour Pressure Measurements.

The vapour pressure of pure methane and four mixtures of methane + 2-methylpentane was determined at the triple point of krypton. The triple point of krypton was taken to be  $115.95^{\circ} \text{K}$  <sup>53, 54, 55</sup>.

The experimental values obtained in this work for three samples of pure methane are listed in Table 16. The average value is compared with those of other workers in Table 17.

It can be seen that the results obtained here seem to be a little low. This may be explained by the fact that there were small traces of impurity in the krypton. This, however, should have no effect on the values of  $g^E$  obtained for the mixtures. It merely means that the temperature scale used here does not correspond exactly with the absolute temperature scale.

The values of the vapour pressure of the liquid mixture at a mole fraction  $x_2$  are listed in Table 18. From these results the  $p - x_2$  graph shown in Fig. 23 was plotted, and the values of  $\ln\gamma_1$  and  $\ln\gamma_2$  calculated as previously described. These were fitted to the equations:-

$$\ln\gamma_1 = 3.385 x_2^2 - 3.38 x_2^3$$

$$\ln\gamma_2 = -1.235 x_1^2 + 3.38 x_1^3$$

using graphical methods.

Hence  $g^E$  was calculated from the expression

$$g^E = RT (x_1 \ln \gamma_1 + x_2 \ln \gamma_2)$$

The values obtained are shown in Table 19, whilst Fig. 24 shows the form of the  $g^E$  against  $x_2$  plot.

### Discussion.

Qualitative conclusions can be drawn fairly easily from these results. As we have mentioned earlier in this thesis, the thermodynamic requirements for a system to show a L.C.S.T. is that:-

$$g^E > 0, h^E < 0, s^E < 0 \text{ and } v^E < 0$$

From the results obtained, it can be seen that the system methane + 2-methylpentane which show a L.C.S.T. at  $194.7^\circ$  K conforms to these requirements even at very low temperatures, since at  $116^\circ$  K,  $v^E$  is negative and  $g^E$  is positive. As we have shown experimentally  $v^E$  becomes more negative as the temperature increases and for this system we should expect it to have a maximum value of about  $-10 \text{ cc. mole}^{-1}$  when separation occurs.

Comparison with the system methane + isopentane, which has been shown to be miscible over the whole liquid range, suggests that there must be a critical value of  $v^E$  where separation occurs in these methane + hydrocarbon systems. As we have stated earlier, a

negative value of  $v^E$  is a necessary but not sufficient requirement for a system to show a L.C.S.T. and it can be seen that the value of  $v^E$  for the system methane + isopentane becomes quite highly negative as the temperature increases, though it is not as negative as  $v^E$  for the system methane + 2-methylpentane. It is in fact usual for  $v^E$  to be negative for molecules of different sizes,  $v^E$  becoming more negative the greater the difference in size between the two molecules. This is in fact found with these two systems.

For both these systems, the plot of  $v^E - x_2$  is asymmetric, the ~~symmetry~~ <sup>minima</sup> being displaced to the side of the ~~larger~~ <sup>smaller</sup> component. For the system methane + 2-methylpentane, the maximum value of  $v^E$  occurs when  $x_2 \sim 0.30$  whilst for the system methane + isopentane  $v^E_{\max}$  occurs at  $x_2 \sim 0.35$ . Thus as expected, the curve becomes more asymmetric as the difference in molecular size increases.

The  $g^E - x_2$  curve is also slightly asymmetric for the system methane + 2-methylpentane. About  $115.95^\circ \text{K}$ , the maximum value of  $g^E$  is  $339 \text{ joules mole}^{-1}$  and it occurs when  $x_2 = 0.375$ . For very simple systems of non-polar liquids  $g^E$  is usually of the order of  $0 \rightarrow 0.15RT$  whilst for aliphatic hydrocarbons of similar size,  $g^E$  is quite often very small. Even for the system

n-hexane + n-hexadecane,  $g^E$  is only of the order of  $-0.03RT$  at  $20^\circ$  C. Thus, the value of  $g^E$  of  $\sim 0.35RT$  obtained here is quite large (in fact it is more comparable with the values of  $g^E$  obtained for a liquid mixture of an aliphatic and an aromatic hydrocarbon). This suggests that there is a large difference in molecular energies between methane and 2-methylpentane as is to be expected for a system that separates into two liquid phases.

We can conclude therefore that the production of a L.C.S.T. in a system containing two hydrocarbons depends on all the thermodynamic functions  $g^E$ ,  $h^E$ ,  $s^E$  and  $v^E$  having the right sign and size. It is however very difficult to deduce anything about the difference in energies and sizes of similar molecules that determine whether a hydrocarbon is miscible with liquid methane or not. It is hoped that when the present results have been looked into from a more quantitative angle, this will be possible.

Table 4.

Volume of pure methane (cc. mole<sup>-1</sup>)

Temperature °K.	Sample A	Sample B	Sample C	Average Value
115.39	38.51	38.53	38.44	38.49
117.53	38.83	38.85	38.74	38.81
119.66	39.14	39.16	39.04	39.11
121.77	39.46	39.49	39.36	39.44
123.88	39.79	39.82	39.69	39.77
125.97	40.11	40.14	40.02	40.09
128.05	40.43	40.46	40.36	40.42
130.12	40.78	40.82	40.70	40.77
132.17	41.13	41.17	41.07	41.12
134.22	41.48	41.52	41.43	41.43
136.27	41.85	41.89	41.80	41.85
138.31	42.23	42.26	42.18	42.22
140.39	42.63	42.66	42.57	42.62
142.40	43.02	43.06	42.97	43.02
144.38	43.43	43.47	43.38	43.43
146.32	43.85	43.89	43.81	43.85
148.24	44.29	44.34	44.26	44.30
150.13	44.75	44.79	44.71	44.75
152.01	45.22	45.26	45.20	45.23
153.88	45.71	45.75	45.68	45.71

Table 5.

Volumes of pure isopentane  
and pure 2-methylpentane.

---

Temperature °K	Pure Isopentane (cc. mole <sup>-1</sup> )	Pure 2-methylpentane (cc. mole <sup>-1</sup> )
115.39	91.81	106.61
117.53	92.05	106.89
119.66	92.30	107.15
121.77	92.54	107.40
123.88	92.78	107.66
125.97	93.01	107.92
128.05	93.24	108.16
130.12	93.47	108.42
132.17	93.70	108.66
134.22	93.93	108.90
136.27	94.14	109.14
138.31	94.38	109.38
140.39	94.60	109.62
142.40	94.81	109.86
144.38	95.03	110.08
146.32	95.25	110.31
148.24	95.46	110.55
150.13	95.68	110.77
152.01	95.91	110.99
153.88	96.11	111.24

---

Table 6.

Volumes and mole fractions of mixtures  
of methane + 2-methylpentane.

Temperature (°K)	$x_2$	Volume cc/mole	$x_2$	Volume cc/mole	$x_2$	Volume cc/mole
115.39	0.043	40.85	0.094	43.89	0.156	48.09
117.53	0.043	41.12	0.094	44.14	0.156	48.32
119.66	0.043	41.41	0.094	44.38	0.156	48.58
121.77	0.043	41.68	0.094	44.65	0.156	48.83
123.88	0.043	41.97	0.094	44.90	0.156	49.07
125.97	0.043	42.24	0.094	45.15	0.157	49.31
128.05	0.043	42.53	0.094	45.41	0.157	49.56
130.12	0.043	42.82	0.094	45.66	0.157	49.80
132.17	0.043	43.04	0.094	45.93	0.157	50.04
134.22	0.043	43.41	0.094	46.20	0.157	50.29
136.27	0.043	43.72	0.094	46.46	0.157	50.53
138.31	0.043	44.01	0.094	46.74	0.157	50.78
140.39	0.043	44.34	0.094	47.00	0.157	51.03
142.40	0.043	44.66	0.094	47.28	0.157	51.28
144.38	0.043	44.99	0.094	47.56	0.157	51.54
146.32	0.043	45.32	0.094	47.84	0.157	51.79
148.24	0.043	45.65	0.094	48.12	0.157	52.04
150.13	0.043	45.99	0.094	48.41	0.157	52.29
152.01	0.043	46.34	0.094	48.71	0.157	52.55
153.88	0.043	46.70	0.095	49.01	0.158	52.81

Table 7.

Volumes and mole fractions of  
methane + 2-methylpentane.

Temperature (°K)	$x_2$	Volume (cc. mole <sup>-1</sup> )	$x_2$	Volume (cc. mole <sup>-1</sup> )
115.39	0.251	54.44	0.339	60.41
117.53	0.251	54.63	0.339	60.62
119.66	0.251	54.85	0.339	60.86
121.77	0.251	55.08	0.339	61.11
123.88	0.251	55.29	0.339	61.34
125.97	0.251	55.47	0.339	61.55
128.05	0.251	55.67	0.339	61.78
130.12	0.251	55.86	0.339	61.99
132.17	0.252	56.06	0.340	62.12
134.22	0.252	56.24	0.340	62.41
136.27	0.252	56.44	0.340	62.62
138.31	0.252	56.62	0.340	62.83
140.39	0.252	56.82	0.340	63.05
142.40	0.252	57.01	0.340	63.26
144.38	0.252	57.19	0.341	63.46
146.32	0.252	57.38	0.341	63.67
148.24	0.253	57.55	0.341	63.86
150.13	0.253	57.74	0.341	64.08
152.01	0.253	57.92	0.341	64.27
153.88	0.253	58.10	0.342	64.48



Table 8.

Volumes and mole fractions of  
methane + 2-methylpentane.

Temperature (°K)	$x_2$	Volume (cc. mole <sup>-1</sup> )	$x_2$	Volume (cc. mole <sup>-1</sup> )
115.39	0.476	69.81	0.677	83.89
117.53	0.476	70.04	0.677	84.11
119.66	0.477	70.25	0.678	84.32
121.77	0.477	70.48	0.678	84.54
123.88	0.477	70.69	0.678	84.75
125.97	0.477	70.89	0.678	84.95
128.05	0.477	71.09	0.678	85.15
130.12	0.477	71.30	0.678	85.35
132.17	0.477	71.49	0.678	85.55
134.22	0.477	71.71	0.679	85.73
136.27	0.478	71.89	0.679	85.92
138.21	0.478	72.09	0.679	86.09
140.39	0.478	72.28	0.679	86.27
142.40	0.478	72.47	0.679	86.44
144.38	0.479	72.65	0.680	86.60
146.32	0.479	72.84	0.680	86.76
148.24	0.479	73.02	0.680	86.92
150.13	0.479	73.19	0.681	87.07
152.01	0.480	73.36	0.681	87.22
153.88	0.480	73.52	0.681	87.35

Table 9.

Volumes and mole fractions of mixtures  
of methane + isopentane.

Temperature (°K)	$x_2$	Volume cc/mole	$x_2$	Volume cc/mole	$x_2$	Volume cc/mole
115.39	0.040	39.81	0.107	43.00	0.236	49.85
117.53	0.040	40.09	0.107	43.25	0.236	50.08
119.66	0.040	40.38	0.107	43.51	0.236	50.30
121.77	0.040	40.66	0.107	43.76	0.236	50.53
123.88	0.040	40.95	0.107	44.00	0.236	50.75
125.97	0.040	41.23	0.107	44.25	0.236	50.97
128.05	0.040	41.53	0.107	44.51	0.236	51.19
130.12	0.040	41.83	0.107	44.76	0.237	51.41
132.17	0.040	42.13	0.107	45.02	0.237	51.64
134.22	0.040	42.43	0.107	45.28	0.237	51.87
136.27	0.040	42.74	0.107	45.54	0.237	52.09
138.31	0.040	43.06	0.107	45.81	0.237	52.31
140.39	0.040	43.39	0.107	46.09	0.237	52.54
142.40	0.040	43.72	0.107	46.36	0.237	52.76
144.38	0.040	44.05	0.107	46.62	0.237	52.97
146.32	0.040	44.39	0.107	46.90	0.237	53.19
148.24	0.040	44.74	0.107	47.19	0.237	53.42
150.13	0.040	45.10	0.107	47.48	0.238	53.64
152.01	0.040	45.48	0.107	47.77	0.238	53.86
153.88	0.040	45.86	0.107	48.05	0.238	54.08

Table 10.

Volumes and mole fractions of  
methane + isopentane.

Temperature (°K)	$x_2$	Volume (cc. mole <sup>-1</sup> )	$x_2$	Volume (cc. mole <sup>-1</sup> )
115.39	0.401	58.64	0.720	76.18
117.53	0.401	58.82	0.720	76.39
119.66	0.401	59.05	0.720	76.60
121.77	0.401	59.28	0.720	76.82
123.88	0.401	59.49	0.720	77.02
125.97	0.402	59.69	0.720	77.20
128.05	0.402	59.90	0.720	77.40
130.12	0.402	60.10	0.721	77.58
132.17	0.402	60.29	0.721	77.77
134.22	0.402	60.49	0.721	77.95
136.27	0.402	60.70	0.721	78.13
138.31	0.402	60.89	0.721	78.30
140.39	0.402	61.07	0.721	78.46
142.40	0.403	61.26	0.722	78.63
144.38	0.403	61.45	0.722	78.79
146.32	0.403	61.64	0.722	78.96
148.24	0.403	61.83	0.722	79.10
150.13	0.403	62.02	0.722	79.25
152.01	0.404	62.21	0.723	79.39
153.88	0.404	62.39	0.723	79.51

Table 11.

Excess Volumes and mole fractions of mixtures  
of methane + 2-methylpentane.

Temperature (°K)	$x_2$	$v^E$ (cc/mole)	$x_2$	$v^E$ (cc/mole)	$x_2$	$v^E$ (cc/mole)
115	0.043	-0.57	0.094	-0.87	0.156	-1.03
120	0.043	-0.65	0.094	-1.12	0.156	-1.18
125	0.043	-0.76	0.094	-1.28	0.157	-1.35
130	0.043	-0.87	0.094	-1.46	0.157	-1.56
135	0.043	-1.00	0.094	-1.67	0.157	-1.80
140	0.043	-1.16	0.094	-1.91	0.157	-2.07
145	0.043	-1.35	0.094	-2.20	0.157	-2.42
150	0.043	-1.60	0.094	-2.57	0.157	-2.84
155	0.043	-1.92	0.095	-3.00	0.158	-3.36

Table 12.

Excess volumes and mole fractions of mixtures  
of methane + 2-methylpentane.

Temperature (°K)	$x_2$	$v^E$ (cc/mole)	$x_2$	$v^E$ (cc/mole)
115	0.251	-1.21	0.339	-1.18
120	0.251	-1.35	0.339	-1.30
125	0.251	-1.61	0.339	-1.49
130	0.251	-1.91	0.339	-1.75
135	0.252	-2.25	0.340	-2.01
140	0.252	-2.65	0.340	-2.34
145	0.252	-3.12	0.341	-2.73
150	0.253	-3.68	0.341	-3.21
155	0.253	-4.34	0.342	-3.75

Table 13.

Excess volumes and mole fractions of mixtures  
of methane + 2-methylpentane.

Temperature (°K)	$x_2$	$v^E$ (cc/mole)	$x_2$	$v^E$ (cc/mole)
115	0.476	-1.17	0.677	-0.76
120	0.477	-1.29	0.678	-0.87
125	0.477	-1.49	0.678	-1.05
130	0.477	-1.73	0.678	-1.27
135	0.478	-2.00	0.679	-1.51
140	0.478	-2.34	0.679	-1.82
145	0.479	-2.74	0.680	-2.18
150	0.479	-3.21	0.681	-2.63
155	0.480	-3.77	0.681	-3.12

Table 14.

Excess volumes and mole fractions of  
mixtures of methane + isopentane.

Temperature (°K)	$x_2$	$v^E$ (cc/mole)	$x_2$	$v^E$ (cc/mole)
115	0.040	-0.77	0.107	-1.15
120	0.040	-0.85	0.107	-1.29
125	0.040	-0.92	0.107	-1.45
130	0.040	-1.03	0.107	-1.63
135	0.040	-1.14	0.107	-1.83
140	0.040	-1.28	0.107	-2.08
145	0.040	-1.44	0.107	-2.37
150	0.040	-1.65	0.107	-2.73
155	0.040	-1.89	0.107	-3.16

Table 15.

Excess volumes and mole fractions of mixtures  
of methane + isopentane.

Temperature (°K)	$v^E$		$v^E$		$v^E$	
	$x_2$	cc/mole	$x_2$	cc/mole	$x_2$	cc/mole
115	0.236	-1.22	0.401	-1.26	0.720	-0.69
120	0.236	-1.39	0.401	-1.39	0.720	-0.80
125	0.236	-1.58	0.401	-1.62	0.720	-0.95
130	0.237	-1.82	0.402	-1.85	0.721	-1.14
135	0.237	-2.07	0.402	-2.13	0.721	-1.36
140	0.237	-2.39	0.402	-2.44	0.721	-1.63
145	0.237	-2.75	0.403	-2.81	0.722	-1.93
150	0.238	-3.20	0.403	-3.27	0.722	-2.29
155	0.238	-3.58	0.404	-3.81	0.723	-2.74

Table 16.

Vapour Pressure of Pure Methane at 115.95° K.

Sample	Pressure (mm. Hg)
1.	1056.1
2.	1057.2
3.	1058.4

The average value for the vapour pressure of methane at 115.95° K was taken as 1057.2 ± 1.5 mms.

Table 17.

Vapour Pressure of pure methane deduced  
from other workers at 115.95° K.

Source	Pressure (mm. Hg).
National Bureau of Standards (A.P.I. Project 1953)	1065.7
National Bureau of Standards (I.C.T. Value)	1067
Keyes and co-workers (1922)	1077
Bloomer and Parent	1067
This work	1057.2

Table 18.

Vapour Pressures of mixtures of methane  
+ 2-methylpentane at 115.95° K.

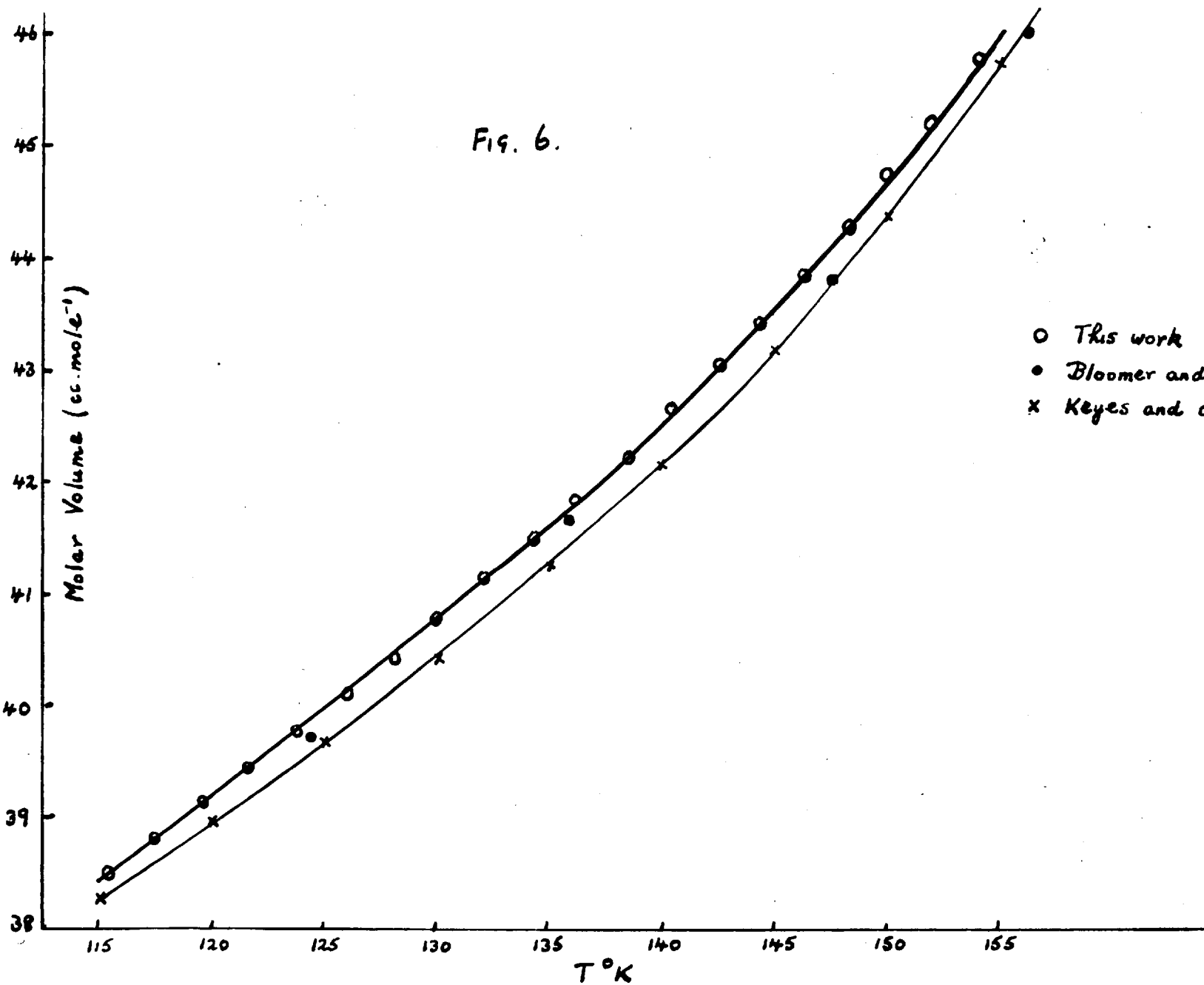
Mole Fraction ( $x_2$ )	Vapour Pressure (mm. Hg).
0.102	1012.6
0.274	956.3
0.482	906.9
0.741	575.2

Table 19.

Excess Free Energy of mixtures of  
methane + 2-methylpentane.

Mole Fraction ( $x_2$ )	$g^E$ (joules mole <sup>-1</sup> )
0.102	173.9
0.274	323.8
0.482	315.8
0.741	168.2

Fig. 6.



- This work
- Bloomer and Parent.
- × Keyes and coworkers.



2-METHYLPENTANE

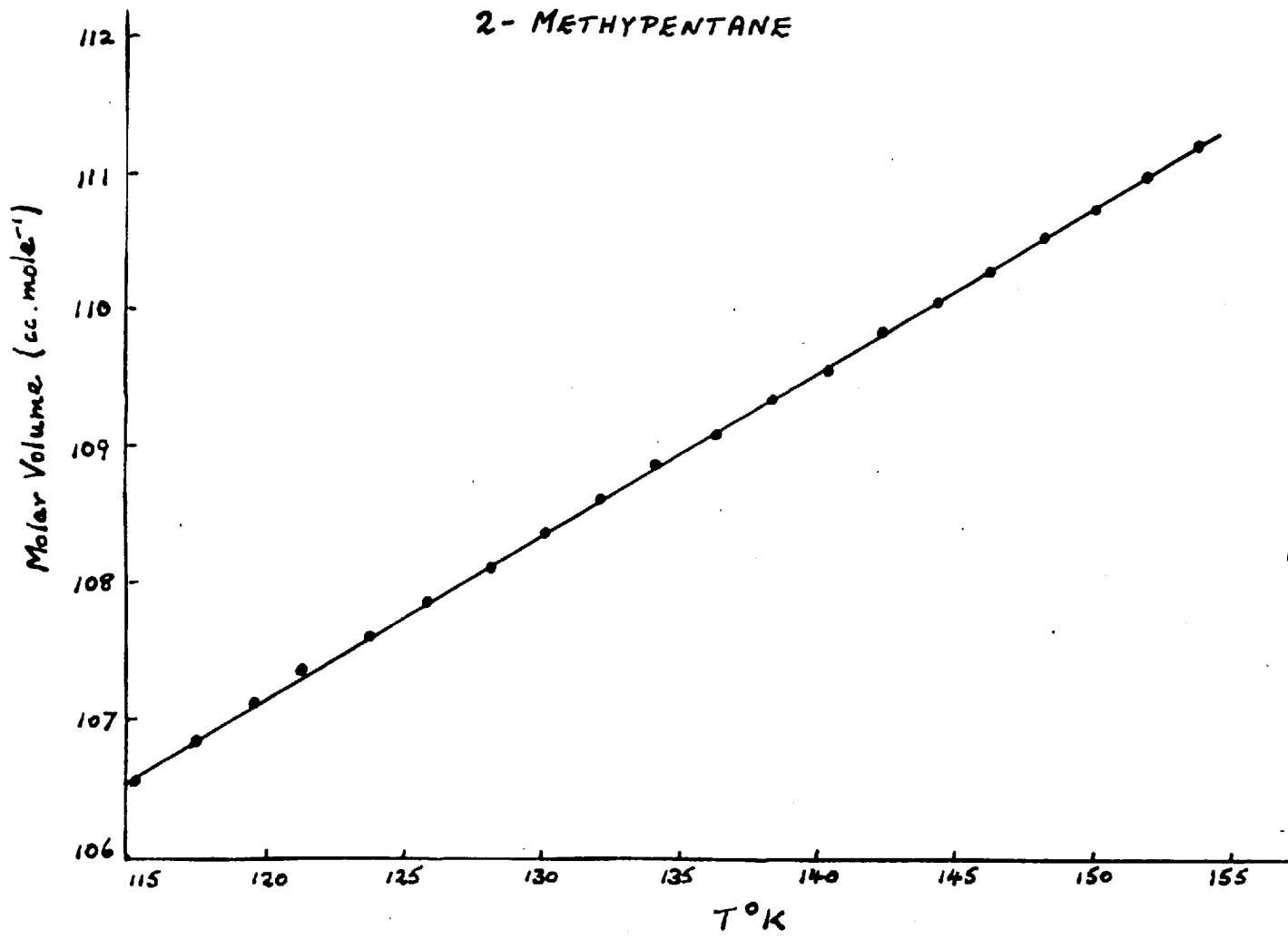


FIG. 7.

ISOPENTANE

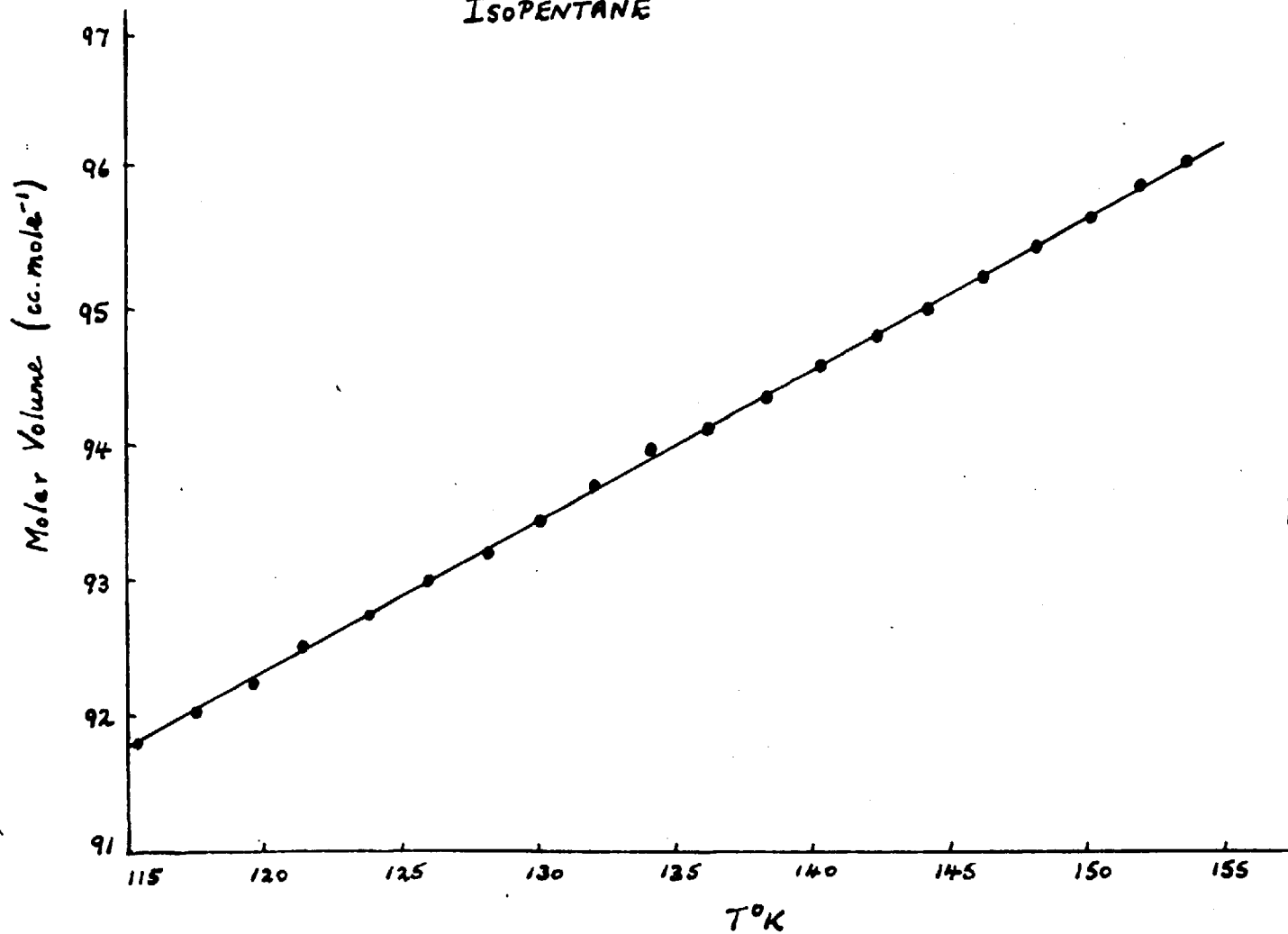
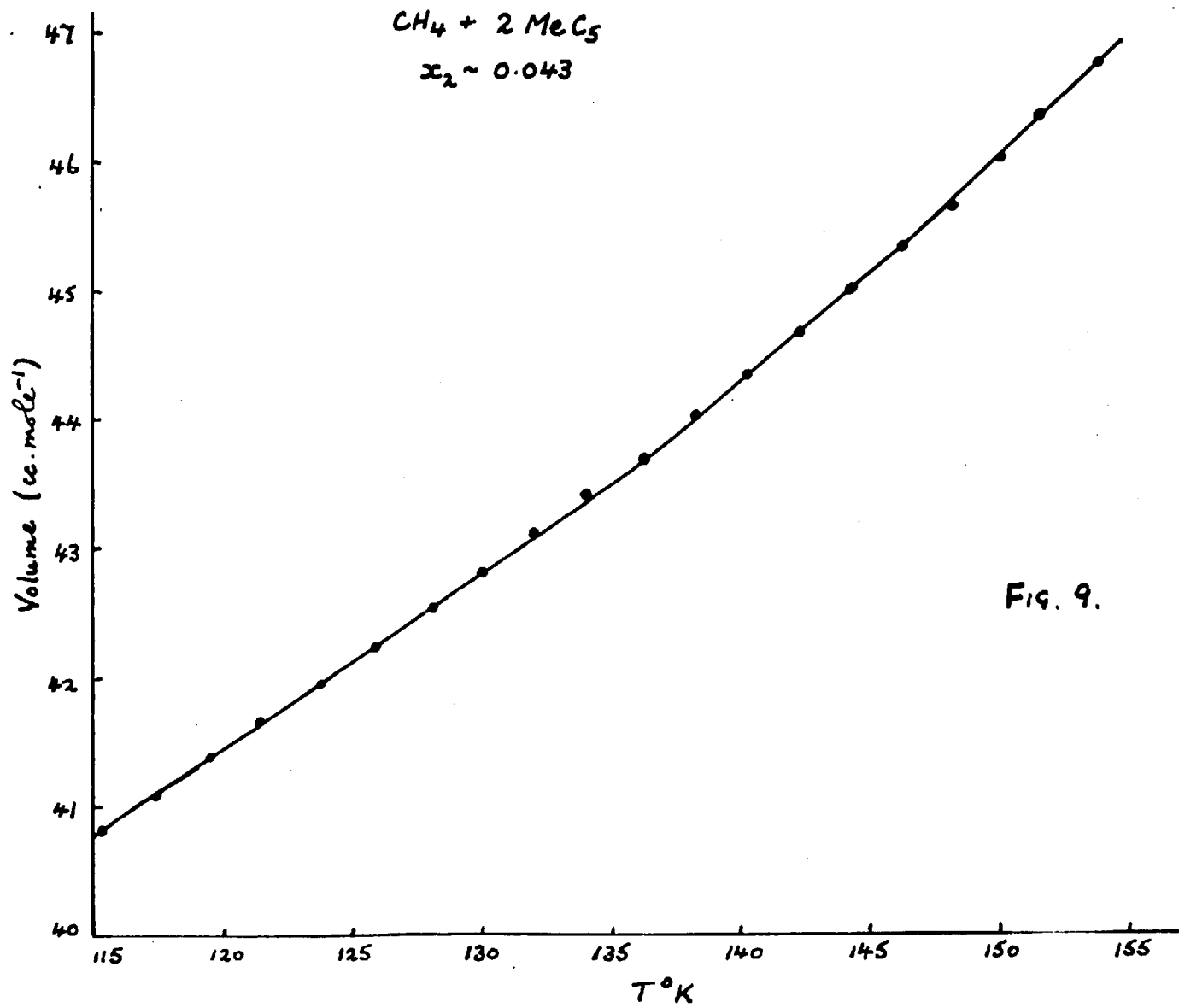


Fig. 8.



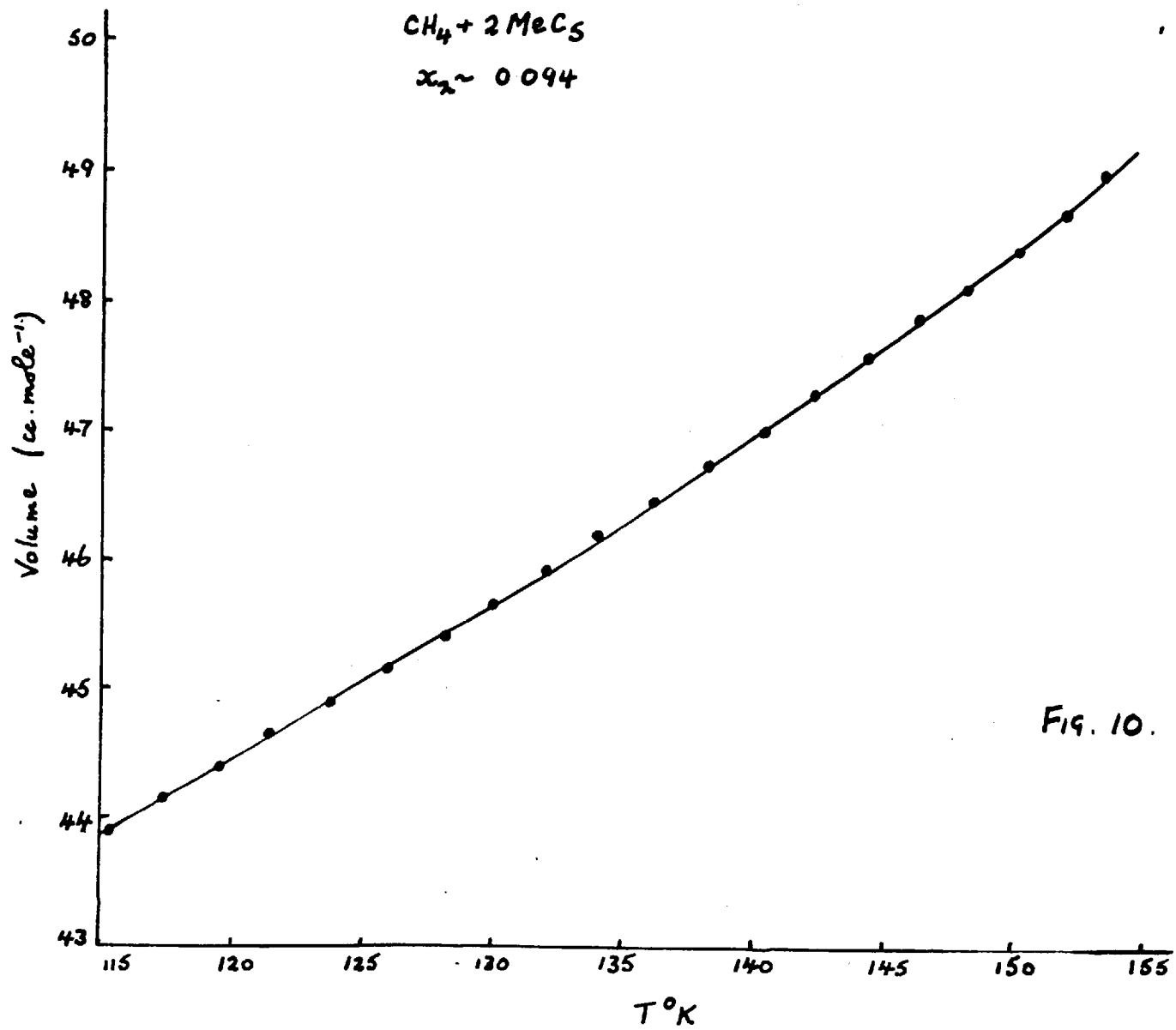


Fig. 10.

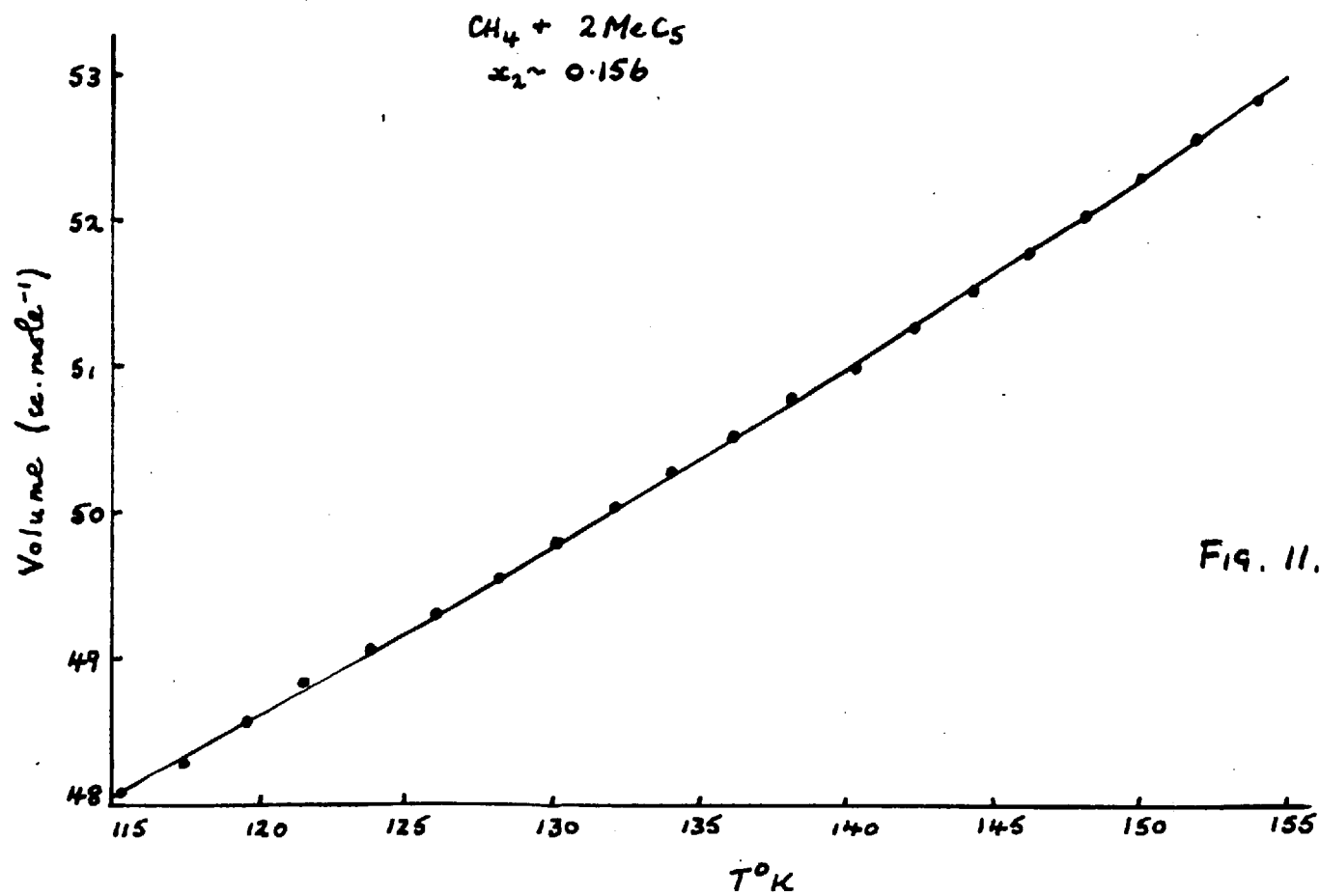


Fig. 11.

$\text{CH}_4 + 2 \text{MeCs}$

$x_2 \sim 0.251$

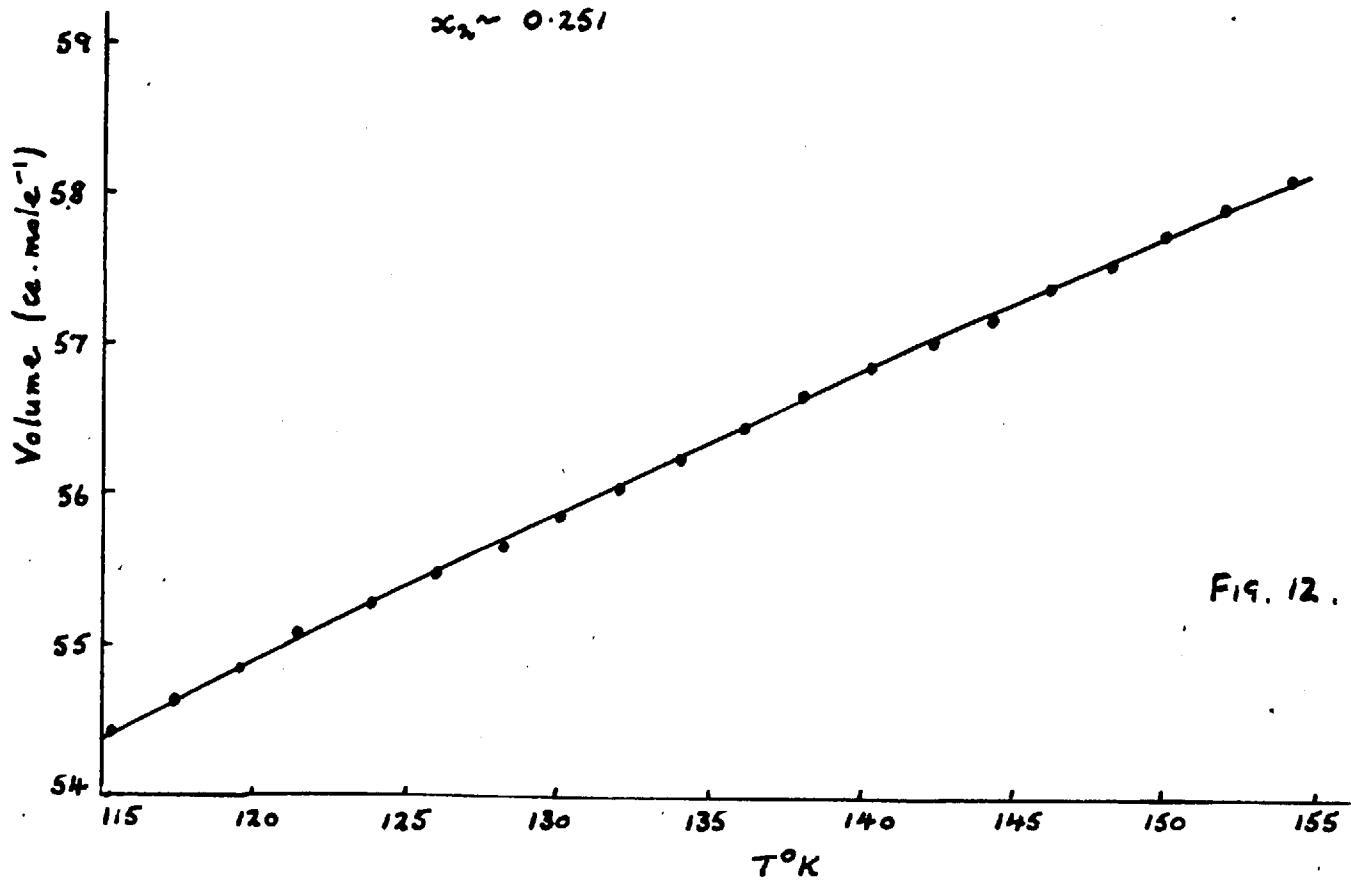


FIG. 12.

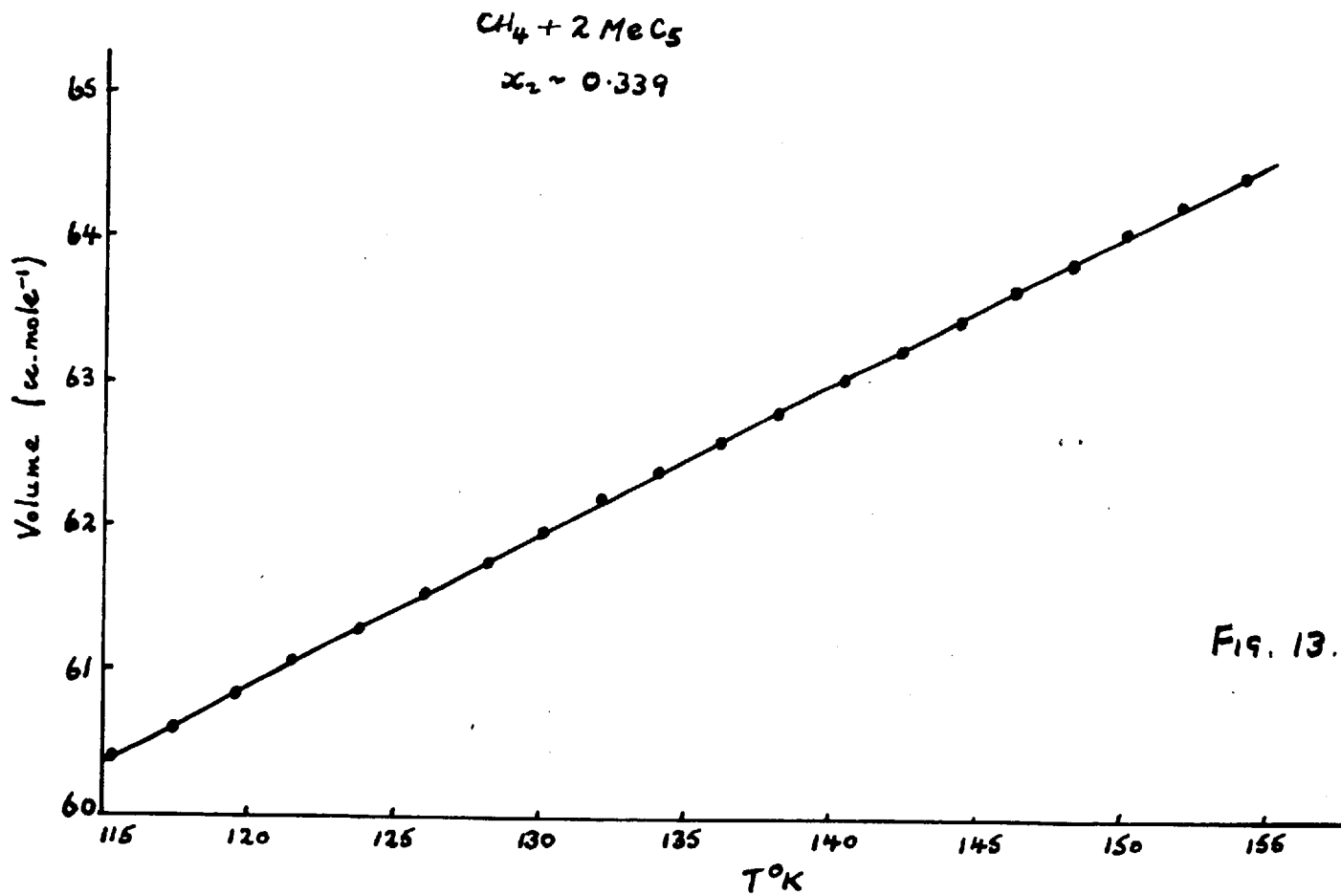


FIG. 13.

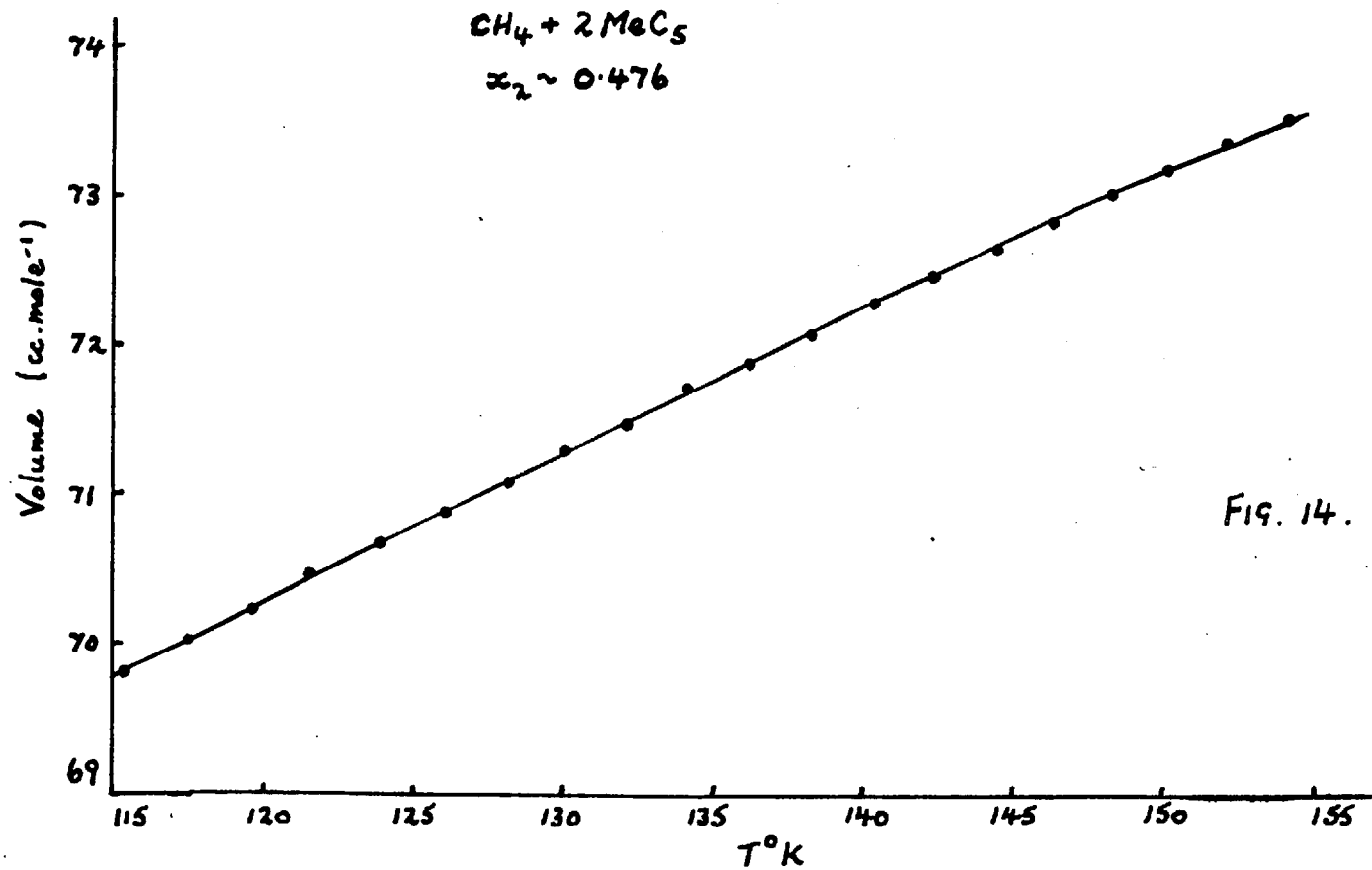


FIG. 14.



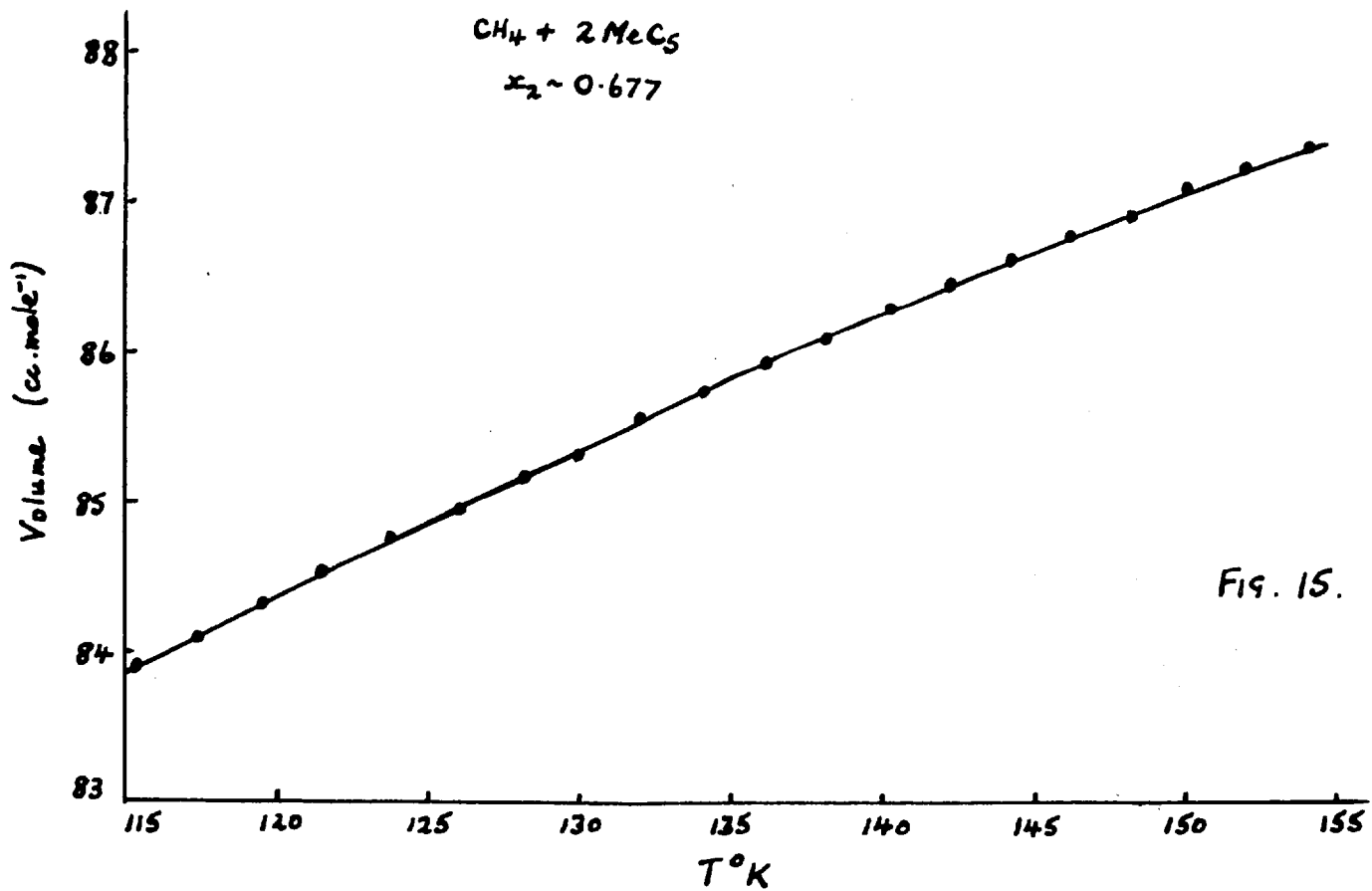


Fig. 15.

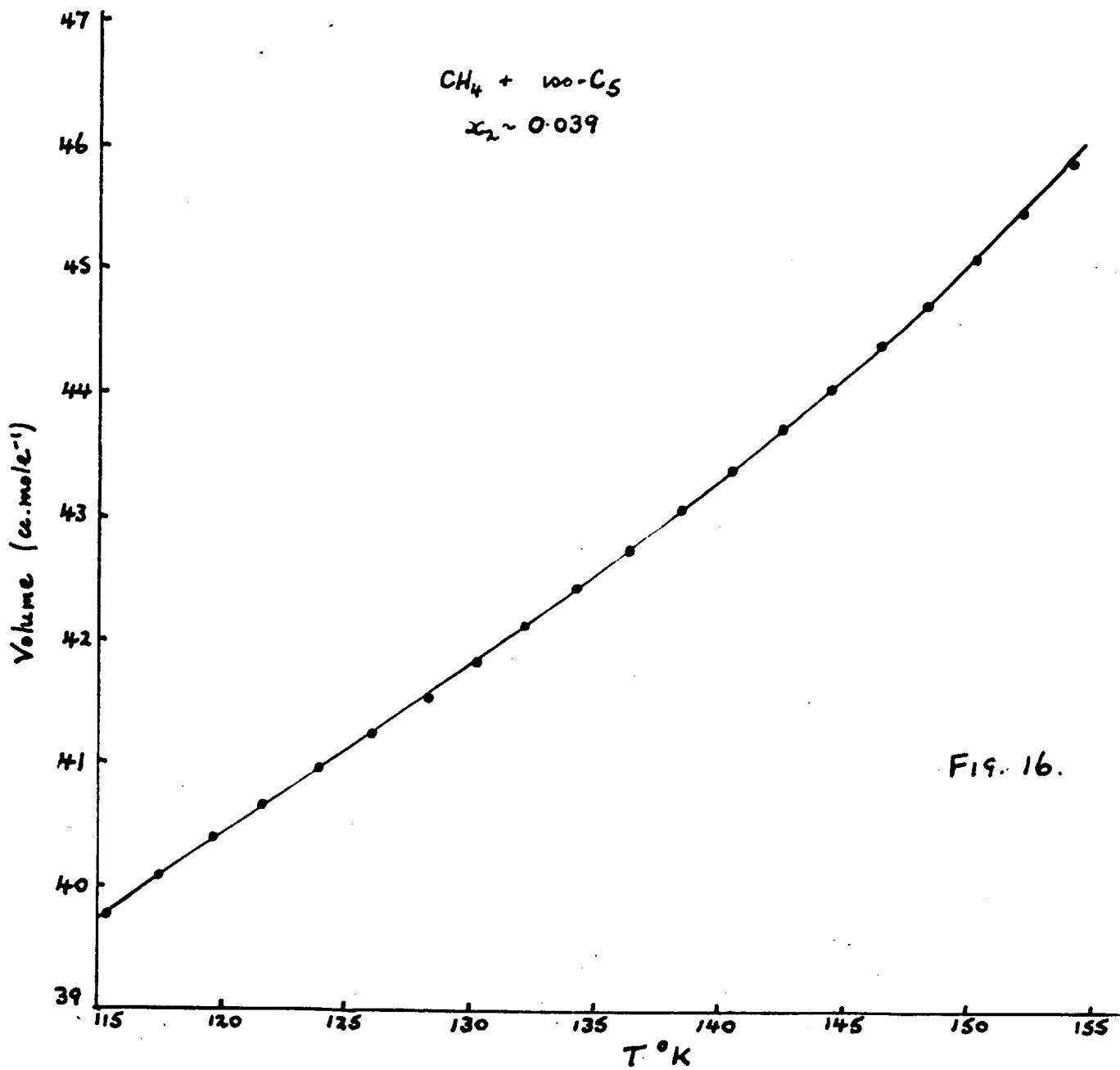


Fig. 16.

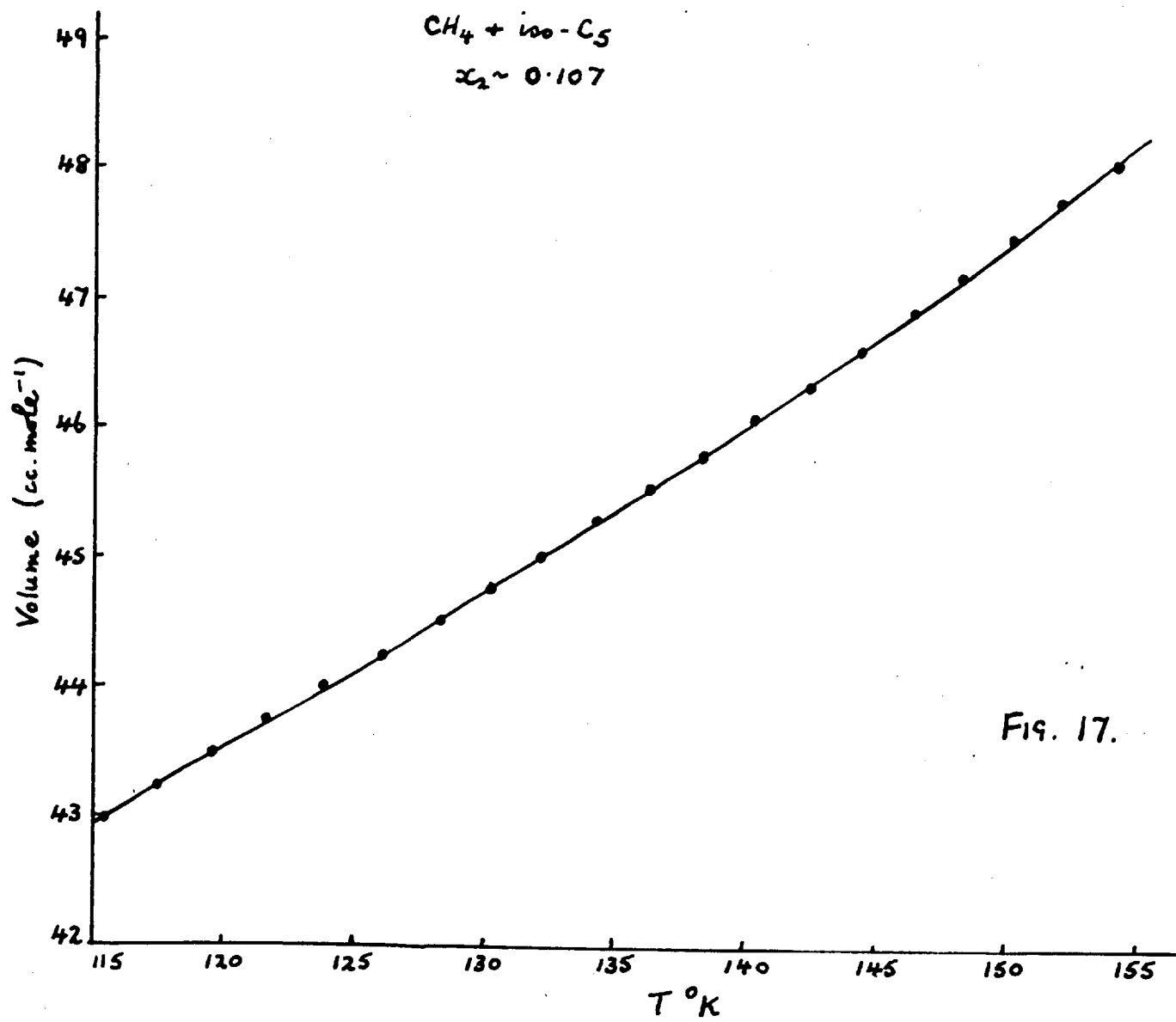


Fig. 17.

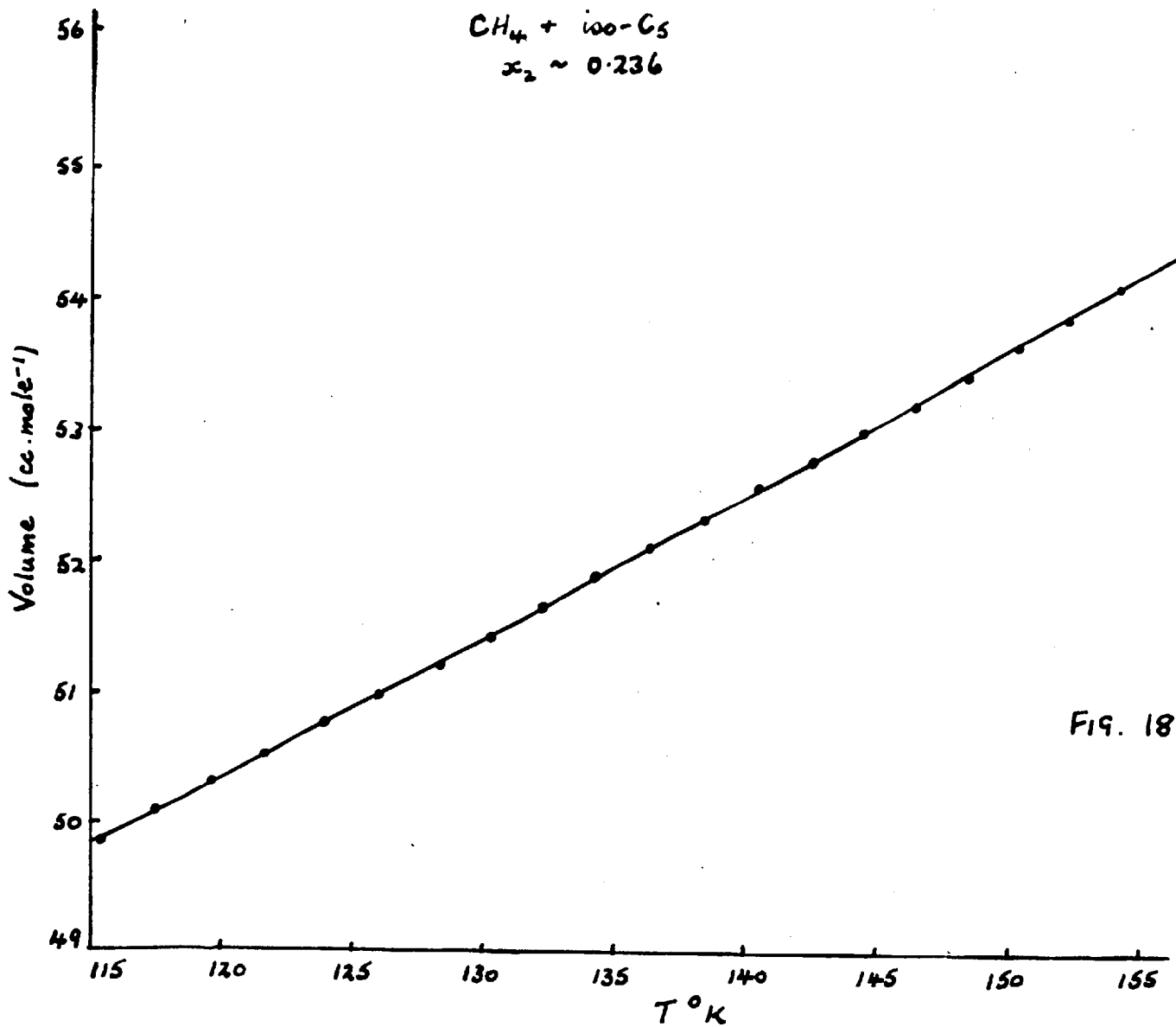


FIG. 18.

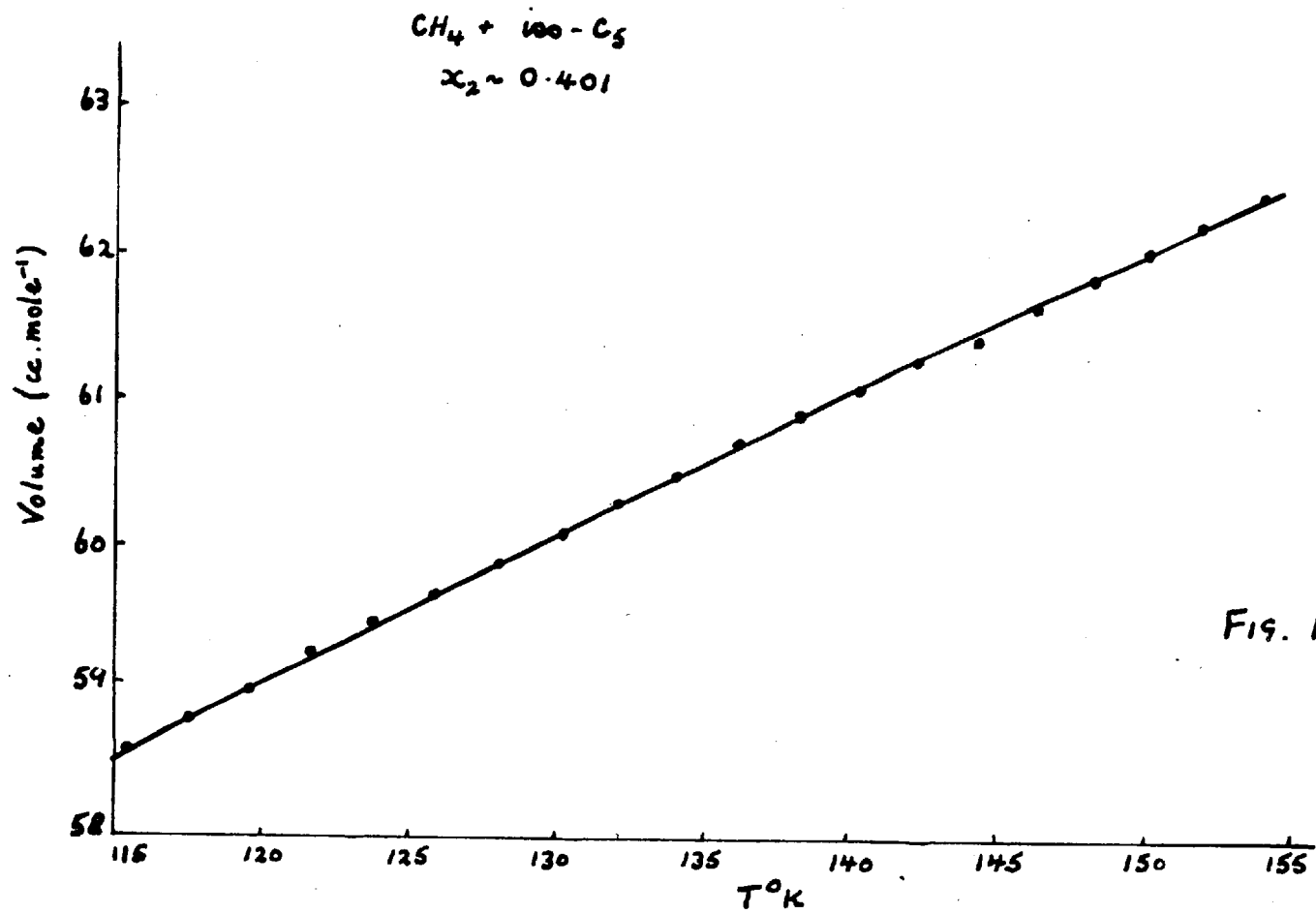


Fig. 19.

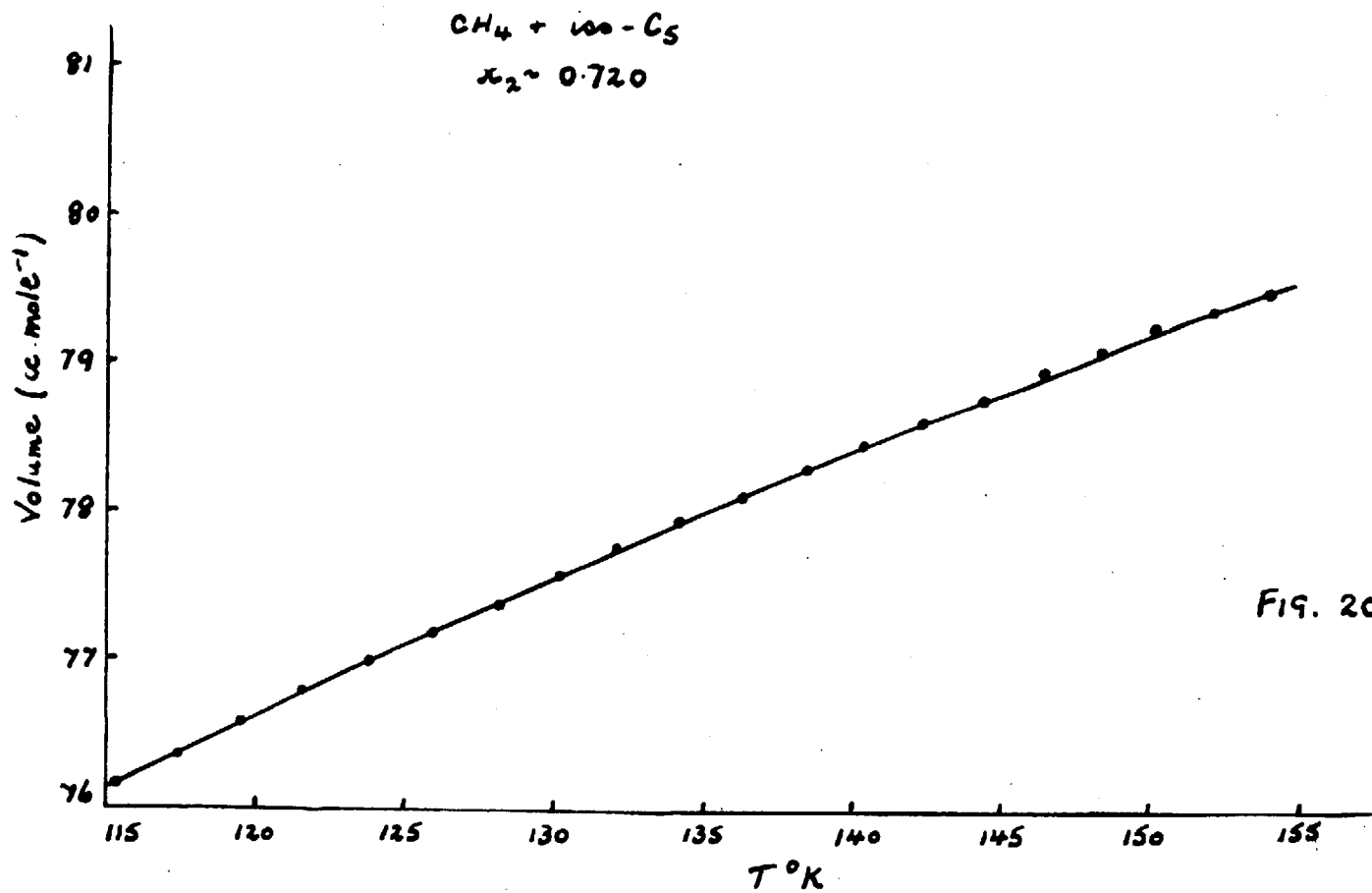
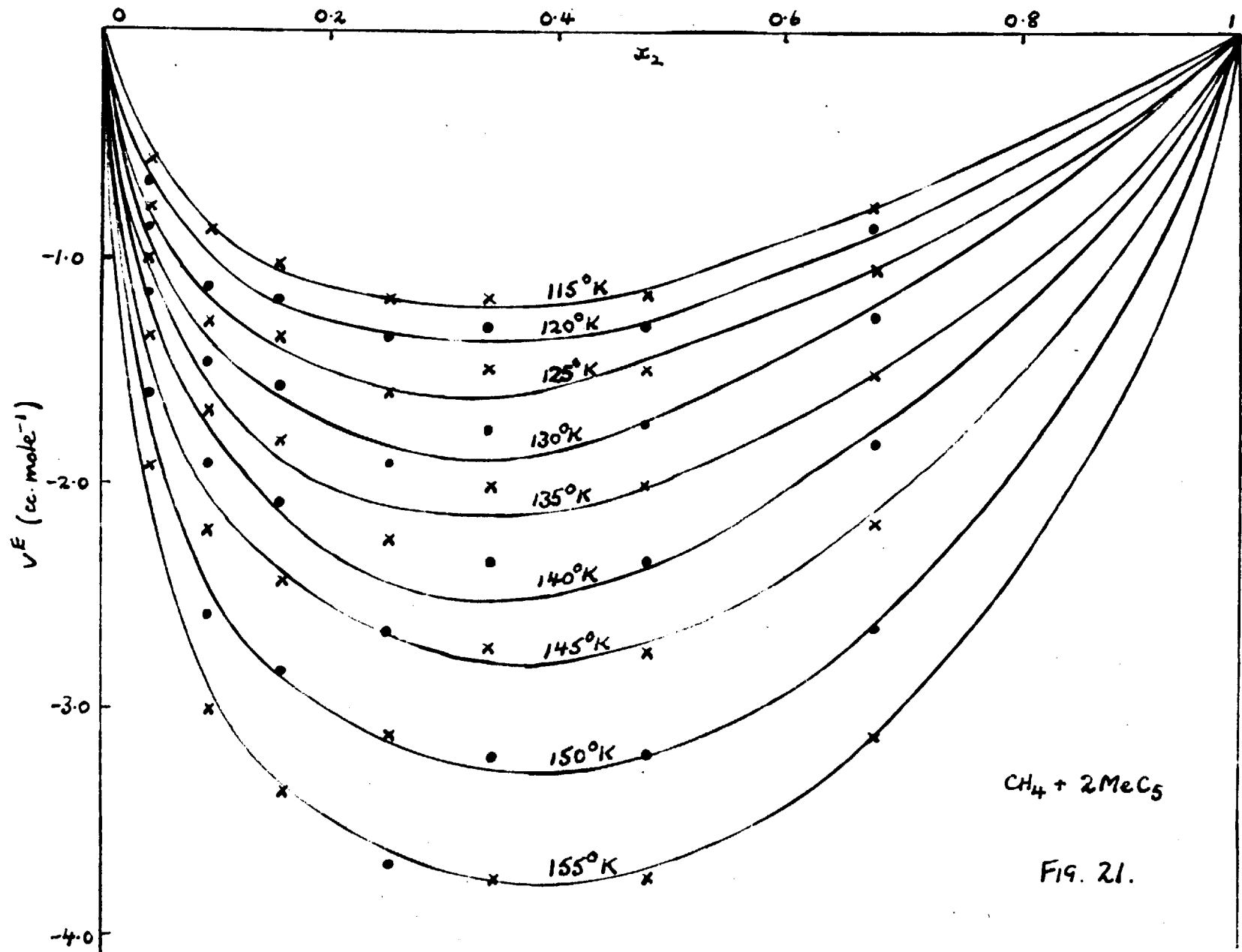
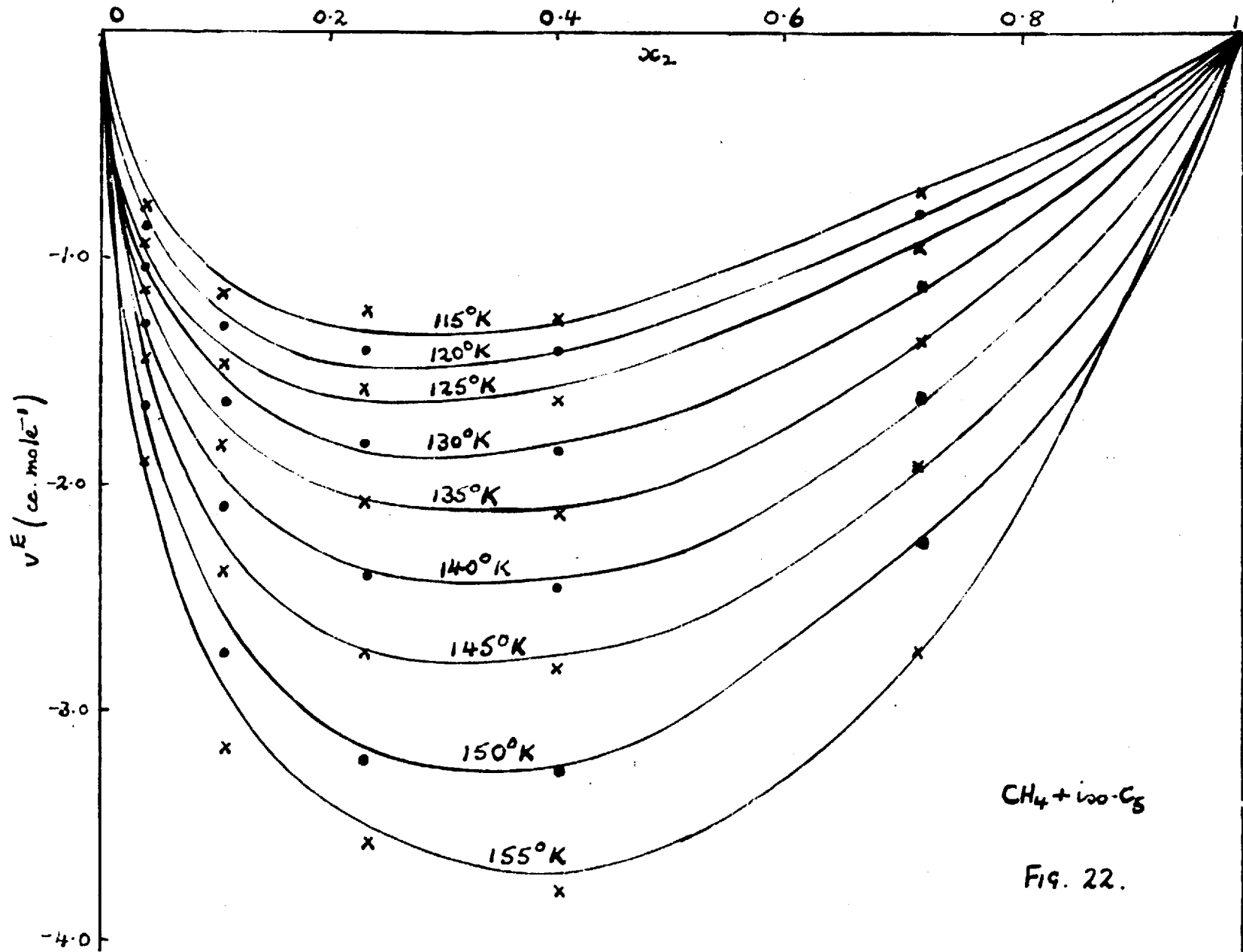


FIG. 20.





$\text{CH}_4 + \text{iso-C}_5$

Fig. 22.



FIG. 23.

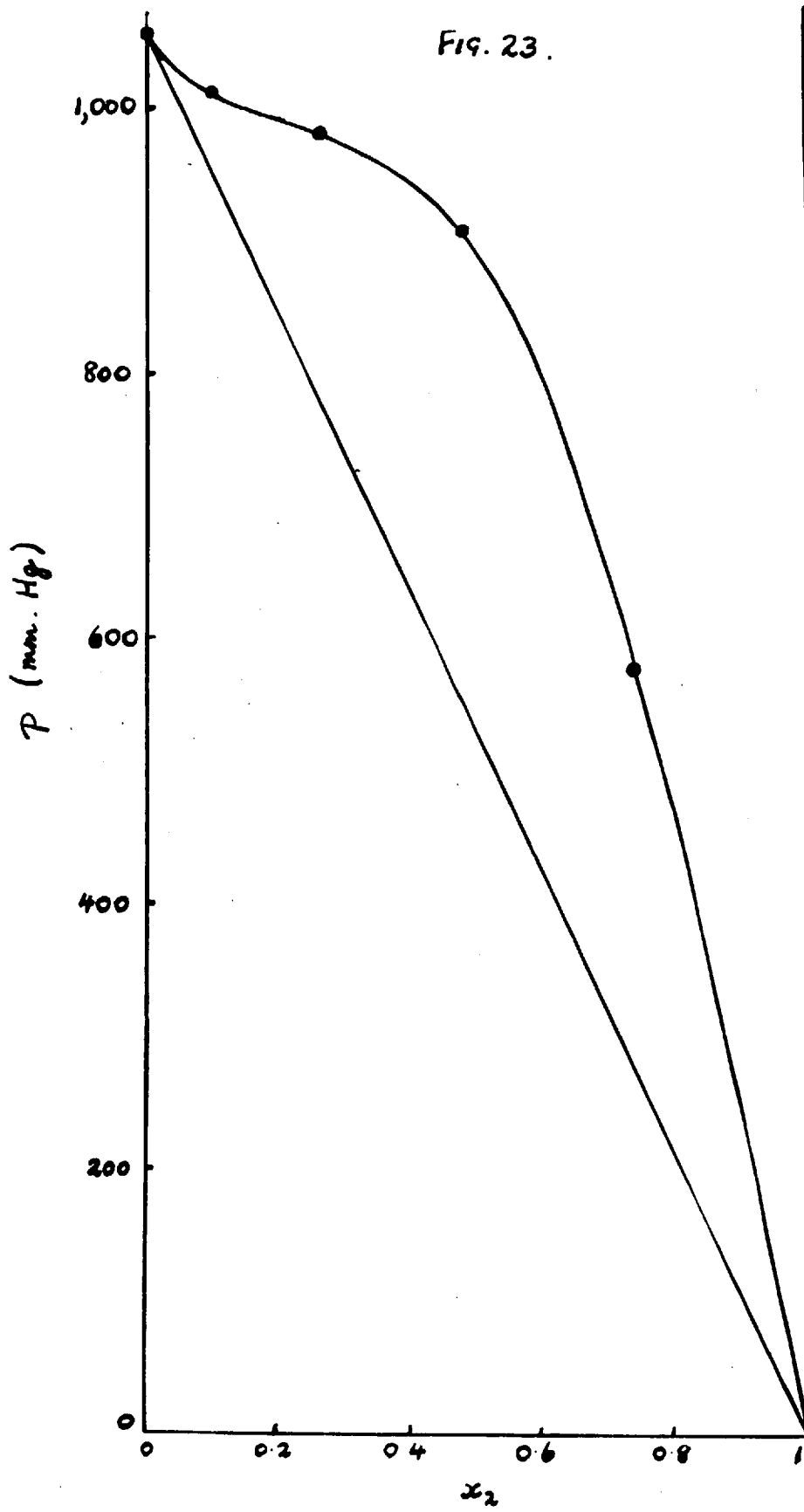
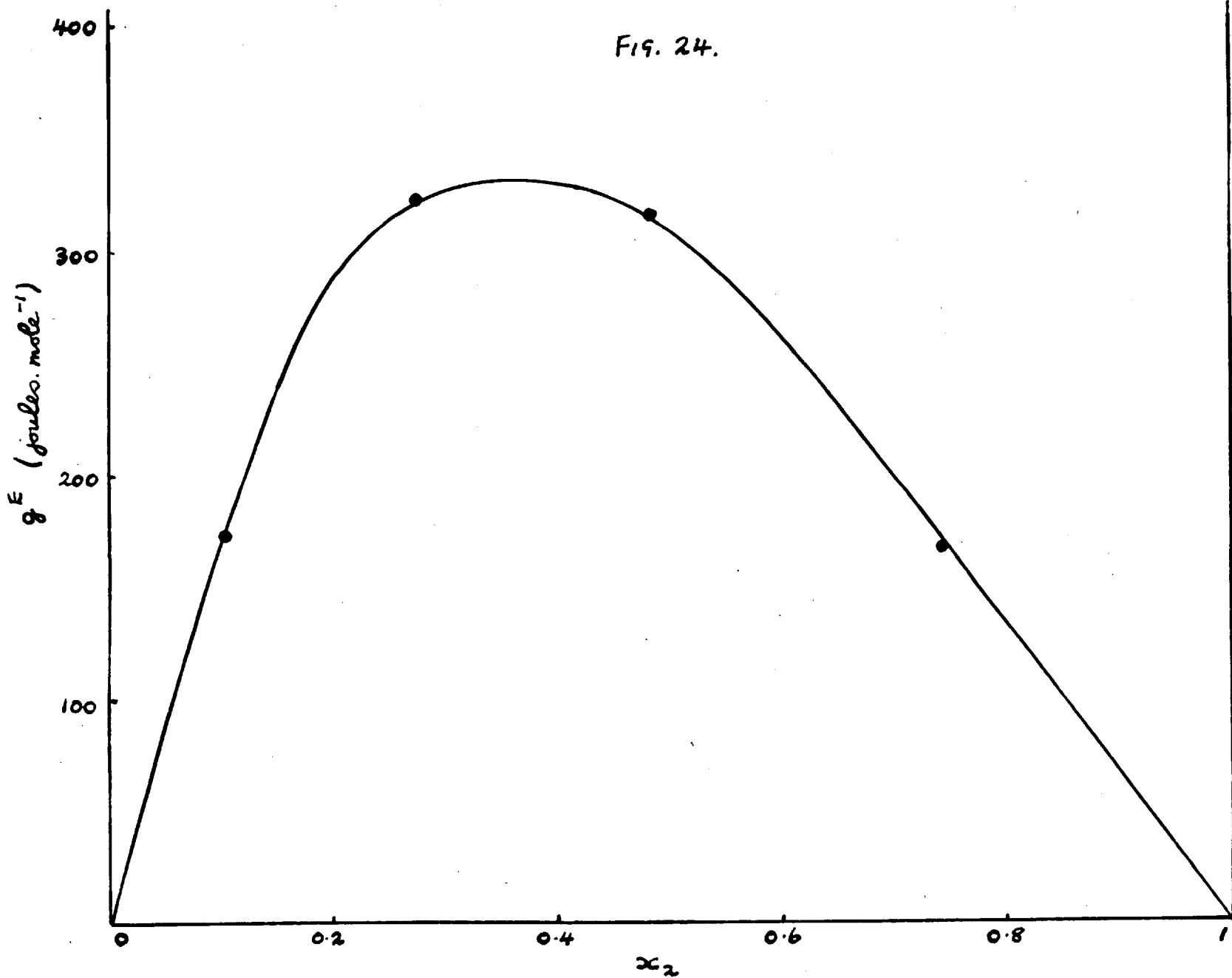


FIG. 24.



## BIBLIOGRAPHY.

- 1) Wilson, Keith and Haylett, Ind. Eng. Chem.,  
28 (1936) 1065.
- 2) Kalichevsky and Kobe, Petroleum Refining with  
Chemicals p. 390-2, Elsevier, Amsterdam 1956.
- 3) Rowlinson and Freeman, Pure Appl. Chem., 1961,  
2, 329.
- 4) Freeman and Rowlinson, Polymer, 1960, 1, 20.
- 5) Kohn, Amer. Inst. Chem. Eng. J., 1961, 7, 514.
- 6) Davenport, Freeman and Rowlinson, Amer. Inst.  
Chem. Eng. J. 1962, 7, 428.
- 7) Hanson and Croley, U.S. Patent Office, No. 2837  
(1958), 504.
- 8) Scatchard, Chem. Rev., 1931, 28, 321.
- 9) Hildebrand and Scott, Solubility of Non-Electrolytes,  
p. 46, 121, (3rd Edition), Reinhold, New York,  
1950; Hildebrand, Disc. Farad. Soc., 15,  
(1953), 9.
- 10) Copp and Everett, Disc. Farad. Soc., 15 (1953), 183.
- 11) Andon, Cox and Herington, Disc. Farad. Soc., 15  
(1953), 168.
- 12) Mitchell and Wynne-Jones, Disc. Farad. Soc., 15  
(1953), 161.
- 13) Hirschfelder, Stevenson and Eyring, J. Chem. Phys.,  
1937, 5, 896
- 14) Baker and Fock, Disc. Farad. Soc., 15 (1953), 188.

- 15) Kohnstamm and Reeders, Pro. Acad. Sci. Amsterdam,  
14 (1911-12), 270.
- 16) Scheffer and Smittenberg, J. Rec. Trav.  
Pays-Bas 52 (1933), 982.
- 19) Hixson and Hixson, Trans. Amer. Inst. Chem.  
Engrs. 37 (1941) 927; Hixson and Bockelmann,  
Trans. Amer. Inst. Chem. Engrs., 38 (1942)  
981; Drew and Hixson, Trans. Amer. Inst.  
Chem. Engrs., 40 (1944) 675.
- 20) Clusius and Riccobini, Z. Physik. Chem. B. 1937,  
38, 81.
- 21) American Petroleum Institute, Research Project 44  
(Carnegie Press, Pittsburgh, 1950).
- 22) Michels and Nederbraght, Physica., 2, 1000, 1935.
- 23) Hamann and Lambert, Australian J. Chem., 1954, 2, 1.
- 24) Lambert, Roberts, Rowlinson and Wilkinson, Pro.  
Royal Soc. A., 1949, 196, 113.
- 25) Ambrose, Britt. J. Appl. Physics, 1957, 8, 32.
- 26) Krigbaum and Flory, J. Amer. Chem. Soc., 1953,  
25, 5254.
- 27) Patterson, Private communication.
- 28) Baker, Brown, Gee, Rowlinson, Stubley and Yeadon,  
Polymer, 1962, 3, 215.
- 29) Myrat, Private communication.
- 30) Jenkel and Keller, Z. Naturf. 5a, (1950) 317.
- 31) Schultz and Flory, J. Amer. Chem. Soc., 74 (1952),  
4760.

- 32) Rowlinson, Liquids and Liquid Mixtures,  
Butterworths, London 1959, p. 146.
- 33) Everett and Mumm, To be published in the  
Transactions of the Faraday Society.
- 34) Guggenheim, Mixtures, (O.U.P. 1952) Chapter X.
- 35) (a) McGlashan and Morcom, Trans. Farad. Soc.,  
1961, 57, 581.  
(b) McGlashan and Williamson, Trans. Farad. Soc.,  
1961, 57, 588.  
(c) McGlashan, Morcom and Williamson, Trans.  
Farad. Soc., 1961, 57, 608.
- 36) (a) Delmas, Patterson and Somcynsky, J. Polymer  
Sc. Vol. 57 (1962) p. 79.  
(b) Delmas, Patterson and Bohme, Trans. Farad.  
Soc., 1962, 58, 2116.
- 37) Guggenheim, Mixtures, (O.U.P. 1952).
- 38) Flory, J. Chem. Phys., 9 (1941) 660; J. Chem.  
Phys., 10 (1942) 51.
- 39) Huggins, J. Chem. Phys., 9 (1941) 440.
- 40) Lennard, Jones and Devonshire, Pro. Royal Soc.,  
1937, A, 163, 53; Pro. Royal Soc., 1938,  
A, 165, 1.
- 41) Pitzer, J. Chem. Phys., 1939, 2, 583.
- 42) Longuet-Higgins, Pro. Royal Soc., 1951, 205A, 247.
- 43) (a) Prigogine, Bellemans and Englert-Chowles,  
J. Chem. Phys., 1956, 24, 518.

- (b) Prigogine, Molecular Theory of Solutions,  
North Holland 1957.
- 44) Scott, J. Chem. Phys., 1956, 25, 193.
- 45) Byers-Brown, Phil. Trans., 1957, 250A, 221.
- 46) (a) Prigogine, Trappemiers and Mathot, Disc. Farad.  
Soc., 15 (1953), 93.
- (b) Prigogine, Trappemiers and Mathot, J. Chem.  
Phys., 21 (1953) 559.
- (c) Prigogine, Bellemans and Naar-Colin, J. Chem.  
Phys., 26 (1957) 751.
- (d) Prigogine, Molecular Theory of Solutions,  
North Holland 1957, Ch. XVI.
- 47) Saville, Private communication.
- 48) Coulson and Herington, Laboratory Distillation  
Practice, Neunes 1958.
- 49) Kistemaker, Physica, 1945, 11, 277.
- 50) Keyes, Taylor and Smith, J. Math. Phys. (M.I.T.)  
1922, 211.
- 51) Bloomer and Parent, Inst. of Gas Research Bull.  
(Chicago) 1952, 17.
- 52) Mathot, Staveley, Young and Parsonage, Trans.  
Farad. Soc., 1956, 52, 1488.
- 53) Clusius, Krius and Konnertz, Ann. Physik., 1938,  
33, 642.
- 54) Clusius, Z. Phys. Chem., 1936, 31B, 459.
- 55) Keesom, Magur and Meihuizen, Physica., 1935, 2, 669.